

AD-A119 112

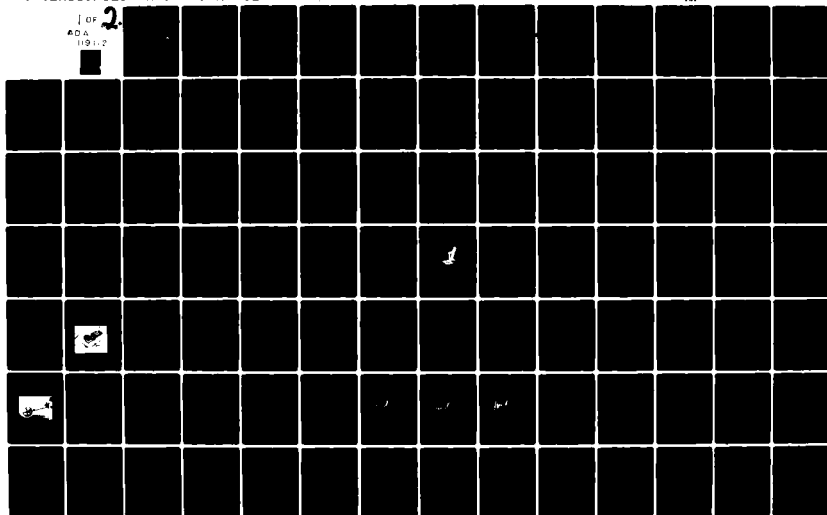
AIR FORCE INST OF TECH WRIGHT-PATTERSON AFB OH  
MEASUREMENT OF VEHICLE TIRE-TO-ROAD COEFFICIENT OF FRICTION WIT--ETC(U)  
AUG 82 R L COKE  
AFIT/CI/NR/82-35T

F/G 13/6

UNCLASSIFIED

NI

1 OF 2  
ADA  
119 112



UNCLASS

SECURITY CLASSIFICATION OF THIS PAGE (When Data Entered)

## REPORT DOCUMENTATION PAGE

READ INSTRUCTIONS  
BEFORE COMPLETING FORM

1. REPORT NUMBER AFIT/CI/NR/82-35T		2. GOVT ACCESSION NO. AD-A119112	3. RECIPIENT'S CATALOG NUMBER
4. TITLE (and Subtitle) Measurement of Vehicle Tire-To-Road Coefficient of Friction With A Portable Microcomputerized Transducer		5. TYPE OF REPORT & PERIOD COVERED THESIS/DISSERTATION	
7. AUTHOR(s) Ronnie Lynn Coke		6. PERFORMING ORG. REPORT NUMBER	
9. PERFORMING ORGANIZATION NAME AND ADDRESS AFIT STUDENT AT: University of Texas - Austin		8. CONTRACT OR GRANT NUMBER(s)	
11. CONTROLLING OFFICE NAME AND ADDRESS AFIT/NR WPAFB OH 45433		10. PROGRAM ELEMENT, PROJECT, TASK AREA & WORK UNIT NUMBERS	
14. MONITORING AGENCY NAME & ADDRESS (if different from Controlling Office)		12. REPORT DATE August 1982	
		13. NUMBER OF PAGES 152	
		15. SECURITY CLASS. (of this report) UNCLASS	
		15a. DECLASSIFICATION DOWNGRADING SCHEDULE	
16. DISTRIBUTION STATEMENT (of this Report) APPROVED FOR PUBLIC RELEASE; DISTRIBUTION UNLIMITED			
17. DISTRIBUTION STATEMENT (of the abstract entered in Block 20, if different from Report)			
18. SUPPLEMENTARY NOTES APPROVED FOR PUBLIC RELEASE: IAW AFR 190-17 30 AUG 1982 LYNN E. WOLAVER Dean for Research and Professional Development AFIT, Wright-Patterson AFB OH			
19. KEY WORDS (Continue on reverse side if necessary and identify by block number)			
20. ABSTRACT (Continue on reverse side if necessary and identify by block number) ATTACHED COPY			

DTIC  
ELECTE  
SEP 9 1982  
H

DD FORM 1473

EDITION OF JAN 65, OBSOLETE

UNCLASS

SECURITY CLASSIFICATION OF THIS PAGE (When Data Entered)

## ABSTRACT

Accurate measurement of the tire-to-road coefficient of friction is a necessary factor in the analysis of vehicle dynamics when sliding composes part of the motion. In the past, numerous methods have been used to measure the coefficient of friction but the results of these methods seldom agree or yield the requisite accuracy necessary for a detailed analysis of vehicle dynamics.

Tire traction is a complex process which has many variables. The method of using a portable accelerometer and a microcomputerized data acquisition and storage device was chosen as the best way to measure the coefficient of friction because it permits a test procedure which closely approximates the event being analyzed. Therefore, leaving the least number of variables unaccounted for.

A portable accelerometer/microcomputer device was implemented and used at three different skid test sites. Skid test results from the accelerometer, verified by an independent fifth-wheel device, confirm the accuracy of using this type of device and procedure to determine the coefficient of friction.

DTIC	1
COPY	1
INSPECTED	1
2	
1	
2	
3	
4	
5	
6	
7	
8	
9	
10	
11	
12	
13	
14	
15	
16	
17	
18	
19	
20	
21	
22	
23	
24	
25	
26	
27	
28	
29	
30	
31	
32	
33	
34	
35	
36	
37	
38	
39	
40	
41	
42	
43	
44	
45	
46	
47	
48	
49	
50	
51	
52	
53	
54	
55	
56	
57	
58	
59	
60	
61	
62	
63	
64	
65	
66	
67	
68	
69	
70	
71	
72	
73	
74	
75	
76	
77	
78	
79	
80	
81	
82	
83	
84	
85	
86	
87	
88	
89	
90	
91	
92	
93	
94	
95	
96	
97	
98	
99	
100	



8-2-85

MEASUREMENT OF VEHICLE TIRE-TO-ROAD  
COEFFICIENT OF FRICTION WITH A  
PORTABLE MICROCOMPUTERIZED  
TRANSDUCER

APPROVED:

Walter S. Reed  
N. J. Rylander

MEASUREMENT OF VEHICLE TIRE-TO-ROAD  
COEFFICIENT OF FRICTION WITH A  
PORTABLE MICROCOMPUTERIZED  
TRANSDUCER

BY

RONNIE LYNN COKE, B.S.

THESIS

Presented to the Faculty of the Graduate School of  
The University of Texas at Austin  
in Partial Fulfillment  
of the Requirements  
for the Degree of  
MASTER OF SCIENCE IN ENGINEERING

THE UNIVERSITY OF TEXAS AT AUSTIN

August 1982

#### ACKNOWLEDGMENTS

The author thanks Dr. Walter S. Reed for his guidance toward the accomplishment of this thesis. Appreciation is also due Dr. H. Grady Rylander for his careful reading and suggestions for improving the text. Mr. Grover A. Edmiston, Jr., provided invaluable assistance by constructing the microcomputer and connecting the accelerometer to it. Mr Frank Abernathy and Mr. Wayne Wedemeyer also contributed significantly by providing the equipment and time to store the computer's operational program in the memory chip.

Thanks also go to Officer Charles Chipman, Investigator for the Austin Police Department, for help in setting up and performing several skid tests. Mr. Hal Fitzpatrick and Mr. Richard Fredrick also provided invaluable assistance during the testing phase of this work.

The financial support for the author's graduate studies was provided by the United States Air Force, Air Force Institute of Technology. Without this support, the graduate work would not have been completed.

Finally, the author wishes to thank his wife, Ellen and son, John for their patience and moral support throughout graduate school.

## ABSTRACT

Accurate measurement of the tire-to-road coefficient of friction is a necessary factor in the analysis of vehicle dynamics when sliding composes part of the motion. In the past, numerous methods have been used to measure the coefficient of friction but the results of these methods seldom agree or yield the requisite accuracy necessary for a detailed analysis of vehicle dynamics.

Tire traction is a complex process which has many variables. The method of using a portable accelerometer and a microcomputerized data acquisition and storage device was chosen as the best way to measure the coefficient of friction because it permits a test procedure which closely approximates the event being analyzed. Therefore, leaving the least number of variables unaccounted for.

A portable accelerometer/microcomputer device was implemented and used at three different skid test sites. Skid test results from the accelerometer, verified by an independent fifth-wheel device, confirm the accuracy of using this type of device and procedure to determine the coefficient of friction.



## TABLE OF CONTENTS

	Page
ACKNOWLEDGMENTS. . . . .	iii
ABSTRACT . . . . .	iv
LIST OF TABLES . . . . .	vi
LIST OF FIGURES. . . . .	vii
CHAPTER I     INTRODUCTION. . . . .	1
CHAPTER 2     SYSTEM DESIGN REQUIREMENTS. . . . .	11
CHAPTER 3     MICROCOMPUTER AND FIFTH-WHEEL DESIGN AND DEVELOPMENT AND ACCELEROMETER INCORPORATION . . . . .	31
CHAPTER 4     SYSTEM TESTING AND DATA EVALUATION. . .	55
CHAPTER 5     CONCLUSIONS AND RECOMMENDATIONS . . . .	94
APPENDIX A     FIGURES FOR TEST SITE ONE . . . . .	97
APPENDIX B     FIGURES FOR TEST SITE THREE . . . . .	116
REFERENCES     . . . . .	147
VITA            . . . . .	152

## LIST OF TABLES

Table		Page
3.1	First Resonant Frequency, Damping Ratio, and Time Constant for Undamped and Lightly Damped System. . . . .	36
4.1	Results of Skid Testing on Guadalupe Drive June 18, 1982 . . . . .	72
4.2	Results of Skid Testing on Crossing Place June 18, 1982 . . . . .	91
4.3	Results of Skid Testing on Texas Highway 29 Near Burnet, Texas, June 29, 1982 . . . . .	92

## LIST OF FIGURES

Figure		Page
1.1a	Constant Deceleration as a Function of Time . .	7
1.1b	Velocity Curve Resulting from Constant Deceleration . . . . .	7
1.2	Typical Deceleration for an Automobile Skid Test . . . . .	8
2.1	The Four Major Components of Tire-Pavement Friction [14] . . . . .	14
2.2	Braking Force Due to Adhesion and Skidding Effects as a Function of Time . . . . .	16
2.3	Slip Angle . . . . .	21
3.1	Spring, Mass, Damper, Limiter Arm, and Strain Gage Accelerometer. . . . .	33
3.2	Transfer Function of the Undamped Accelerometer Showing First Resonant Frequency [22] . .	34
3.3	Transfer Function of Lightly Damped Accelerometer Showing First Resonant Frequency [22] . .	35
3.4	Block Diagram of Computer Board and Accelerometer and Fifth-Wheel Interconnection . . . . .	40
3.5	Accelerometer and Microcomputer Unit . . . . .	41
3.6	Memory Map . . . . .	47
3.7	RAM Memory Map . . . . .	48
3.8	Fifth-Wheel . . . . .	54
4.1	Deceleration vs. Time June 18, 1982 Test One Unfiltered . . . . .	60
4.2	Deceleration vs. Time June 18, 1982 Test Two Unfiltered . . . . .	61
4.3	Deceleration vs. Time June 18, 1982 Test Three Unfiltered . . . . .	62

## LIST OF FIGURES (Continued)

Figure		Page
4.4	Deceleration vs. Time June 18, 1982 Test One Filtered. . . . .	64
4.5	Deceleration vs. Time June 18, 1982 Test Two Filtered. . . . .	65
4.6	Deceleration vs. Time June 18, 1982 Test Three Filtered . . . . .	66
4.7	Deceleration vs. Time June 18, 1982 Test One Filtered One G Calibration Range . . . . .	69
4.8	Deceleration vs. Time June 18, 1982 Test Two Filtered One G Calibration Range . . . . .	70
4.9	Deceleration vs. Time June 18, 1982 Test Three Filtered One G Calibration Range . . . . .	71
4.10	Velocity vs. Time June 18, 1982 Test One. . .	74
4.11	Velocity vs. Time June 18, 1982 Test Two. . .	75
4.12	Velocity vs. Time June 18, 1982 Test Three. .	76
4.13	Distance vs. Time June 18, 1982 Test One. . .	77
4.14	Distance vs. Time June 18, 1982 Test Two. . .	78
4.15	Distance vs. Time June 18, 1982 Test Three. .	79
4.16	Distance vs. Time June 18, 1982 Test One Fifth-Wheel Data. . . . .	80
4.17	Distance vs. Time June 18, 1982 Test Two Fifth-Wheel Data. . . . .	81
4.18	Distance vs. Time June 18, 1982 Test Three Fifth-Wheel Data. . . . .	82
4.19	Distance vs. Velocity Test Site Two. . . . .	86
4.20	Distance vs. Velocity Test Site Two Example Velocity Estimation . . . . .	87

## LIST OF FIGURES (Continued)

Figure		Page
4.21	Distance vs. Velocity June 17, 1982 Test Site One. . . . .	88
4.22	Distance vs. Velocity June 29, 1982 Test Site Three Uphill Skid . . . . .	89
4.23	Distance vs. Velocity June 29, 1982 Test Site Three Downhill Skid . . . . .	90

## APPENDIX A FIGURES

A.1	Deceleration vs. Time June 17, 1982 Test One Unfiltered. . . . .	98
A.2	Deceleration vs. Time June 17, 1982 Test Two Unfiltered. . . . .	99
A.3	Deceleration vs. Time June 17, 1982 Test Three Unfiltered. . . . .	100
A.4	Deceleration vs. Time June 17, 1982 Test One Filtered. . . . .	101
A.5	Deceleration vs. Time June 17, 1982 Test Two Filtered. . . . .	102
A.6	Deceleration vs. Time June 17, 1982 Test Three Filtered. . . . .	103
A.7	Deceleration vs. Time June 17, 1982 Test One Filtered One-G Calibration Range. . . . .	104
A.8	Deceleration vs. Time June 17, 1982 Test Two Filtered One-G Calibration Range. . . . .	105
A.9	Deceleration vs. Time June 17, 1982 Test Three Filtered One-G Calibration Range. . . . .	106
A.10	Velocity vs. Time June 17, 1982 Test One. . .	107
A.11	Velocity vs. Time June 17, 1982 Test Two. . .	108
A.12	Velocity vs. Time June 17, 1982 Test Three. .	109

## LIST OF FIGURES (Continued)

Figure		Page
A.13	Distance vs. Time June 17, 1982 Test One. . .	110
A.14	Distance vs. Time June 17, 1982 Test Two. . .	111
A.15	Distance vs. Time June 17, 1982 Test Three. .	112
A.16	Distance vs. Time June 17, 1982 Test One Fifth-Wheel Data. . . . .	113
A.17	Distance vs. Time June 17, 1982 Test Two Fifth-Wheel Data. . . . .	114
A.18	Distance vs. Time June 17, 1982 Test Three Fifth-Wheel Data. . . . .	115

## APPENDIX B FIGURES

B.1	Deceleration vs. Time June 29, 1982 Test One Unfiltered. . . . .	117
B.2	Deceleration vs. Time June 29, 1982 Test Two Unfiltered. . . . .	118
B.3	Deceleration vs. Time June 29, 1982 Test Three Unfiltered. . . . .	119
B.4	Deceleration vs. Time June 29, 1982 Test Four Unfiltered. . . . .	120
B.5	Deceleration vs. Time June 29, 1982 Test Five Unfiltered. . . . .	121
B.6	Deceleration vs. Time June 29, 1982 Test One Filtered. . . . .	122
B.7	Deceleration vs. Time June 29, 1982 Test Two Filtered. . . . .	123
B.8	Deceleration vs. Time June 29, 1982 Test Three Filtered. . . . .	124
B.9	Deceleration vs. Time June 29, 1982 Test Four Filtered. . . . .	125

## LIST OF FIGURES (Continued)

Figure		Page
B.10	Deceleration vs. Time June 29, 1982 Test Five Filtered. . . . .	126
B.11	Deceleration vs. Time June 29, 1982 Test One Filtered One-G Calibration Range. . . . .	127
B.12	Deceleration vs. Time June 29, 1982 Test Two Filtered One-G Calibration Range. . . . .	128
B.13	Deceleration vs. Time June 29, 1982 Test Three Filtered One-G Calibration Range. . . . .	129
B.14	Deceleration vs. Time June 29, 1982 Test Four Filtered One-G Calibration Range. . . . .	130
B.15	Deceleration vs. Time June 29, 1982 Test Five Filtered One-G Calibration Range. . . . .	131
B.16	Velocity vs. Time June 29, 1982 Test One. . .	132
B.17	Velocity vs. Time June 29, 1982 Test Two. . .	133
B.18	Velocity vs. Time June 29, 1982 Test Three. .	134
B.19	Velocity vs. Time June 29, 1982 Test Four . .	135
B.20	Velocity vs. Time June 29, 1982 Test Five . .	136
B.21	Distance vs. Time June 29, 1982 Test One. . .	137
B.22	Distance vs. Time June 29, 1982 Test Two. . .	138
B.23	Distance vs. Time June 29, 1982 Test Three. .	139
B.24	Distance vs. Time June 29, 1982 Test Four . .	140
B.25	Distance vs. Time June 29, 1982 Test Five . .	141
B.26	Distance vs. Time June 29, 1982 Test One Fifth-Wheel Data. . . . .	142
B.27	Distance vs. Time June 29, 1982 Test Two Fifth-Wheel Data. . . . .	143

## LIST OF FIGURES (Continued)

Figure		Page
B.28	Distance vs. Time June 29, 1982 Test Three Fifth-Wheel Data. . . . .	144
B.29	Distance vs. Time June 29, 1982 Test Four Fifth-Wheel Data. . . . .	145
B.30	Distance vs. Time June 29, 1982 Test Five Fifth-Wheel Data. . . . .	146



## CHAPTER I

### INTRODUCTION

The law enforcement and legal communities are increasingly relying on the expertise of the mechanical engineer to ascertain detailed relationships causing and comprising vehicle collisions. This process, which will be referred to as accident reconstruction, generally involves three basic steps:

1. Accident data acquisition.
2. Analytical reconstruction of the vehicle dynamics.
3. Presentation of results.

This thesis deals with the first of these steps, the accident data acquisition step, and specifically with the development of an accurate and consistent method of determining the coefficient of friction, ( $\mu$ ) between a vehicle's tires and the road surface. The nature of all forces controlling the vehicle's motion are a function of this coefficient of friction except during short periods when the vehicle is impacting another vehicle or object. Determining the exact characteristics of  $\mu$  is therefore essential if accuracy of vehicle dynamics is going to be achieved.

In a sample of 1000 accident cases studied during

the Multidisciplinary Accident Investigation Program (MDAI) nearly twenty percent of all cases involved braking, nine percent involved steering, and nearly six percent involved both braking and steering. In addition, nearly sixty-six percent involved no evasive action at all [1]. Therefore, approximately seventy-four percent of the accidents where evasive actions were taken involved braking.

When locked wheel skidding has occurred the measured length of the skid marks, the coefficient of friction, and the estimated velocity at the time of impact can be used to determine the velocity of a vehicle prior to the skid. An accurate measurement of  $\mu$  must be made at the accident site if the above velocity estimate is to be precise. Therefore, the methods used in obtaining  $\mu$  must be precise and repeatable.

In the past however,  $\mu$  has been one of the least credible factors. The equipment used to gather the data at the accident site has generally been quite unsophisticated. In some cases, only a vehicle and a measuring tape were used [2]. In this type of test, the procedure requires the investigator to drive his vehicle at a documented speed (usually 30 miles per hour) and skid to a stop. The investigator then measures the length of the skid marks with a measuring tape and calculates the coefficient of friction

by using the following equation:

$$\mu = (V)^2 / (2gs) \quad (1)$$

where

$\mu$  is the average coefficient of friction (dimensionless),

$V$  is the velocity of the vehicle prior to the skid (feet per second),

$s$  is the length of the skid (feet), and

$g$  is the gravitational acceleration (feet per second squared).

This is easily converted to the following approximation for ease and convenience:

$$\mu \approx (v)^2 / (30s) \quad (2)$$

where

$v$  is the velocity of the vehicle prior to the skid (miles per hour),

$s$  is the length of the skid (feet), and

$30 \approx 2(32.2 \text{ ft/sec}) / (1.466666 \text{ ft/sec/MPH})^2$ .

There are, however, several inaccuracies built into the above equations and, therefore, into this procedure. The vehicle's velocity prior to the skid is difficult to obtain with the requisite accuracy. If it is not accurate, the error is increased by the squaring factor. The distance is also difficult to obtain because the actual skid marks may not begin until the vehicle has skidded for

several feet. Even then, the beginning of the skid marks are sometimes hard to pinpoint. It should be noted also that this procedure yields a single valued coefficient (i.e.  $\mu_{ave}$ ) that contains no information concerning the nature of  $\mu$  with respect to time, distance, or velocity.

Equation (1) was developed from the work-energy theorem. The assumption is made that all the vehicle's kinetic energy is transformed by the forces acting at the tire-road interface with most being converted to heat and dissipated into the tire or at the road interface. The kinetic energy,  $E$  of the vehicle moving at velocity,  $V$  is:

$$E = m(V)^2/2 \quad (3)$$

where

$m$  is the vehicle mass.

The work,  $W$  performed by the road on the skidding tires is:

$$W = Fs \quad (4)$$

where

$F$  is the force applied by the road to the tires, and  $s$  is the distance of the skid.

The work required to stop a moving vehicle is equal to the initial kinetic energy or:

$$Fs = m(V)^2/2 \quad (5)$$

The only force applied to a skidding vehicle is through the tires and hence a function of the coefficient

of friction. This equates to:

$$F = \mu N \quad (6)$$

where

$N$  is the normal component of force  
acting on the tires, and

$\mu$  is the dynamic coefficient of friction.

The combined normal force of all the tires is equal to the total weight,  $w$  of the vehicle.

With Newton's Second Law of Motion:

$$F = ma \quad (7)$$

where

$a$  is the acceleration, and

$m$  is the vehicle mass,

Equation (6) becomes:

$$\begin{aligned} F &= \mu w \\ &= \mu mg \end{aligned} \quad (8)$$

Combining Equations (5) and (8) yields:

$$\mu mg = m(V)^2 / 2 \quad (9)$$

Rearrangement of Equation (9) produces Equation (1). At one time, this method was considered the interim standard for measuring  $\mu$  [3].

The  $\mu$  calculated from Equation (1) is an average dynamic coefficient of friction between a vehicle's tires and the road surface over a velocity range from the initial velocity down to zero. Since  $\mu$  is directly proportional

to the vehicle's deceleration by a factor of  $g$  (see Ch 2), Equation (1) implies that the deceleration of a vehicle is constant throughout the skid as depicted in Figure 1.1a. With a constant deceleration the velocity decrease will be linear.

Testing of this phenomena began during the early 1950's and showed that the deceleration of a skidding vehicle is not in fact constant [4]. Typically, the deceleration of a vehicle in a locked-wheel skid acts more like that depicted in Figure 1.2. Braking forces build up from zero to the incipient peak where skidding begins. The deceleration drops off slightly and slowly increases again as the skid continues.

In addition to those noted above, there are other inaccuracies built into Equation (1) also. This equation assumes that all the kinetic energy dissipated during a skid is done through the tire-road surface interface. During the actual skid this is true, but there is a short period of time, approximately 0.12 seconds [1,5], where the brakes are applied and the wheels are not locked. This brake build-up time, in addition to the fact that the initial skid marks may not actually start for several feet after brake lock-up, causes the calculated  $\mu$ , from (1) to actually be higher than the true  $\mu$ . This discrepancy is very undesirable because it severely limits the accuracy

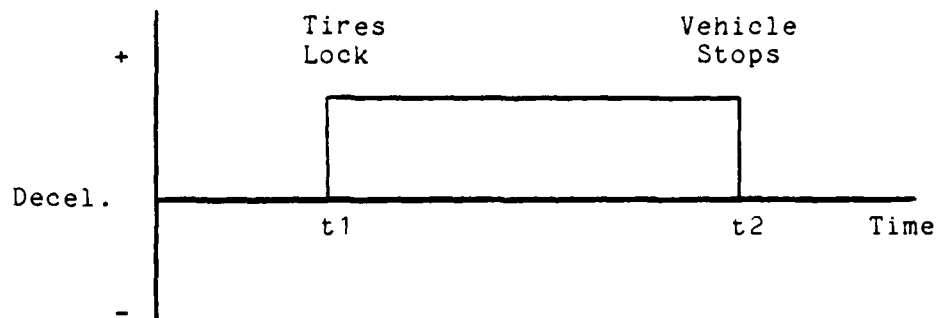


Figure 1.1a Constant Deceleration as a Function of Time

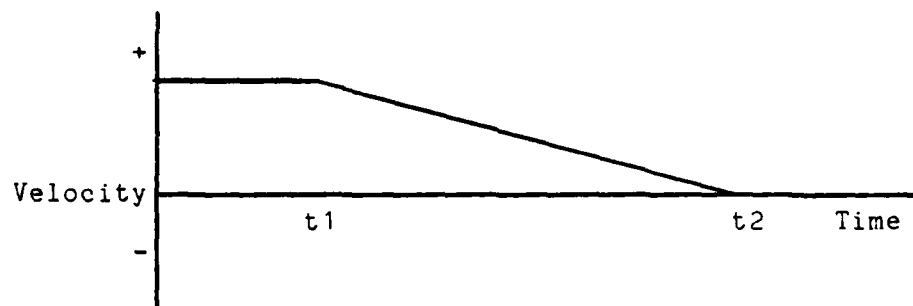


Figure 1.1b Velocity Curve Resulting from Constant Deceleration

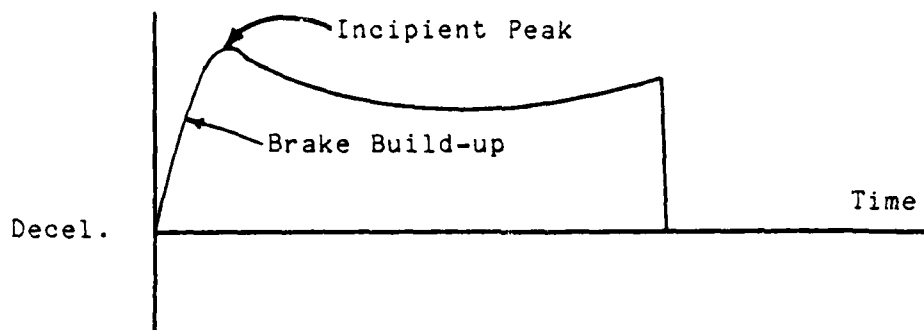


Figure 1.2 Typical Deceleration Curve for an Automobile Skid Test

of the analytical accident reconstruction.

The coefficient of friction,  $\mu$  is a function of many variables which affect the tire-road surface interface. These variables include, but are not limited to:

1. Speed [1,2,4,5,6,7,8,9,10,11],
2. Tire construction and materials  
[1,2,5,7,9,10,12,13,14,15],
3. Vehicle suspension and geometry conditions  
[1,5,7,16],
4. Vehicle mass [1,5,7,10,12,16],
5. Ambient conditions [1,8,16],
6. Tire temperature [1,8,10,12,16,17,18,19],
7. Tire inflation pressure [10,18],
8. Road surface roughness  
[1,2,7,9,10,12,15,17,18,20,21], and



#### 9. Road contaminants [1,2,12].

These variables for a particular accident or test site can be grouped according to how they affect the test procedure and results. Group "A" variables are "site" specific and are not considered functions of vehicle speed. Group "A" variables include ambient conditions, tire temperature, tire pressure, road surface roughness and road contaminants. This group is set at the time of the accident. Group "B" variables include the vehicle's mass, the vehicle's suspension and geometric conditions, tire construction, and tire materials. These variables also affect  $\mu$  but are not site specific. Group "B" may change, however, as the suspension system parts wear. As a result, these variables are also established at the time of the accident. Group "B" variables are considered "vehicle" parameters, whereas Group "A" variables are considered "site" parameters. The Group "C" variable, vehicle speed, is the only one that is directly controlled by the driver and is not part of the vehicle or site. It is, however, the variable which ultimately is to be determined from the skid length measurements and the coefficient of friction.

The goal of this research is to show how the different variables influence the coefficient of friction and then to develop an accurate and consistent method of

obtaining an instantaneous  $\mu$  during a locked-wheel or yaw skid, recording that information and using it to reconstruct the vehicle dynamics. A transducer has previously been developed which will accurately convert the deceleration into an electrical signal [22]. This research will use the previously developed and tested accelerometer and will expand on the system by developing a dependable method of recording, analyzing, and verifying the data from the accelerometer.

This system will provide the engineer with an extremely useful tool for motor vehicle accident reconstruction. It is not limited to the accident reconstruction area, however. For example, slippery road surfaces could be identified and evaluated before accidents happen or runway surfaces could be evaluated to determine if rubber or other contaminant removal procedures should be initiated.

## CHAPTER II

### SYSTEM DESIGN REQUIREMENTS

The coefficient of friction at the tire-road interface is a complex phenomenon. An accelerometer has been designed and constructed to measure this phenomenon [22] but it is necessary to understand the mechanisms of tire friction before the operation of the accelerometer can be fully understood. This chapter discusses the mechanisms of tire friction and the various methods of measuring and recording continuous values of  $\mu$  and distance throughout the duration of a locked-wheel skid.

#### The Coefficient of Friction

The physics of the tire-road friction at this point in time is not completely understood. This is primarily a result of the lack of test equipment sophisticated enough to accurately measure and record the data and then to evaluate the data. Numerous methods have been used in the past to measure and record  $\mu$  but none have truly been able to accurately represent this phenomenon. This is partly because the total coefficient of friction is influenced by many variables which are impossible to isolate from the whole. The Society of Automotive Engineers (SAE) defines eleven kinematic and geometric variables that completely describe the steady state motion and orientation of the

tire to the road [16]. When these variables are added to the list of variables discussed in Chapter I, it is easy to see how complex the phenomenon of tire traction really is.

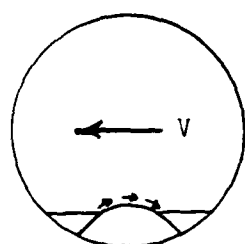
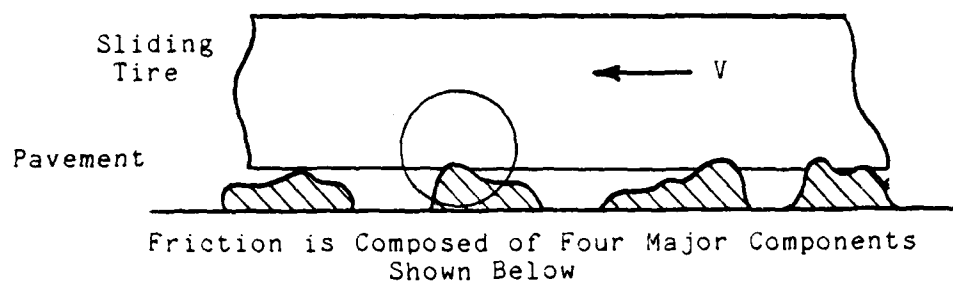
There are four basic elements which contribute to the total coefficient of friction: adhesion, deformation, tearing, and wear [1,9,14,17,18]. Adhesion results from the molecular attraction between the tire and the road surface asperities. It is considered a static property because it is not a function of the relative motion of the pavement and the tire. Adhesion is a property which follows the definition of Coulomb friction in which the frictional force is a function of  $\mu$  and the normal force, but is not a function of the contact area [23]. During a skid, the temperature increase of the tire-road contact surface results from adhesion.

Also during sliding, the rubber deforms at the macroscopic tire to road surface asperity and tends to wrap around the asperity in a direction opposite the direction of the skid. This deformation contributes to  $\mu$  because it takes more energy to deform the rubber than is regained when the rubber returns to the undeformed state. This process is called hysteresis. Modulus is another property of rubber that contributes to the overall coefficient of friction. It is a measure of the hardness of the rubber and reflects the ease in which it deforms. Most

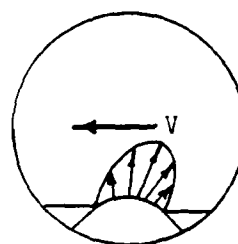
automobile tires today use synthetic rubber which has a relatively lower modulus than natural rubber, of which most truck or severe service tires are made. The lower the modulus, the easier the rubber deforms around the asperity resulting in a higher  $\mu$  but at a sacrifice to the wear characteristics [14]. The deformation of the rubber results in a heat build-up beneath the tire contact surface.

Tearing and wear are both associated with abrasion. These factors are functions of the tensile and shear strengths of the tire material. A higher tensile strength will result in higher abrasive friction, assuming all other variables remain unchanged. The distinction between tearing and wear lies in the fact that wear results in the formation of loose wear particles and therefore, material loss while in tearing the material remains attached.

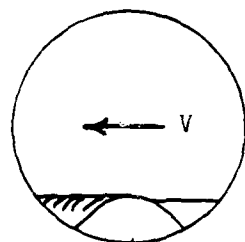
The four basic factors which affect tire friction are pictorially represented in Figure 2.1. "Experts" in the tire friction area concur that these four basic factors combine to form the total coefficient of friction but the agreement stops there. There is little agreement on how each of the factors contributes to the overall  $\mu$  or how the physical variables (speed, temperature, road contaminants, etc.) affect the contribution of the four factors. Some "experts" claim that 80 percent of the total  $\mu$  is caused by adhesion [9], while others claim that friction is an



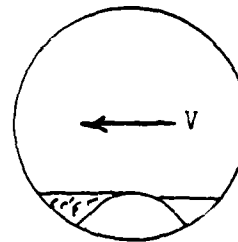
Adhesion



Deformation



Tearing



Wear

Figure 2.1 The Four Major Components of Tire-Pavement Friction [14]

energy-dissipating process and only through hysteresis can energy be dissipated [9,12]. A third view of the tire-road surface friction process is that adhesion is the main component of  $\mu$  at low speeds while deformation, tearing, and wear occur at high relative velocities [17]. This theory is graphically represented in Figure 2.2. The curve shows how  $\mu$  changes as slipping increases from no skidding to 100 percent skidding depending on whether the primary component is adhesion, deformation, tearing, or wear. Curve ABC depicts  $\mu$  as a function of pure adhesion and curve FDE depicts  $\mu$  as a function of deformation, tearing, and wear. In this case,  $\mu$  is a function of vehicle velocity. Neither curves ABC or FDE occur in actual automobile skids but a combination of the two, curve ABGDE, does. The value of  $\mu$  is limited to the lower value because the lower  $\mu$  dominates in the friction process. The peak of the ABGDE curve at G never reaches the intersection of ABC and FDE; this is because BGD is considered the transition region between the curves ABC and FDE.

The tire-to-road frictional interaction is complex in itself, but when additional variables such as speed, temperature, etc. are considered the measurement of  $\mu$  becomes an exhaustive task. Numerous studies have been made to determine  $\mu$  using various methods in laboratory and field environments. These studies are at first more

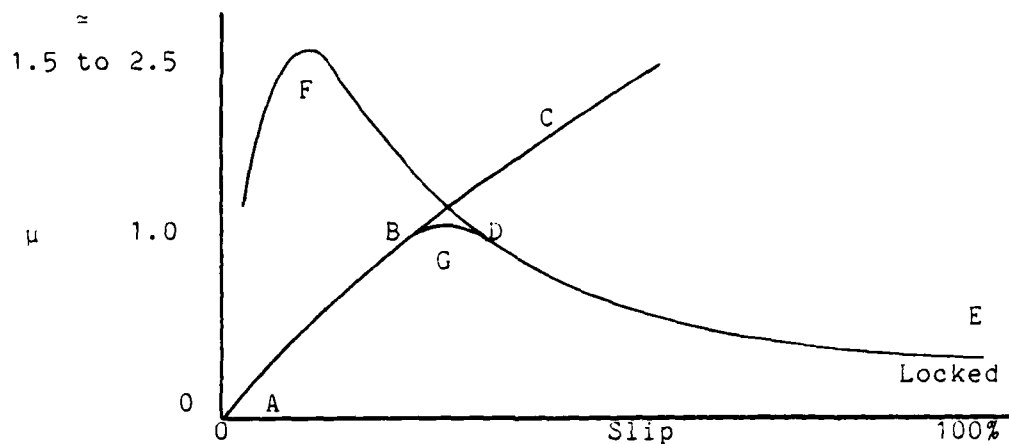


Figure 2.2 Braking Force Due to Adhesion and Skidding Effects as a Function of Tire Slip [17]

confusing than informative to a student studying tire friction, because the results are usually contradictory without close examination. With further study, the differences in test procedures become apparent. The compared goals, data, methods, and results are different in most cases. Therefore, subject tests often can not be effectively compared with others. Some of the disagreements between "experts" in this field result from non-uniform test procedures. For example, Grough [17] states:

Most laboratory measurements of friction of various rubbers or polymer blends have been made under steady state sliding at low speeds. It is commonly noted that initial values are



lower than at final steady state; or put another way, movement between rubber and ground is necessary to achieve maximum friction pertinent to the materials and operating conditions.

While Meyer and Kummer [19] state, "As sliding speed is increased friction decreases, but eventually increases again." These two tests can not be compared without realizing that in reference [17], the sliding speeds were low but not specifically explained; whereas, reference [19] specifically explains that sliding velocities were less than one foot per second. The friction in reference [17] may have involved deformation, tearing, and wear, where reference [19] probably involved mostly adhesion.

There is general agreement, however, in the belief that most of the energy dissipated in a locked-wheel skid is through heat generation and loss of the heat to the road surface and tire. Grosch [8] explains in detail the relationship between different test conditions and the amount of heat build-up in rubber and compares them with standard empirical equations. The relationships between temperature and heat transfer for a skidding vehicle partially explains why laboratory and field friction tests rarely produce similar values of  $\mu$ .

With the complexities of the frictional components

not being completely understood, determination of the "correct" method to measure  $\mu$  is difficult if not impossible, but it is reasonable to assume that duplication of as many of the variables as possible is the "safest" way to accomplish the task.

#### Measurement Techniques

There have been numerous methods employed to measure the coefficient of friction [1-22,24] but there has been little correlation of the results from one test procedure to another. Some of the most popular methods used in the past are:

1. Specialized laboratory tests;
2. Analytical methods;
3. Pulled trailer skid force methods;
4. Pulled trailer slip angle methods;
5. Automobile length of skid tests;
6. Accelerometers in automobiles;
7. Fifth-wheel automobile skid tests;
8. Automobile dynamometer tests;
9. Specially instrumented automobile and automobile test models; and
10. Photographic test procedures.

The reasons for performing these tests are as varied as the different procedures themselves. The most prevalent reason has been to compare the coefficient of

friction from one road surface to another and to compare  $\mu$  on the same road surface under different atmospheric conditions. Very little has been done in determining  $\mu$  for the purposes of automobile accident reconstruction. Each of the above methods were evaluated prior to deciding the best method for determining  $\mu$  for this application.

Specialized laboratory tests display the broadest range of  $\mu$ . The types of tests that have been devised are numerous [5,8,9,16,17]. While the laboratory environment provides the best control of variables which are uncontrollable in a field test, the laboratory does not have the inputs from the test site which are important in the accident reconstruction area. Laboratory tests have measured  $\mu$  as high as 3 for rubber materials similar to those used in automobile tires [8], but a  $\mu$  this high at a test site is extremely unrealistic. For these reasons, laboratory tests have been ruled out as a method for measuring  $\mu$  for this research.

Analytical methods [8,12,16,17,20], by themselves, suffer within the context of this research because they have no way to accurately account for many "real world" variables which are prime considerations in accident reconstruction.

The pulled trailer skid test method is one of the most popular techniques for measuring the coefficient of

friction on various road surfaces [5,7,21]. The procedure utilizes a vehicle to pull a trailer which has one or more tires locked. The force required to pull the trailer is measured at the trailer tongue by a load cell. This force is proportional to the coefficient of friction by a factor of the tire loading. Many variations to the basic trailer method have been devised. These variations include different ways to load and lock the trailer's tire(s), various sensing devices, and general construction of the trailer. Some trailers are also equipped to measure the "incipient force" (friction force just prior to lock-up). During testing, the trailers are usually pulled at a constant speed. The tow vehicle can also be equipped with a water storage tank and a wetting system for making tests on wet pavement.

Pulled trailer slip angle force testers are very similar to the trailer skid force testers except that the trailer's tire(s) are positioned such that the longitudinal axis of the tire-wheel assembly is at an angle (called the slip angle) to the direction of the trailer motion. Figure 2.3 pictorially describes the slip angle. Most trailers are designed such that the slip angle can be changed.

The advantages of the trailer methods are that specialized test equipment can be incorporated into the trailers and that the trailers can be towed at a constant

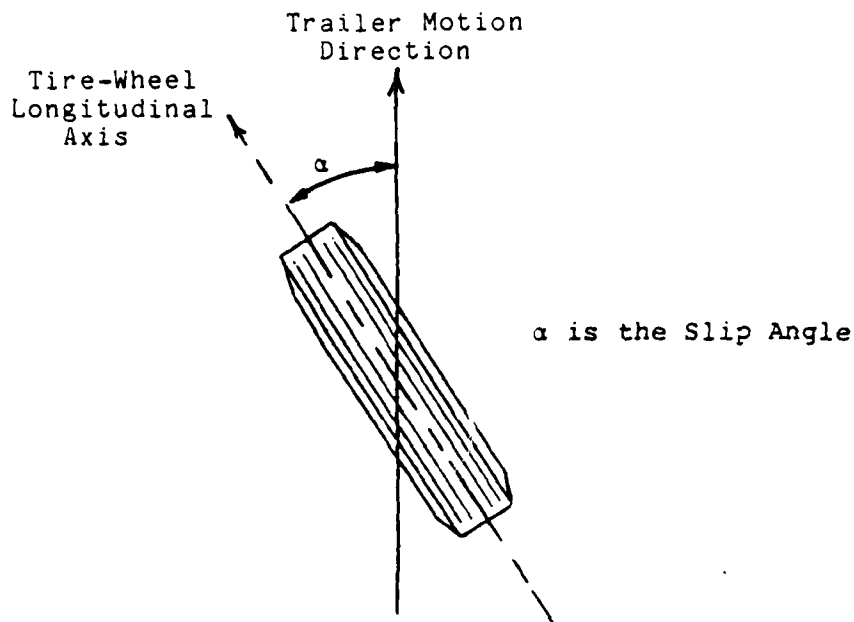


Figure 2.3 Slip Angle

speed. Therefore, testing can be performed without significantly disrupting traffic flow. The disadvantages of the trailers are that they are large, expensive, usually require a specialized tow vehicle, and have dynamic characteristics different from the automobile. Additionally, correlation of data between trailer testing methods has been poor [7]. Due partly to the fact that the skid trailer does not reproduce many of the variables in the vehicle skid, this method has also been ruled out.

The automobile length of skid test method [2,4,5,6,7,15] was described in detail in Chapter I. This

method involves skidding an automobile from a known velocity to a stop and measuring the skid length. The initial speed (V) and the skid length (s) are used in the equation:

$$\mu = V^2 / 2gs$$

to find the average coefficient of friction ( $\mu$ ). The advantages of this type of test are that it requires very little equipment, it is simple to perform, measure and calculate the results, and, most importantly, it can closely approximate the actual skid variables, especially if a similar vehicle and tires are used. The disadvantages arise from the inaccuracies of observing the initial speed, determining the initial skid location, and from the fact that the calculated  $\mu$  is only an average value for speeds from the initial velocity to zero. Very little additional information is available from the length of skid test method. This method is also ruled out for the purposes of motor vehicle accident reconstruction in this research, although it is the basic method for obtaining  $\mu$  for this purpose.

Instrumenting an automobile with an accelerometer for measuring deceleration during skid tests [2,4,5,6] has all the advantages of the length-of-skid tests and also gives the instantaneous  $\mu$  over the skid duration. Therefore, an accurate measurement of the skid length and

initial velocity are no longer required. Instantaneous values of velocity and distance can also be obtained by successive integrations of the acceleration versus time data. With the accelerometer calibrated in g's, the acceleration is equal to  $\mu$ . As described in Chapter I, the classical definition of friction force (Eqn. 5) is:

$$F = \mu N$$

where

$F$  is the friction force;

$\mu$  is the coefficient of dynamic friction; and

$N$  is the normal force between the two subject objects.

Additionally, from Newton's Second Law (Eqn. 6), a force ( $F$ ) is equal to a mass ( $m$ ) under acceleration ( $a$ ):

$$F = ma$$

When the vehicle under the influence of a 1 g gravitational attraction, the normal force is:

$$N = m(1g)$$

$$= w$$

(10)

where  $w$  is the total weight of the vehicle. Combining Equations 5, 6, and 10 yields:

$$\mu w = ma$$

or,

$$\mu = a/g$$

where  $\mu$  is dimensionless. The disadvantages of the

automobile length - of - skid test method using an accelerometer are that it is more costly than automobile length-of-skid tests and that it requires a knowledge of the instrumentation.

Fifth-wheel input to automobile skid tests [5] can make additional information available. The exact skid length can be measured at the time the skid is occurring and it can be used to verify the data from the double integration of the accelerometer data. The disadvantages of a fifth-wheel are mainly the added cost, the required operator knowledge, and the additional equipment. Another disadvantage to the fifth-wheel device is the difficulty in attaching it to the test vehicle. The fifth-wheel should be used cautiously without an accelerometer, however, because of the difficulty in the numerical differentiation of the data to obtain the velocity and acceleration information.

Automobile dynamometers are often used to measure and compare tractive forces of various tires [16], but are of little use for accident reconstruction data acquisition at a test site.

Specially instrumented automobiles [5,24] can be used to gather almost any kind of data desired about the physical phenomenon occurring in an automobile during skids. Photographic analysis can also be incorporated into



this category. More data can be made available for the analytical reconstruction of an accident using these two techniques, but cost prohibits them from being used beyond the extent of an accelerometer in the test vehicle.

In Chapter I, three categories of variables that affect  $\mu$  were described. They were Category "A" (site), Category "B" (vehicle), and Category "C" (vehicle controlled) variables. From the previous discussion of tire traction, it becomes understandable how many of the physical interactions which take place at the tire-road interface remain mysteries to us, especially when the above variables are included. To insure accurate reproduction of the skid which took place prior to a collision, it is necessary to duplicate as closely as possible the variables which were present at the time of the skid. Category "A" variables are duplicated by performing a controlled skid test as soon as possible after the accident in question (or at least before the weather conditions change). Category "B" variables differences are reproduced as closely as possible by using a similar, if not identical, vehicle with similar or like tires as the one(s) involved in the collision. Since all vehicles have mechanical characteristics which vary from one vehicle to another, it is important to understand some of the variables that affect stopping distance and the maximum error that can result from them.

Although by no means complete, the published literature of previous testing indicates the following factors which affect the tire-road friction and measurement testing:

1. The dynamic characteristics and geometric parameters of different vehicles influence tire-road skidding behavior [1,2,4,7].
2. Tire design characteristics (structural and material) affect skid performance [1,2,7,8,9, 10,13,14,15,16,17].
3. Driver input to vehicle affects stopping distance with all other variables remaining constant [1,2,4,10].
4. Load on a tire and tire inflation pressure have a slight influence on skid performance [1,7,10,12,13,16].
5. Vehicle speed affects skid performance [2,5,6, 7,8,10].
6. The maximum variation of  $\mu$  as a result of the automobile variables is approximately 10 percent. This value can be significantly reduced by choosing a test vehicle of similar construction and with similar tires to the accident vehicle [7].

The last variable, speed, is unknown and is the

variable which is to be determined by performing the analysis of  $\mu$ . Performing a skid test in a similar vehicle with similar tires as soon as possible after the accident can duplicate the unknown variables and provide  $\mu(t)$  consistent with performing an accurate analysis of vehicle dynamics.

The published results of previous tests indicate that road surface characteristics have the single greatest effect on variations in the measured coefficient of friction for automobile skid tests [4]. For this reason, as well as equipment size, ease of operation, cost, repeatability, reliability, and adaptability, a portable accelerometer transducer was chosen as the most suitable for the purpose of automobile skid tests.

An accelerometer for this exact purpose was designed and built by Mr. Scott Reid [22]. The accelerometer consists of a small, vertically oriented cantilever beam with a mass attached to the free end and a strain gage bridge mounted near the fixed end. The simplicity, small size and mass, low cost, and reliability were key considerations for deciding to continue with this type of accelerometer.

The accelerometer, however, is of no use by itself. There must be a method of recording the instantaneous values of acceleration over the entire skid duration so

that the data can be integrated to acquire the velocity and distance versus time data.

There are numerous ways in which this recording and analysis can be accomplished. For example:

1. Manual observation and recording;
2. High speed photographic methods;
3. Hard copy real time plotting;
4. Recording oscilloscope and photographic techniques;
5. Real time magnetic tape recording of transducer output; and
6. Computerized data acquisition, storage, and transfer.

Manual observations were eliminated from consideration because of the speed at which the acceleration changes during the skid process. It would be humanly impossible to record all the necessary data.

High speed photographic recording of the accelerometer output would be an accurate and permanent record of the skid process especially if a timing device were included in the photographs. The difficulty lies in the analysis of the data once it is obtained. Manual graphing or digitization and integration would be required which is, at best, tedious and time consuming. The expense involved for equipment and film and the inherent inaccuracies of

manual integration prohibit this method from being used in this work.

Hard copy real time plotting, real time magnetic tape recording and the recording oscilloscope and photographic techniques are also accurate ways of recording the output from the accelerometer but as in the photographic method, manual integration of the data would be necessary. Numerical integration techniques by computer could be used in these methods but the data must first be digitized. The inherent inaccuracies of these methods also prohibit them from being used in this work.

Computerized data acquisition, storage, and transfer methods can be adapted for this purpose. The ability of a microprocessor to make thousands of samples of data per second from numerous sources and to store the data in a retrievable memory makes this system ideal for the purpose of automobile accident reconstruction. This system also has the capability of transferring the data in memory to a more permanent type of storage device, like a magnetic recording tape. Once the data is permanently stored on the tape, the computer and memory are free to record the data from another skid test. The recording tape can transfer the same data into another computer at a laboratory for analysis and evaluation. All this can be accomplished without human interpretation of or interaction with the

data. There are some drawbacks to this method, however. The complexities of microcomputers requires a knowledge of microcomputer programming to make the system work, but once the system works correctly it can be operated by anyone with a basic understanding of computers. The added cost is also a drawback but the accuracies gained by this method far outweigh the extra cost. There also must be computer equipment available to perform the analysis of the data once it is collected, but this is true in all of the above methods if any accuracy is to be expected at all. For the above reasons, a microcomputer data acquisition, storage, and transfer system was selected as the best method for the purpose of motor vehicle accident reconstruction.

To verify the results of the numerical integration of the accelerometer data, a fifth-wheel tachometer is also added to the total system. The microcomputer can then store the elapsed distance as a function of time from the instant an external interrupt is triggered.

### CHAPTER III

#### Microcomputer and Fifth-Wheel Design and Developement and Accelerometer Incorporation

##### Accelerometer

The accelerometer designed by Reid [22] is a vertically oriented cantilever beam with a small mass mounted at the free end and a temperature compensated strain gage bridge mounted approximately three quarters of an inch from the fixed end. Constructed of standard spring steel stock 0.020 inches thick, it is three inches long by one half inch wide with a 0.028 pound mass at the free end. With the beam oriented horizontally, the mass will cause a deflection of 0.025 inches under the influence of a one-g gravitational field. To insure that the spring steel would not be overstressed, the maximum stress at the fixed end was calculated at 2523 pounds per square inch, well within the maximum stress for spring steel of 58,000 pounds per square inch.

The undamped natural frequency was also calculated to determine if any undesired resonances would be excited during testing. The calculated frequency, 19.8 cycles per second, is very close to the natural frequency of the automobile suspension (10 to 15 cycles/sec) and decreasing the mass to increase the natural frequency would cause an

undesirably low deflection and a smaller strain gage output. To reduce the chances that the automobile frequencies will cause the undesired vibrations in the beam, a damper system was used to modify the beam dynamic response.

The damper consists of a friction lever arm connected to the mass by a link. By varying the tension on the spring which presses the lever arm between two washers, the amount of damping can be adjusted. A Hewlett-Packard Model 5423A Structural Dynamics Analyzer was used to analyze the beam, mass, and damper shown in Figure 3.1. The first resonant frequency for the undamped system (damper, link, and lever arm removed), was 19.4 cycles/sec, which is very close to the predicted frequency. For the undamped system, the damping ratio (percent of critical damping) is 1.9 percent, and the time constant (time for the system to damp motion to  $1/e$  times its original displacement) is 0.428 seconds. Figure 3.2 shows the response of the undamped system and Figure 3.3 shows the system's response with varying amounts of damping. The plot in Figure 3.3 with the lowest peak is representative of the damper setting that allowed the best output from the completed system in actual skid tests. As the amount of damping increases by tightening the damper pivot nut, the damping ratio is increased and the time constant is decreased. Table 3.1 lists the resonant frequency, damping ratio, and



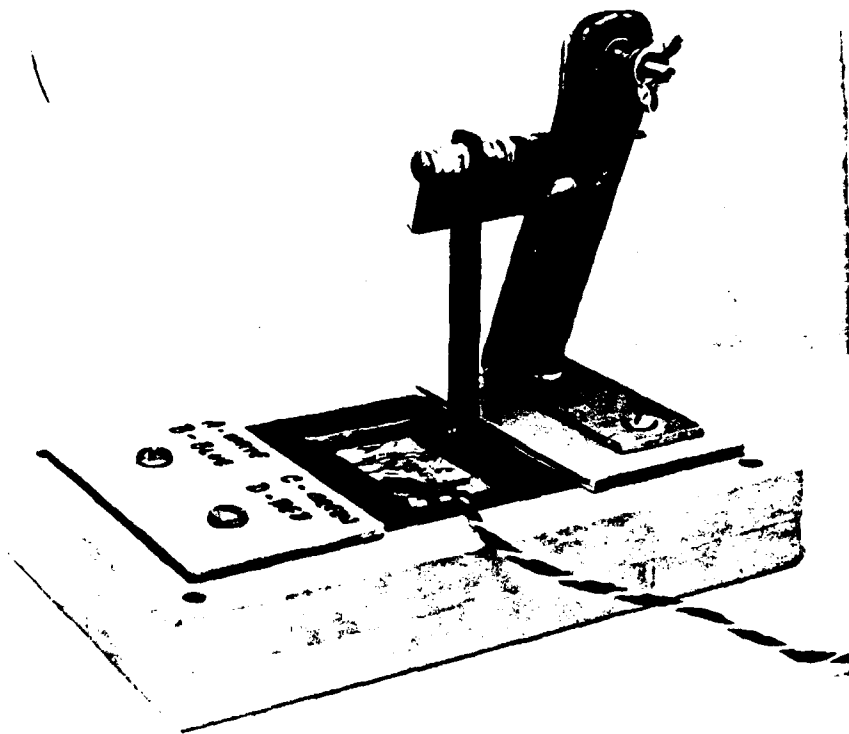


Figure 3.1 Spring, Mass, Damper, Limiter Arm and Strain Gage Accelerometer

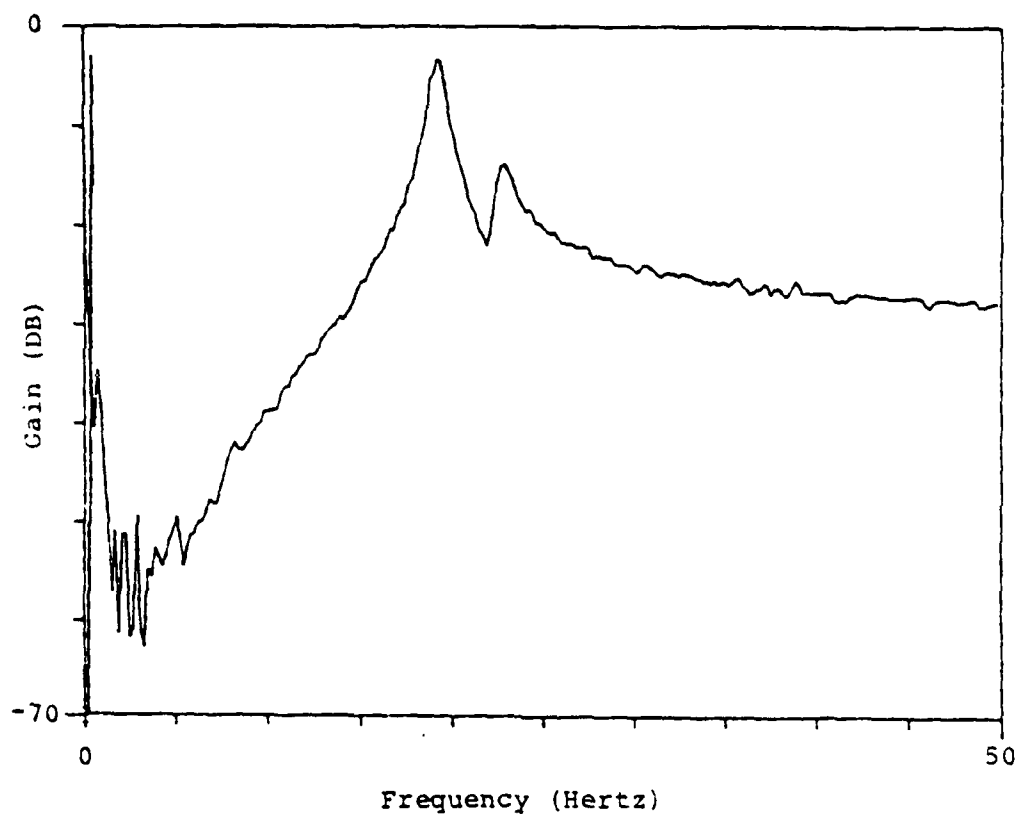


Figure 3.2 Transfer Function of the Undamped Accelerometer  
Showing the First Resonant Frequency [22]

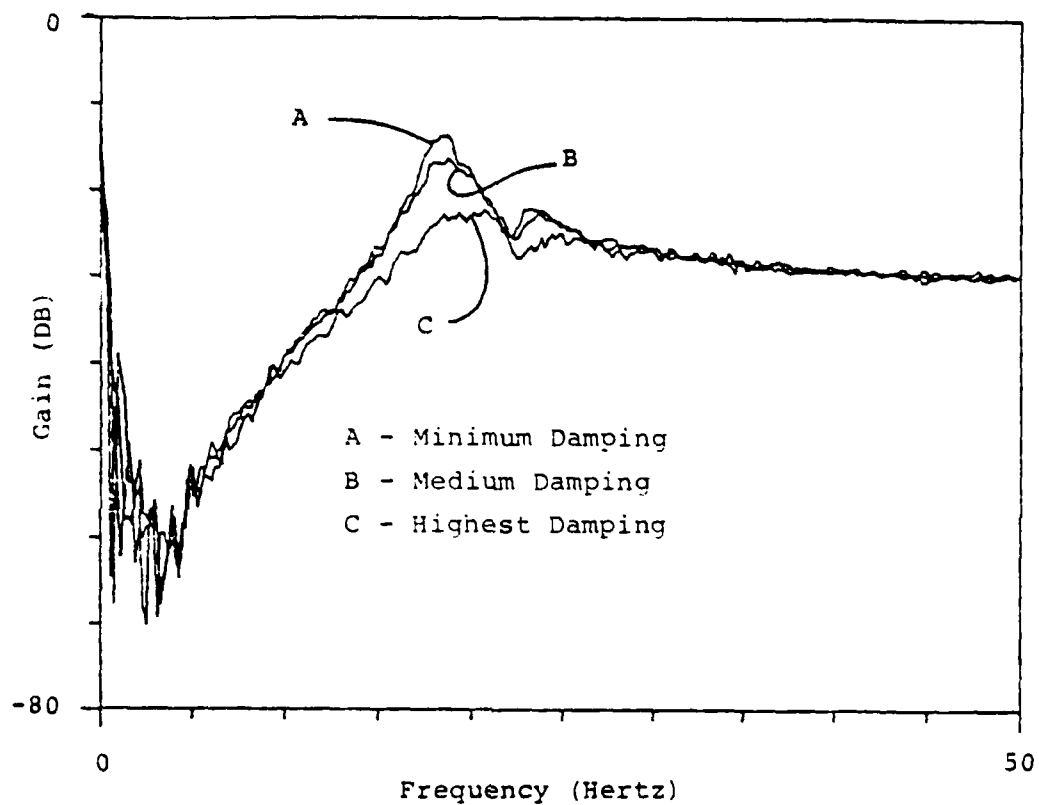


Figure 3.3 Transfer Function of Lightly Damped Accelerometer Showing First Resonant Frequency [22]

SYSTEM	FREQUENCY (HERTZ)	DAMPING RATIO (PERCENT)	TIME CONSTANT (SECONDS)
Undamped	19.14	1.9	0.428
Minimum Damping(A)*	18.39	5.5	0.156
Medium Damping(B)*	18.51	7.6	0.113
Highest Damping(C)*	19.27	13.5	0.061

\*A, B, and C refer to Figure 3.3

Table 3.1 First Resonant Frequency, Damping Ratio, and Time Constant for Undamped and Lightly Damped System [22]

time constant for the undamped system (from Figure 3.2) and for the three settings of the damper system (from Figure 3.3). Although the first natural frequency can be damped so that unwanted oscillations do not confound the test data during tests, no usable information with frequencies near or above 19 cycles/sec can be obtained from the accelerometer.

The limiter arm, also shown in Figure 3.1, was installed to prevent the beam from being overstressed during testing and handling.

The cantilever beam spring-mass-damper system was combined with strain gages to become the accelerometer. Four matched, foil-type strain gages were attached to the beam and were connected to act as a temperature compensated wheatstone bridge. Micro-Measurements type EA-06-125BT-120 strain gages were used, each with a nominal resistance of 120 ohms. An electrical circuit was designed and incorporated onto the main computer board to provide the strain gage bridge with an input voltage and to amplify the output by a factor of 1000. The strain gage bridge is not perfectly balanced so the output from the strain gages, after amplification, is a constant of approximately 0.2 volts (beam undeflected). With an amplification factor of this magnitude it proved difficult to find four strain gages which were perfectly matched. When the beam is

deflected by the mass under one-g, the strain gages produce an amplified output of approximately four volts.

The amplified strain gage output is fed into an 8 bit analog-to-digital (A/D) converter which has an input voltage range from zero to five volts. The A/D converter converts the analog voltage to a digital code which is proportional to the analog voltage on a decimal scale of 0 to 255 or a hexadecimal scale from 0 to FF. During the Calibration and Execution phases of operation, the output of the A/D converter is sampled by the microprocessor.

#### Microcomputer

The microcomputer, designed and built by Mr. Grover Edmiston, consists of the following main components:

1. An 8085 based microprocessor manufactured by Intel Corp.;
2. 2 each No. 2516 Texas Instruments 2 K Erasable Programmable Read Only Memory (EPROM) Units;
3. 4 each 1 K No. MK4118A-4 Mostek Random Access Memory (RAM) units;
4. A hexadecimal keypad, a 6 digit hexadecimal display panel, and an Intel Corp. No. 8279 Programmable Keyboard/Display Interface module;
5. An Intel Corp. No. 8253 Programmable Interval Timer;
6. An Analog Devices No. AD7574 8 bit Analog-to-

Digital Converter; and

7. An Analog Devices No. AD521KD Instrumentation Amplifier.

Figure 3.4 is a block diagram of the computer board which shows the interconnection of the components and the connection to the accelerometer and the fifth-wheel. Figure 3.5 shows the actual accelerometer and microcomputer unit.

The microprocessor is programmed to perform various operations which are written in 8085 assembly language [25] and stored in the EPROM. It automatically begins processing the instructions contained in the EPROM starting at memory location 0000 when the power is turned on or when the reset button is pressed. The exact programming procedures used in assembly language are of an extensive and detailed nature and therefore, beyond the scope of description in this thesis.

The Intel 8085 microprocessor was used in this application because of the speed at which it can operate. It is driven by a 6.144 megahertz clock in this system. The 6.144 MHz signal is internally divided by two to clock the actual execution processes within the microprocessor. The different executable instructions require varying numbers of clock cycles depending on the complexity of the instructions. On the average, instructions take

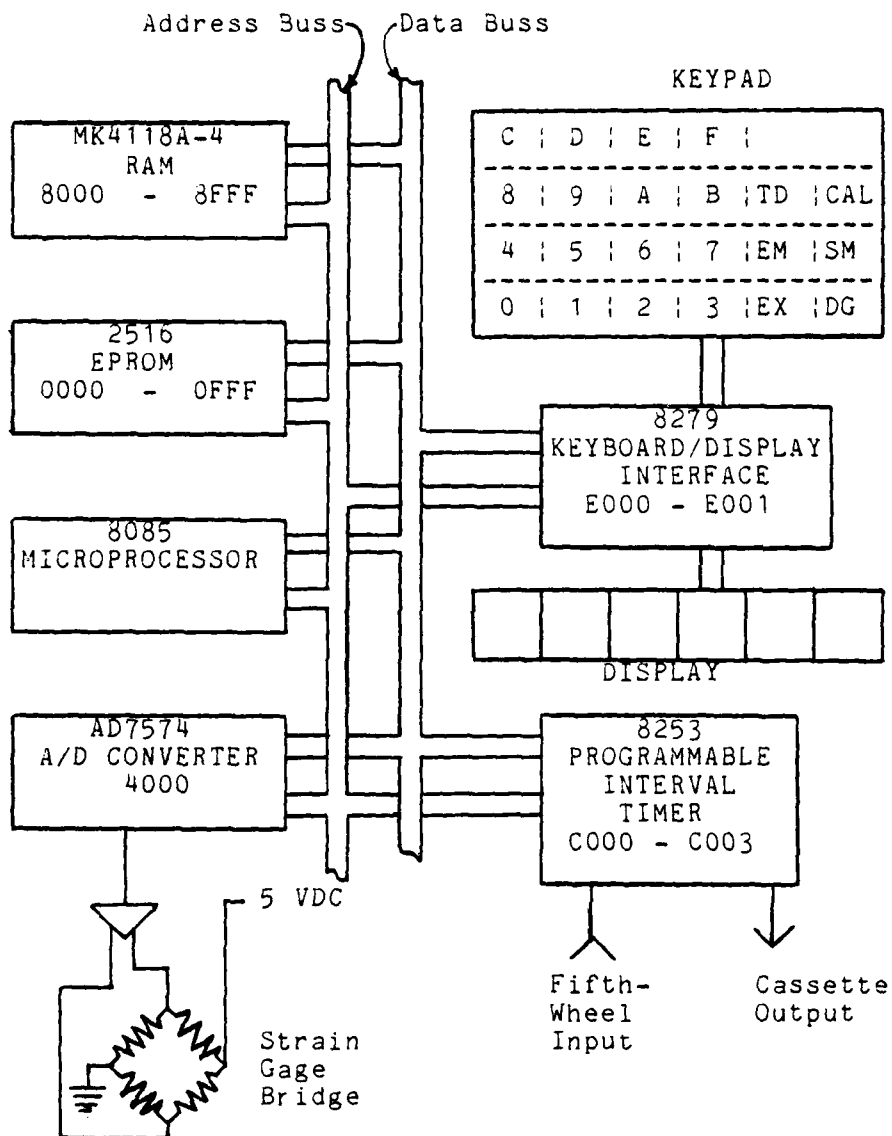


Figure 3.4 Block Diagram of Computer Board and Accelerometer and Fifth-Wheel Interconnection



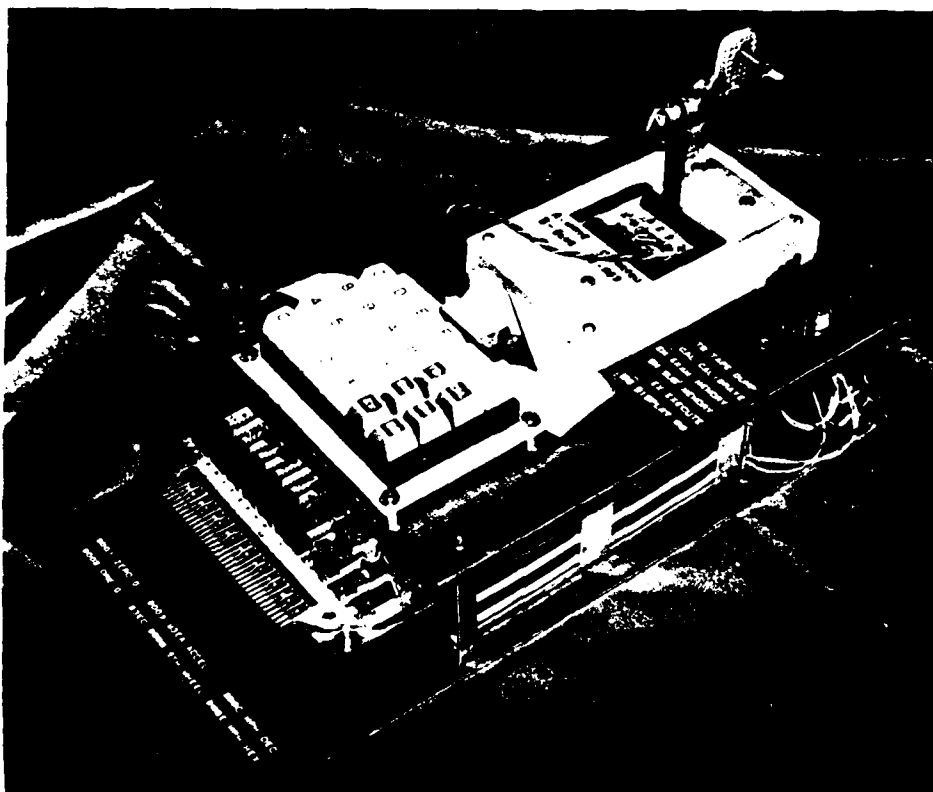


Figure 3.5 Accelerometer and Microcomputer Unit

approximately 10 clock cycles to be executed. With a 3.072 MHz clock, the microprocessor completes approximately 300,000 instructions per second, making it ideal for the high speed data acquisition which is required for this application.

The main functions of the microprocessor in this application are as follows:

1. To program and communicate with the 8279 Keyboard/Display Interface module;
2. To program and communicate with the 8253 Programmable Interval Timer;
3. To sample the data from the A/D converter; and
4. To store the data in the RAM.

The function of the EPROM is to provide non-volatile storage for the executable code. The information stored in the EPROM is not lost when the power is turned off so the microprocessor will always operate when the power is turned on.

The Random Access Memory (RAM) consists of 4 K of 8 bit words. Its primary purpose is to store the data from the accelerometer A/D converter, and the fifth-wheel count provided by the Programmable Interval Timer(PIT). The contents of the RAM can be read by the microprocessor or written over by it. Since the RAM is volatile, its con-

tents must be stored on tape before the power is turned off or before another test is run.

The hexadecimal keypad, hexadecimal display panel, and the Keyboard/Display Interface module provide the operator with a means of controlling the operation of and communication with the microprocessor.

The keypad has 22 keys which perform the following functions:

1. 0 - F hexadecimal number keys;
2. TD Taped Dump;
3. CAL Calibrate;
4. EM Examine Memory;
5. SM Substitute Memory;
6. EX Execute; and
7. DG Display G's.

The TD, CAL, EX, and DG keys will be discussed in detail later in this chapter.

The keyboard/display system allows the operator to examine the contents of any memory location and to deposit into any RAM location data that he or she desires. Upon pressing the hardware reset button on the computer board the display will automatically show memory location 8000 in the left four digits and its contents in the right two digits. The contents of 8000 are automatically set at FB (hex) by the reset routine to mark the beginning of data.

This flag will be used during the tape read operation. If the EM key is pressed, the address is automatically incremented by one and the contents of that location are automatically displayed. Any memory location can be accessed by entering the address using the 0 - F keys (most significant digits first) and its contents will be displayed. If the operator wishes to enter his or her own data into RAM, he or she can enter the address as above, press the SM key, and then enter the data. The data will then be in RAM at that location.

The Programmable Interval Timer (PIT) has three individually programmable 16 bit counters, each of which can operate independently and in various modes depending on the requirements of the main program and the application. Programming the PIT is accomplished through addresses C000 through C003. Addresses C000 through C002 are used to pass data between the microprocessor and counters 0, 1, and 2 and C003 is used to pass programming information to the PIT (See Figure 3.6, Memory Map).

The PIT in this application has two primary functions. First, it produces the required frequencies used in the Tape Dump routine for converting the bit values in the data words to Kansas City Standard data transmission format (see Tape Dump routine in the next section). Second, it acts as a counter for keeping track of the number of pulses

produced by the fifth-wheel device for conversion to distance and miles per hour (see Execute routine).

The AD7574 8 bit Analog-to-Digital Converter and the AD521KD Instrumentation Amplifier combine to amplify the signal from the strain gage bridge on the accelerometer and to convert the amplified output to a digital code. The amplifier raises the output voltage from the accelerometer from 0 to 5 millivolts to 0 to 5 volts, an amplification factor of 1000. The A/D converter then converts the 0 to 5 volts to an 8 bit binary code which is read by the microprocessor during the Execute routine and during the Calibrate routine. The binary code is converted to hexadecimal code for display on the 6 digit display panel. The range of the A/D converter is from 00 to FF (hex).

#### Computer Mode Operations

The first executable routine which the microprocessor must perform is the Reset routine. The primary function of the Reset routine is to initialize all the peripheral devices so communication with them will be possible. The Keyboard/Display Interface module must be programmed to receive data from the keypad and microprocessor and to transmit data to the display panel. Communication with the Keyboard/Display Interface is accomplished through memory locations E000 (data) and E001 (command) which are addressable by the microprocessor. The Reset routine also

initializes the PIT to set the modes and counts of the three individual counters within the PIT. Certain key memory locations are also initialized to specific values during the Reset routine. Figure 3.6 is a memory map of the memory used in this microcomputer. Memory locations in Figure 3.7 (RAM Memory Map) highlighted by an asterisk(\*) are those which are initialized by the Reset routine. After the Reset routine has been completed, the microprocessor is ready to accept instructions and to perform the operations required by the operator.

#### Calibration

During a locked-wheel skid, the vehicle is decelerating at some time varying rate. This rate of deceleration is determined by the coefficient of friction and by the gravitational field acting on the vehicle creating a normal force on the tires. This relationship allows the accelerometer to be calibrated prior to the tests using gravity as a reference without knowing the effects of any of the unknown parameters discussed in Chapter I.

The strain gage bridge produces a small output when the beam is undeflected. When amplified and coded by the A/D converter, the undeflected reading is called the zero-g output. The one-g accelerometer reading can also be obtained simply by orienting the beam horizontally. This

0000	\	EPROM
--		Operating
0FFF	/	System
1000	\	
--		Not Used
3FFF	/	
4000		A/D Converter
4001	\	
--		Not Used
7FFF	/	
8000	\	
--		RAM (See Figure 3.6)
8FFF	/	
9000	\	
--		Not Used
BFFF	/	
C000	\	
--		PIT
C003	/	
C004	\	
--		Not Used
DFFF	/	
E000	\	
--		Keyboard Display Interface
E001	/	
E002	\	
--		Not Used
FFFF	/	

Figure 3.6 Memory Map

8000* (FB)	Data Beginning Flag
8001	Zero G Location
8002	One G Location
8003	\
--	Accelerometer Data (1000)
83EA	/
83EB* (FF)	Data Division Flag
83EC	\
--	Fifth-Wheel Data (2000)
8BBB	/
8BBC	MPH (decimal)
8BBD (00)	
8BBE	MPH (hex)
8BBF (00)	
8BC0* (FF)	Data End Flag
8BC1* (FF)	Data End Flag
8BC2	\
--	Not Used
8FD7	/
8FD8* (03)	Display G's Start LSB
8FD9* (80)	Display G's Start MSB
8FDA	Not Used
8FDB	Not Used
8FDC* (00)	Tape Start LSB
8FDD* (80)	Tape Start MSB
8FDE* (C2)	Tape Stop LSB
8FDF* (8B)	Tape Stop MSB
8FE0	\
--	Stack
8FFF	/

Figure 3.7 RAM Memory Map



will cause a one-g output from the A/D converter. During an actual skid test, the data from the accelerometer will be proportional to one-g by a factor of  $\mu$ . The coefficient of friction at any point in time can be calculated using the following equation:

$$\mu = (\text{DATA} - \text{Zero g}) / (\text{One g} - \text{Zero g})$$

The calibration procedure involves two steps. The first step is to vertically orient the accelerometer in the the vehicle and press the CAL button. Second, rotate the beam toward the front of the vehicle until the beam passes through horizontal. The computer will sample the accelerometer through the A/D converter every 5 milli-seconds for a period of 10 seconds. The zero-g reading is stored at location 8001 immediately after the CAL button is pressed and the maximum value obtained during the 10 second sampling period will be stored at location 8002 in RAM and is the one-g value.

#### Execution

The Execution operation is the data acquisition phase of the system. Upon pressing the EX (Execute) button, the computer begins to process data from the PIT (Programmable Interval Timer) to calculate the velocity of the vehicle in miles per hour. One of the counters in the PIT is clocked by the output from the fifth-wheel. Every second the counter is reset to zero and, for a one second

duration, the counter counts the number of clock pulses. The number of pulses per second is proportional to the velocity in miles per hour by a factor  $f$ , calculated as follows:

$$f = (9.75" * 2 * 3.1415926) / (12 * 36 * 1.466667) \\ = 1/10.3426$$

where

9.75" is the radius of the 5th-wheel tachometer;

$2 * 3.1415926$  is the conversion of radius to circumference;

12 is the conversion from inches to feet;

36 is the number of clock pulses per revolution;

and

1.466667 is the conversion from ft/sec to MPH.

The speed is continuously displayed and is updated every second. Upon pressing the brake pedal, the speed, in miles per hour, is stored in memory and the data acquisition phase of the execution operation begins.

During the data acquisition phase of the execution operation, the accelerometer and fifth-wheel are sampled at incremental periods of time with the RAM size limiting the number of samples that can be taken during a skid test. One sample of the accelerometer takes one 8 bit memory location while one sample of the fifth-wheel requires two 8 bit memory locations because the counters in the PIT are 16 bit

counters. As a result, three memory locations are required for each sample. There are 4096 RAM locations, so therefore, the maximum number of samples is limited to approximately 1350 leaving 46 locations for computer use storage referred to as Stack. The horizontal resolution of the digital plotter used to plot the data is one one-thousandth of the total width, making more than 1000 sample points unnecessary. For these reasons, a sample number of 1000 was chosen.

A "worst case" skid sample was required to calculate the interval between the sample points. Using a "worst case" of  $\mu$  of 0.5 and a speed of 60 miles per hour, the time to stop a skidding vehicle was calculated at 3.7 seconds. To be safe, a time duration of 5 seconds was chosen. This puts the interval between samples at 5 milliseconds. This time interval is maintained by dividing the microprocessor clock down to a 5 millisecond interval by knowing how many steps are required to perform each instruction in the program between samples and adding in a delay loop to make up the difference.

The combined sampling of the accelerometer and the fifth-wheel make up the data to be evaluated by a computer at the laboratory site. The analysis procedures for the data will be discussed in Chapter IV.

### Tape Dump

The Tape Dump routine is a program which transmits the data contained in RAM onto a cassette tape for permanent storage. The data will then be read into another microcomputer in the laboratory for analysis.

The microcomputer steps through the data stored in RAM and examines each bit in the data word one at a time. The microprocessor then programs the PIT to transmit 8 cycles of a 2400 Hz signal if the bit is a 1, or, 4 cycles of a 1200 Hz signal if the bit is a 0. To create the correct frequency, the PIT divides the 3.072 MHz clock by the appropriate number. This format for data coding and transmitting is called the Kansas City Standard format. The output of the counter is then fed into a cassette recorder's auxiliary input jack for recording. Using this method, the entire RAM contents can be stored on tape in approximately two minutes.

### Display G's

The Display G's routine is a program which will display every tenth accelerometer sample with respect to the zero and one-g calibration values. This allows the operator in the field the ability to examine the skid characteristics immediately after the skid test is completed. The values displayed are in percent of one g and are approximately equal to the coefficient of friction at

that point. Each tenth data point is displayed for approximately one second requiring one and one half minutes to examine the acceleration characteristics.

#### Fifth-Wheel

The fifth-wheel device is constructed from a 20 inch bicycle tire, a plastic wheel, an aluminum frame, and a small electrical circuit. Attached around the edge of the wheel are 36 evenly spaced magnets. An electrical circuit using a Hall Effect switch produces a pulse every time a magnet passes by the Hall Effect switch which is mounted on the frame adjacent to the magnets. This pulse clocks the counter during the Execution phase. The fifth-wheel attaches to the rear bumper of the test vehicle with a set of mounting bolts and is free to rotate about the horizontal axis of the mount to allow for vertical movement. The fifth-wheel is not required in all operations of the micro-computer system and may be deleted altogether in some cases. Figure 3.8 shows the fifth-wheel attached to an automobile.

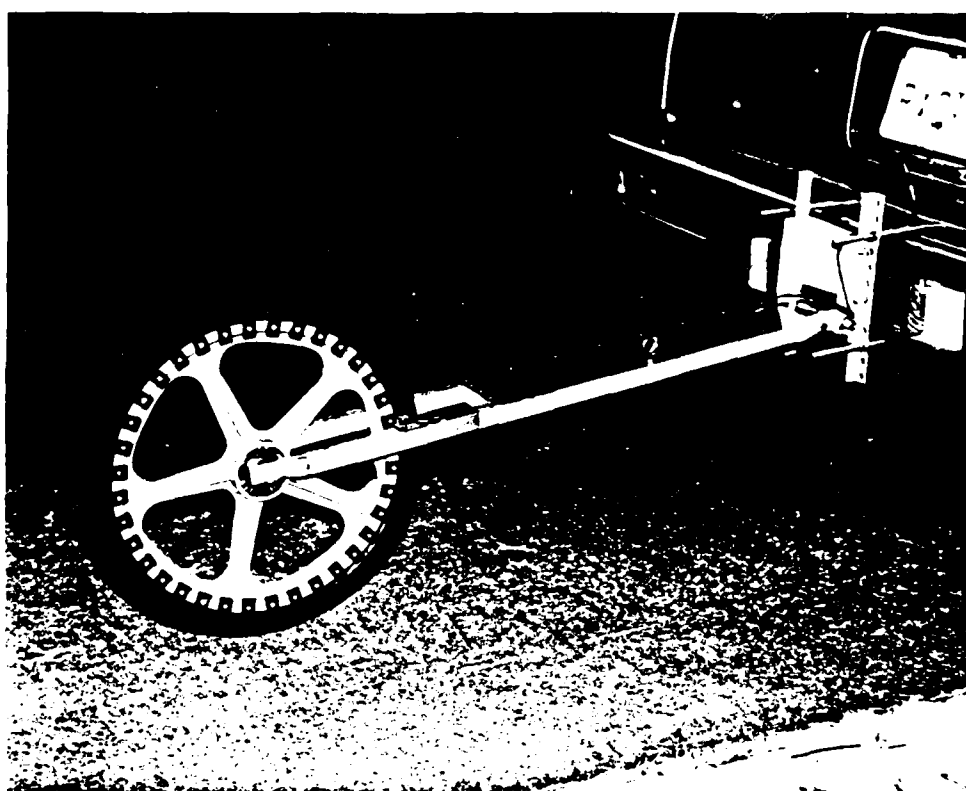


Figure 3.8

Fifth-Wheel

## CHAPTER IV

### System Testing and Data Evaluation

Field tests of the system were conducted at three different locations using two different vehicles. The first two tests were run with the assistance of the Austin Police Department using an APD patrol car. The third test was run with the help of a independent consulting firm using a one ton Ford truck. During the first two test sequences, three people rode in the vehicle: one driver, one person to operate the test device, and one person to monitor the speedometer prior to the skid and to help steady the test equipment. During the test sequence at the third location, only two persons were able to ride in the cab of the truck due to space limitations. Prior to the brake actuation, the vehicle speed is displayed by the computer using the output from the fifth-wheel. The displayed velocity was in complete agreement with the speed indicated by the "certified" patrol car speedometer and with radar during the tests at the second location. Observers outside the vehicle watched for the initial tire lock-up and measured the skid length.

The accelerometer was calibrated prior to each skid to obtain the one-g reference by rotating the beam to the horizontal position. The computer's calibration routine

automatically stores the highest strain gage output it sees during this phase.

The adjustment on the accelerometer damper was modified before each test to obtain the damping ratio which would allow for quick response without unwanted oscillations.

The first test was performed on June 17, 1982, at Crossing Place 0.1 miles north of Riverside Drive in Austin, Texas with a 1979 Ford LTD patrol car. The road was chosen because it had very little use and therefore, deterioration making it a very coarse surface. The temperature was approximately 80 degrees Fahrenheit.

The second series of tests were performed in Austin, Texas, on June 18, 1982, on Guadalupe Drive at the intersection of 24th Street in the northbound lanes. Guadalupe Drive is a main traffic artery for the university area of Austin which is heavily traveled. Therefore, the surface is highly polished and contaminated. The temperature was also approximately 80 degrees Fahrenheit and again, the tests were run using the 1979 Ford LTD.

The third set of tests was done on Texas Highway 29 approximately 8 miles west of Burnet, Texas, 0.3 miles east of the intersection with Inks Lake Park Road. The road was a moderately traveled rural highway which was relatively coarse. Testing was done on a three and one half degree



incline. The temperature was approximately 85 degrees Fahrenheit. The vehicle used was a 1977 Ford F-350 one ton truck.

#### Testing Procedure

Before testing began, the microcomputer-accelerometer unit was electrically connected to the vehicle. The cigarette lighter socket was used as a 12 volt power source. Otherwise, any 12 volt DC source and ground connection could have been used. A conductor was also connected from the lightbulb side of the brake light switch to the computer "BRAKE" input. This served as the triggering source for the data acquisition subroutine.

The fifth-wheel was mounted on the rear of the vehicle and the power and signal lines were run to the computer unit. With all the connections made and the vehicle in position, the accelerometer was calibrated. The CAL button was pressed and the accelerometer was rotated to the horizontal position. When this sequence was complete testing began.

After releasing the brake, the EX button was pressed and the vehicle was accelerated. The velocity at which the test vehicle was traveling was continuously displayed and updated every second by the microcomputer. That same velocity was also stored in a designated memory location for use during the analysis of the data.

At the instant the brake pedal was pushed to initiate the skid, the microcomputer began to sample both the A/D converter (connected to the accelerometer) and the counter (connected to the fifth wheel) every five milliseconds. One thousand samples were taken for a total duration of five seconds. Each sample from the A/D converter and from the counter was stored in the computer RAM.

At the completion of the skid, the data from the skid, which was now in RAM, was converted into Kansas City Standard format and recorded onto a cassette tape. The TD button on the computer is used to initiate this function.

When the test sequence was completed, the cassette tape with the recorded data was read into the memory of a microcomputer development system. To make analysis easier and to eliminate having to read the cassette each time, the data was transferred onto a flexible disk under a filename which reflects the date and test number. The computer utilized in this work is a 64K Z-80 based system running under the CP/M (Control Program/Microcomputer) operating system.

### Test Results

The results from the second tests will be evaluated and explained in detail and the results from the first and third test sites will be presented but not explained in the same detail.

Figures 4.1, 4.2, and 4.3 show the actual deceleration vs. time plots for the three tests performed at the second test site. The heading of each plot indicates the date and test number. Each of the deceleration traces shows that the cantilever beam-mass system was being driven by a frequency close to its natural frequency, thus causing excessive oscillations in the output. The beam does vibrate about its equilibrium position, however, so the equilibrium position of the oscillations would reflect the actual deflection seen by the strain gages.

All of the data recorded by the computer system is in digital form so the use of a digital filter will smooth the data to the beams equilibrium position. A first-order digital filter, as described in reference [26], was used to filter out the unwanted oscillations in the data. The digital filter used in this analysis filters out all oscillations above a frequency of 10 Hz. The following equation is the digital equivalent of a first-order filter:

$$D(n) = D(n-1) + (Ts/(Ts+T))(X(n) - D(n-1)) \quad (12)$$

where

$D(n)$  and  $D(n-1)$  are the filtered values at times  $n$  and  $n-1$ ;

$X(n)$  is the unfiltered value at time  $n$ ;

$Ts$  is the sample interval (0.005 seconds); and

$T$  is the period of the cut-off frequency (0.1 secs).

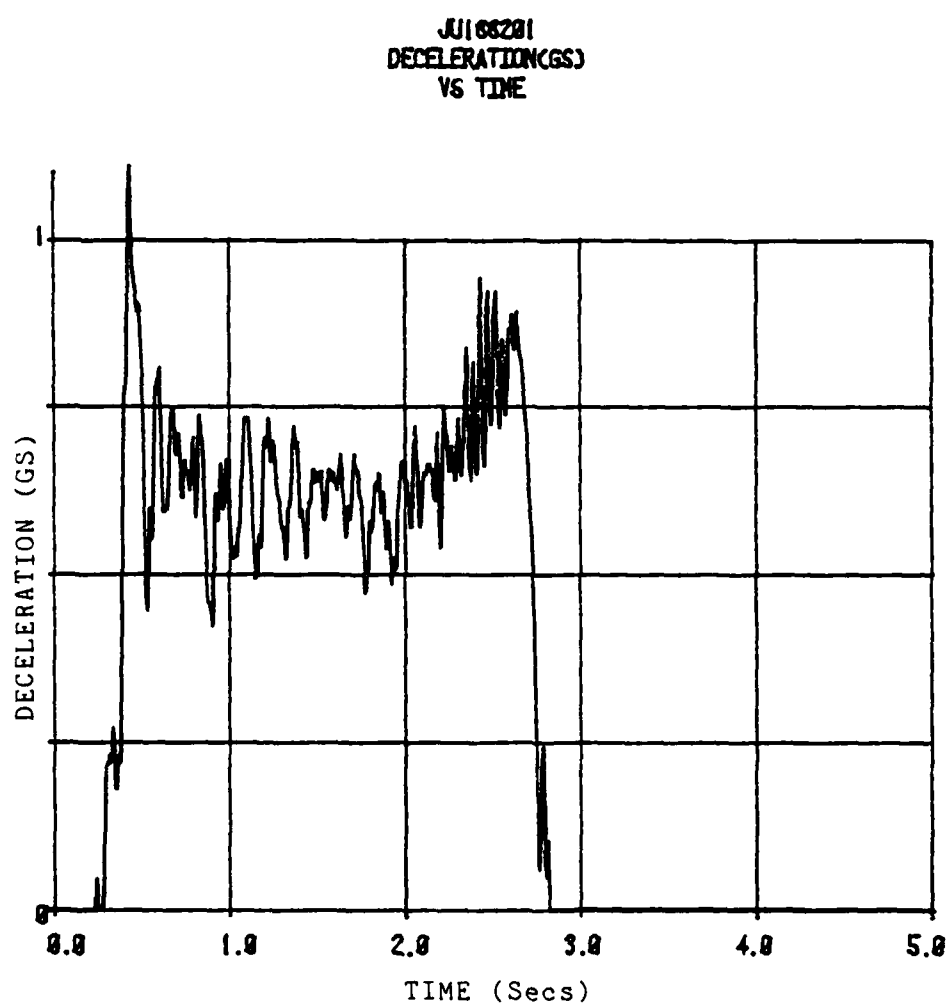


Figure 4.1      Deceleration vs. Time    June 18, 1982 Test One  
Unfiltered

JJ188282  
DECELERATION(GS)  
VS TIME

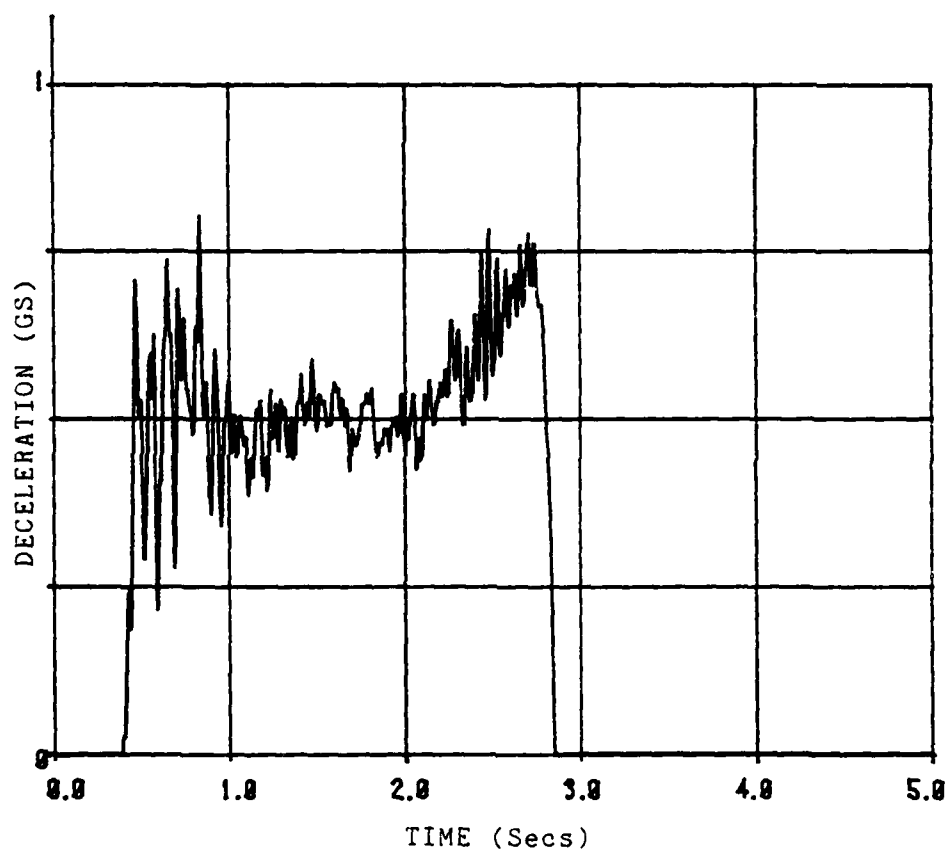


Figure 4.2      Deceleration vs. Time    June 18, 1982 Test Two  
Unfiltered

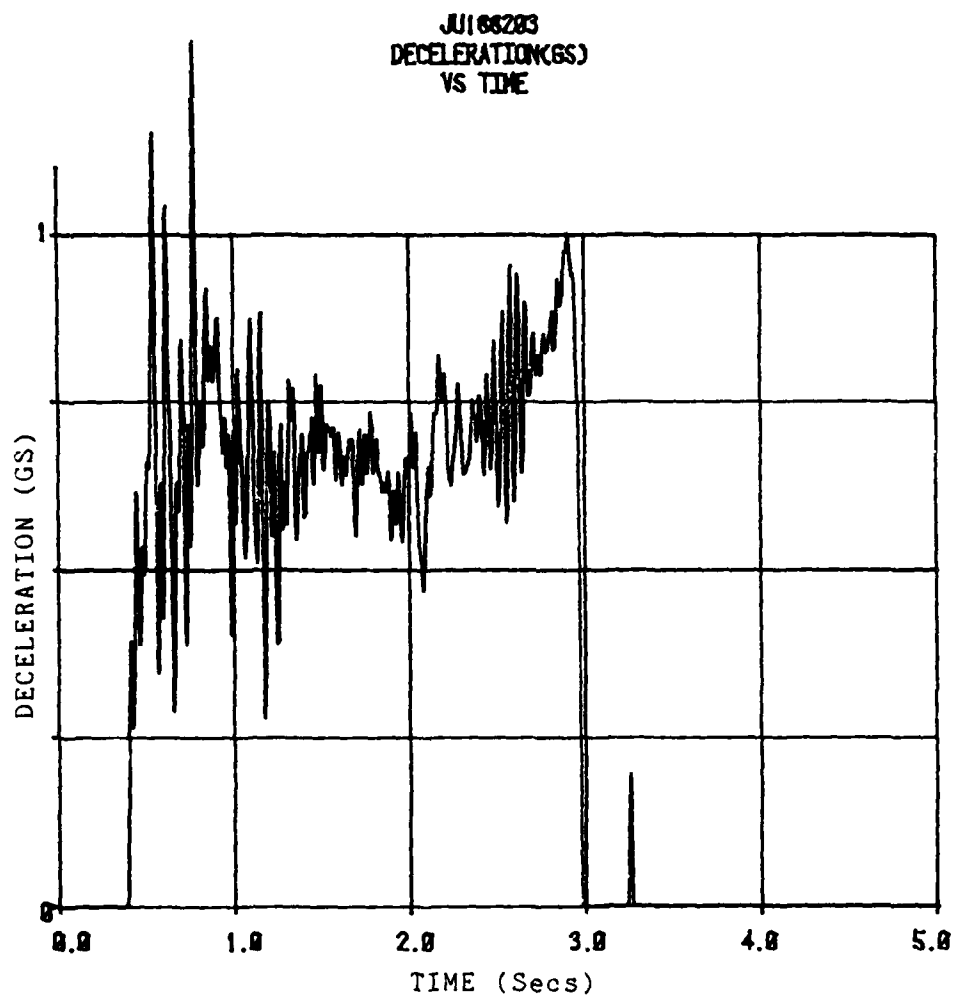


Figure 4.3 Deceleration vs. Time June 18, 1982 Test  
Three Unfiltered

For this case the cut-off frequency is chosen as 10 Hz so the value of  $(T_s/(T_s+T))$  is 1/20 or 0.05.

Figures 4.4, 4.5, and 4.6 represent the deceleration versus time plot employing a digital filter. It can be seen by comparing the equivalent tests that the filtered data represents the equilibrium position of the unfiltered data. To verify that the filtering does not alter the results, an integration with respect to time was performed on the filtered and unfiltered data and the results were in very close agreement, within 0.01 feet per second.

Using simple dynamic principles, the integration of the deceleration versus time curve yields the change in velocity. Since all testing was done to a complete stop, the initial velocity equals the integral of the deceleration versus time curve.

In the skids at test site two, the initial velocity of the vehicle, as recorded by the fifth-wheel-computer combination, did not agree with the integration of the deceleration versus time curve. Since the velocity, as displayed and recorded by the fifth-wheel-computer unit, was closely calibrated and experimentally verified, it must be assumed that the integration of the deceleration versus time curve is incorrect.

The accelerometer records the relative changes in deceleration over the skid time so the only conclusion that

JJ188281  
DECELERATION(GS)  
VS TIME

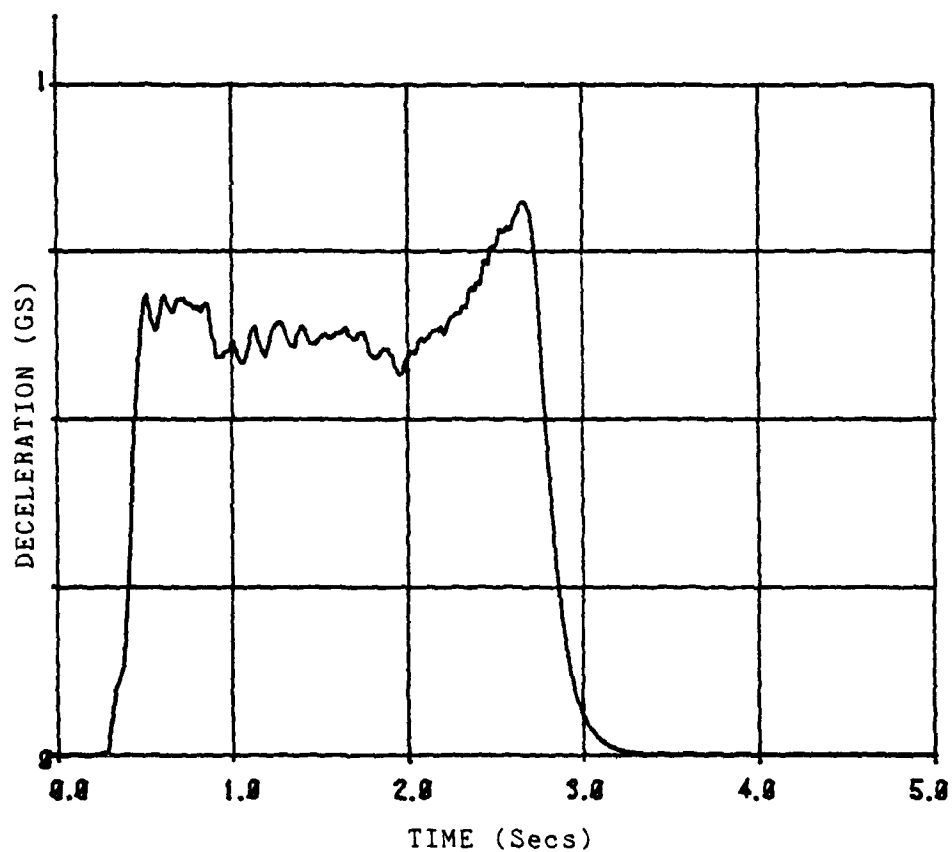


Figure 4.4 Deceleration vs. Time June 18, 1982 Test One  
Filtered



JU165282  
DECELERATION(GS)  
VS TIME

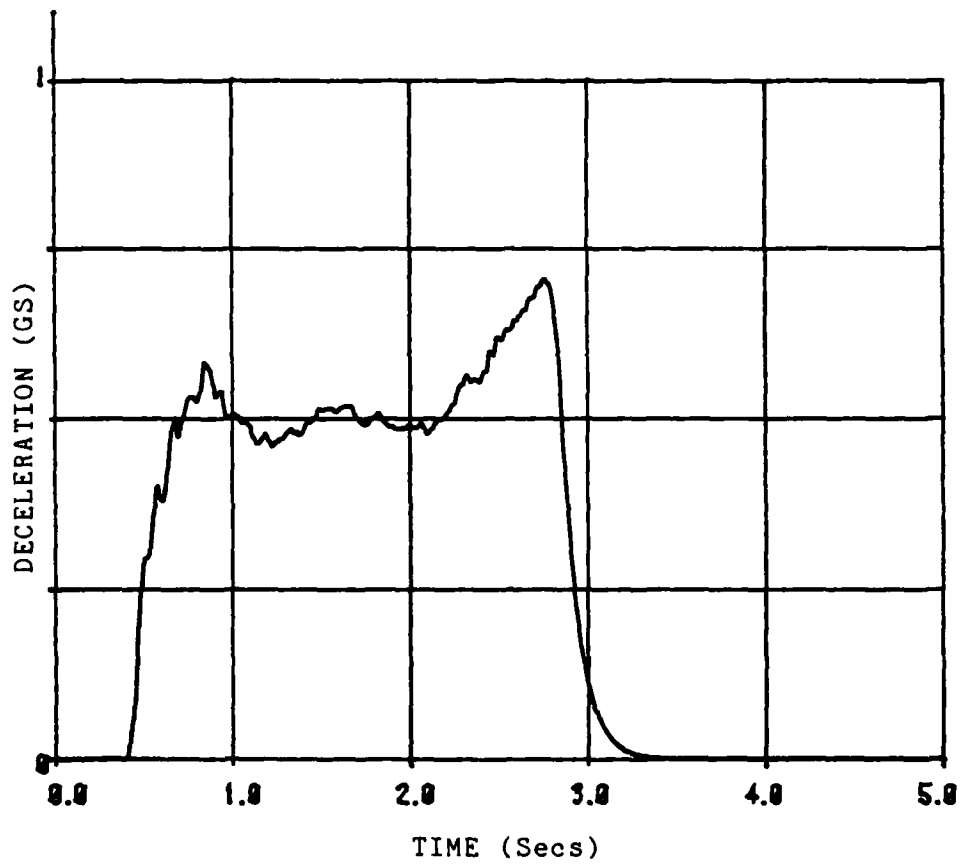


Figure 4.5      Deceleration vs. Time    June 18, 1982 Test Two  
Filtered

JU188283  
DECELERATION(GS)  
VS TIME

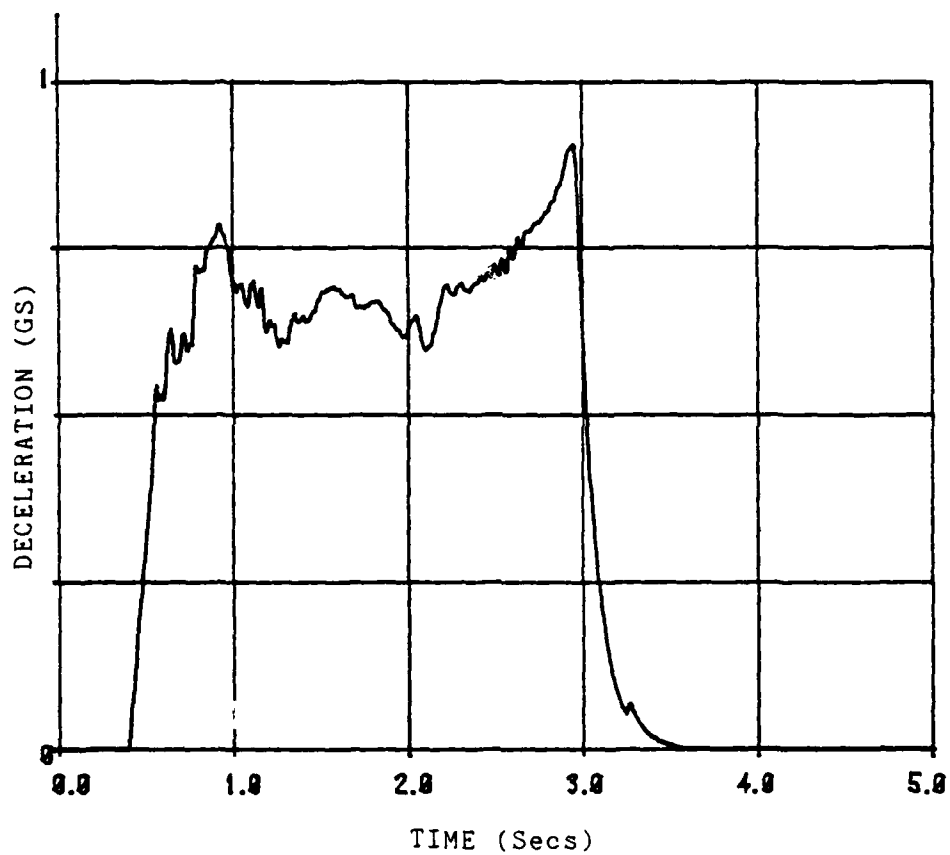


Figure 4.6 Deceleration vs. Time June 18, 1982 Test  
Three Filtered

can be reached is that the exact magnitude of the deceleration data is incorrect. During the calibration phase, the beam is moved slowly, so that it has been essentially statically displaced to the horizontal, one-g position. But when the beam is undergoing deflection during a skid, it is under the influence of a dynamic force and is also being driven by frequencies near its natural frequency. It is concluded that the damping system is preventing the beam from deflecting to its equilibrium position while under the influence of the dynamic force of the mass under acceleration. The damper is necessary, however, since it prevents the beam from being driven too far by the vibrations near its natural frequency.

To make the integration of the deceleration versus time data equal to the initial velocity, the one-g calibration value was recomputed. The displayed fifth-wheel velocity is accurate to within +0 to -0.99 miles per hour or the speed indicated by the computer is the minimum velocity it could be sensing. The actual velocity could be as much as the indicated velocity plus 0.99 miles per hour. In other words, the computer rounds down to the nearest integer velocity. This leads to the fact that there is a range of one-g calibration values which will satisfy the accuracy of the fifth-wheel when the deceleration versus time curve has been integrated. Figures 4.7, 4.8, and 4.9

show the ranges that the deceleration versus time curves can have and still satisfy the accuracy of the indicated initial speed for the three skid tests conducted at site two. The lower deceleration curve reflects the higher one-g calibration value and the higher curve reflects the lower one-g calibration value. These curves also reflect the ranges in the coefficient of friction in dimensionless units from 0 to 1.

Table 4.1 shows the results from the three skid tests done at the second site. The original one-g calibration value is shown for each test as well as the range in the one-g calibration values which satisfy the accuracy of the initial velocity when the deceleration versus time curve is integrated. The initial velocities obtained from the integration of the adjusted deceleration versus time curves are also listed.

The initial velocity of the vehicle is verified and recorded by the fifth-wheel-computer combination and that velocity is obtained by adjusting the one-g calibration factor. The velocity versus time curve can thus be obtained by integrating the deceleration versus time curve once to obtain the initial velocity and then reintegrating the deceleration versus time data one incremental time segment at a time and subtracting it from the previous velocity. Figures 4.10, 4.11, and 4.12 represent

JU186281  
DECELERATION(GS)  
VS TIME

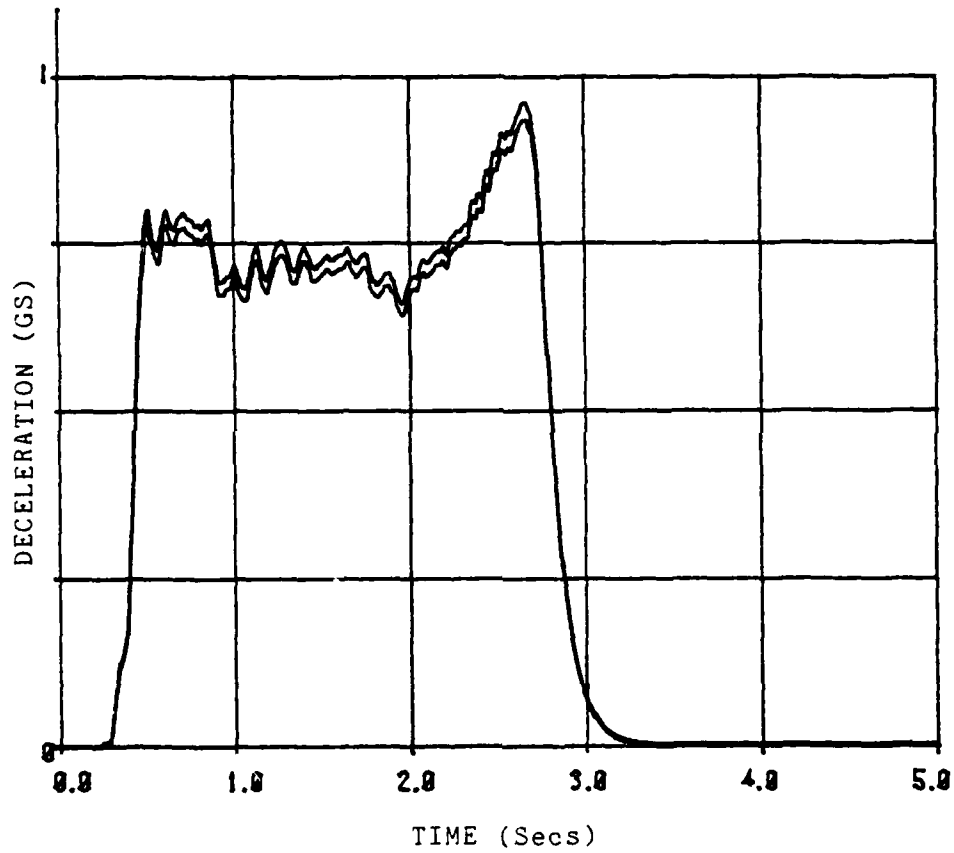


Figure 4.7 Deceleration vs. Time June 18, 1982 Test One  
Filtered, One G Calibration Range

JJ168292  
DECELERATION(GS)  
VS TIME

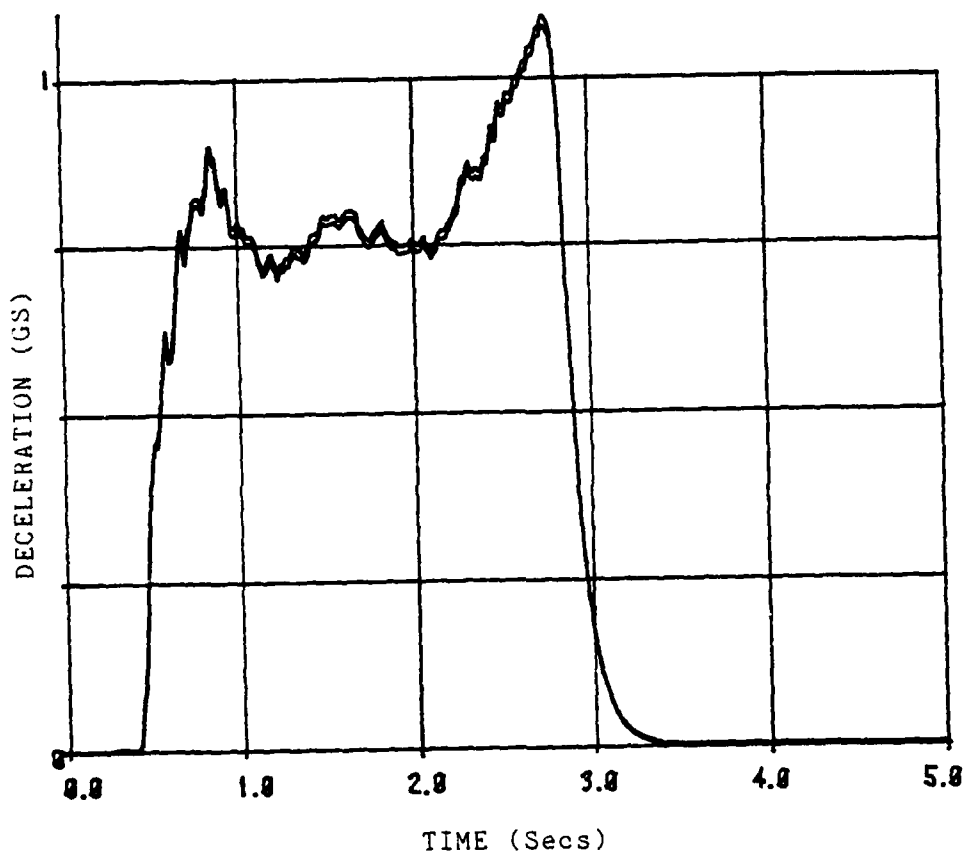


Figure 4.8 Deceleration vs. Time June 18, 1982 Test Two  
Filtered, One G Calibration Range

JJ168203  
DECELERATION(GS)  
VS TIME

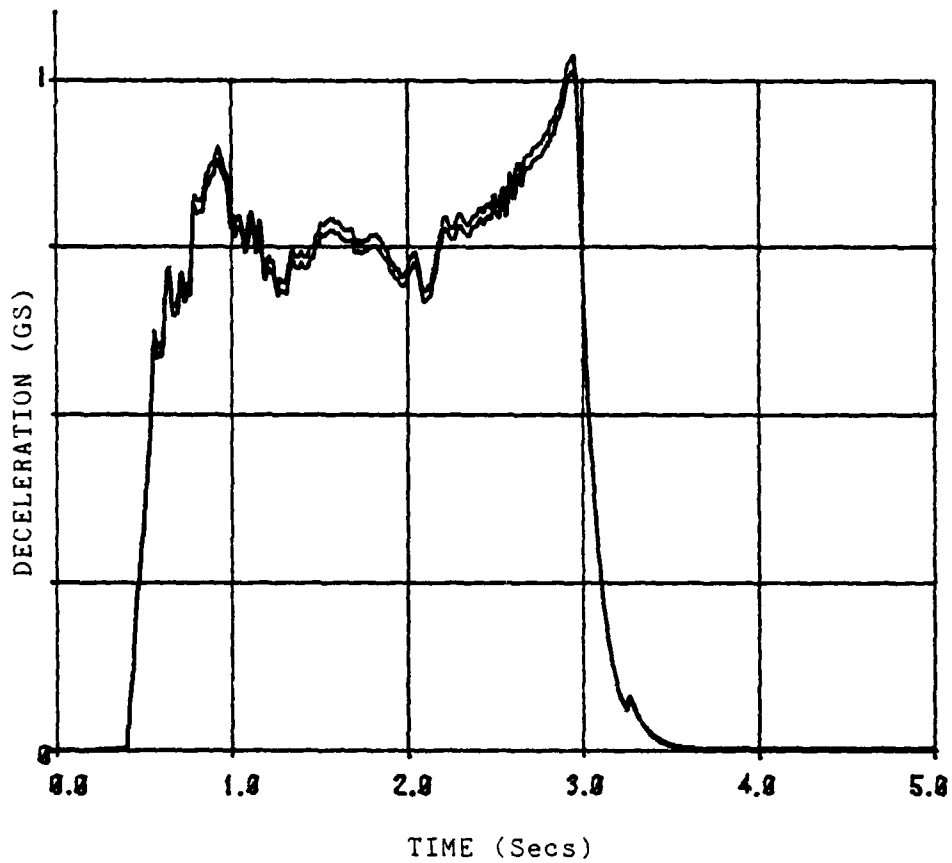


Figure 4.9 Deceleration vs. Time June 18, 1982 Test  
Three Filtered, One G Calibration Range

Description	Test Number		
	1	2	3
1. Initial Velocity (5th-wh)	40 MPH	43 MPH	44 MPH
2. Initial Calibration Value	8F	86	79
3. Calibration Range Adjust	7E - 7B	58 - 57	6C - 6A
4. Velocity Range Using Calib. Range	40.21-40.86 MPH	43.29 - 43.75 MPH	44.10-44.89 MPH
5. Fifth-Wheel Distance	81.5 FT	97.41 FT	107.6 FT
6. Skid Length Measurement	70.5 FT	66.5 FT	76 FT
7. Initial Velocity Using 5th-Wheel Energy	36.62-36.91 MPH	38.86 - 39.08 MPH	41.00-41.38 MPH
8. Calculated Distance Using Double Integration Of Decel. Data	97.8 - 99.4 FT	112.8 - 114.1 FT	118.4-121.9 FT

Table 4.1 Results of Skid Testing at Site Two  
June 18, 1982



the velocity versus time curves for the second series of tests using the above procedure.

The velocity versus time curve can then be integrated to obtain the distance versus time curves shown in Figures 4.13, 4.14, and 4.15.

The cross integration of the deceleration versus distance data will yield the total energy of the skid as defined by Equation (9), where  $g=a$  and  $a$  is the non-constant deceleration. Equation (9) becomes:

$$m \int a \, ds = m V^2 / 2 \quad (12)$$

or

$$V = \left[ 2 \int a \, ds \right]^{1/2} \quad (13)$$

This cross integration was performed with the results in exact agreement with the single integration of the deceleration versus time data. All of the integration carried out in this analysis where time is one of the factors is done numerically using Simpson's method of numerical integration, as defined in Reference [27].

Another distance versus time curve is generated by the sampling of the fifth-wheel counter during the skid process. This fifth-wheel distance versus time curves are shown in Figures 4.16, 4.17, and 4.18 for the three tests at site two.

It is then possible to integrate the deceleration data obtained from the accelerometer with respect to the

JU160281  
VELOCITY (FT/SEC)  
VS TIME

FINAL VELOCITY = 0.0 FT/SEC

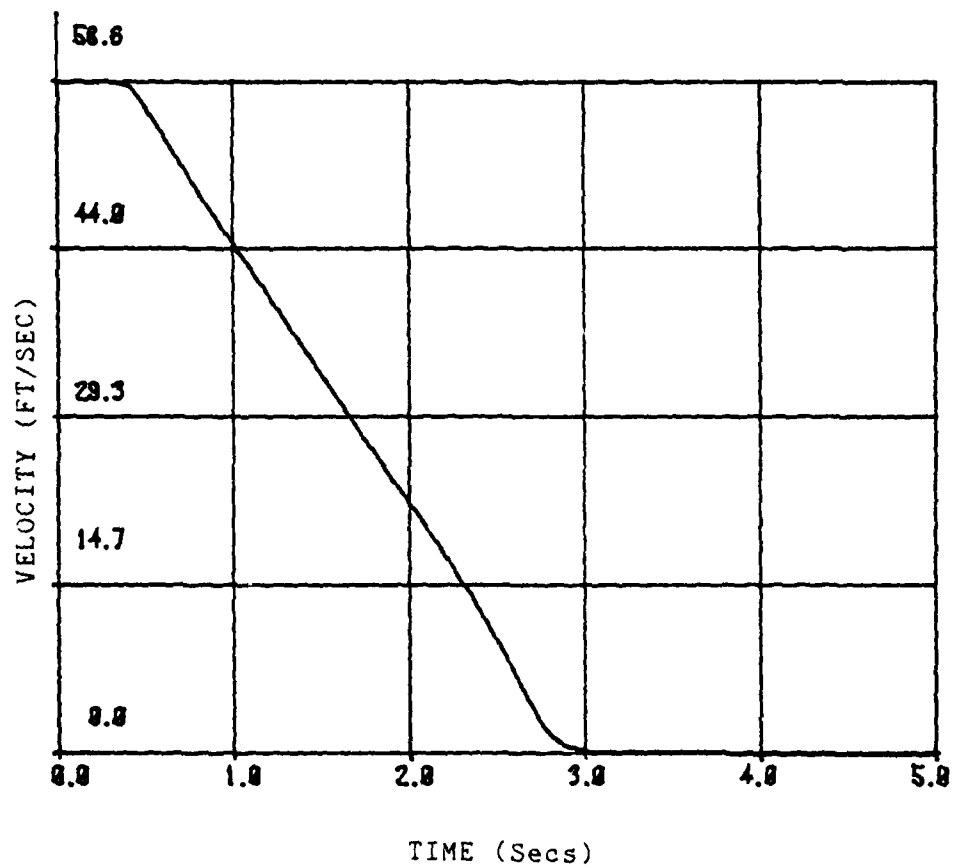


Figure 4.10 Velocity vs. Time June 18, 1982 Test One

JU168282  
VELOCITY (FT/SEC)  
VS TIME

FINAL VELOCITY = 0.0 FT/SEC

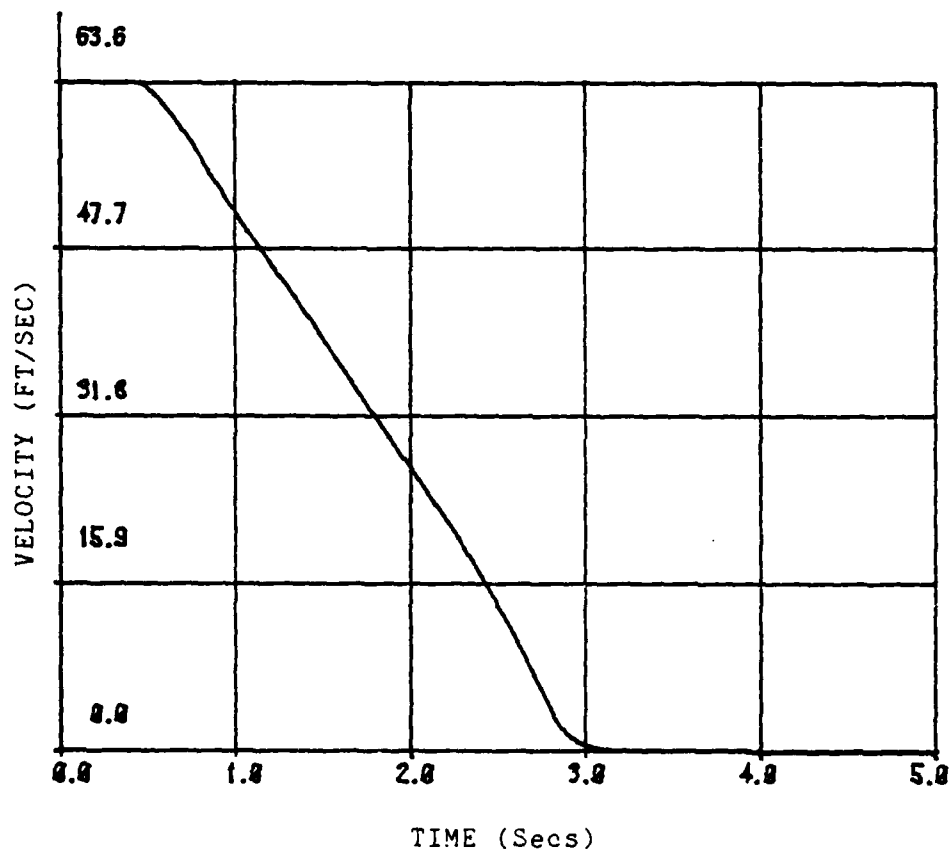


Figure 4.11 Velocity vs. Time June 18, 1982 Test Two

JU188283  
VELOCITY (FT/SEC)  
VS TIME

FINAL VELOCITY = 0.0 FT/SEC

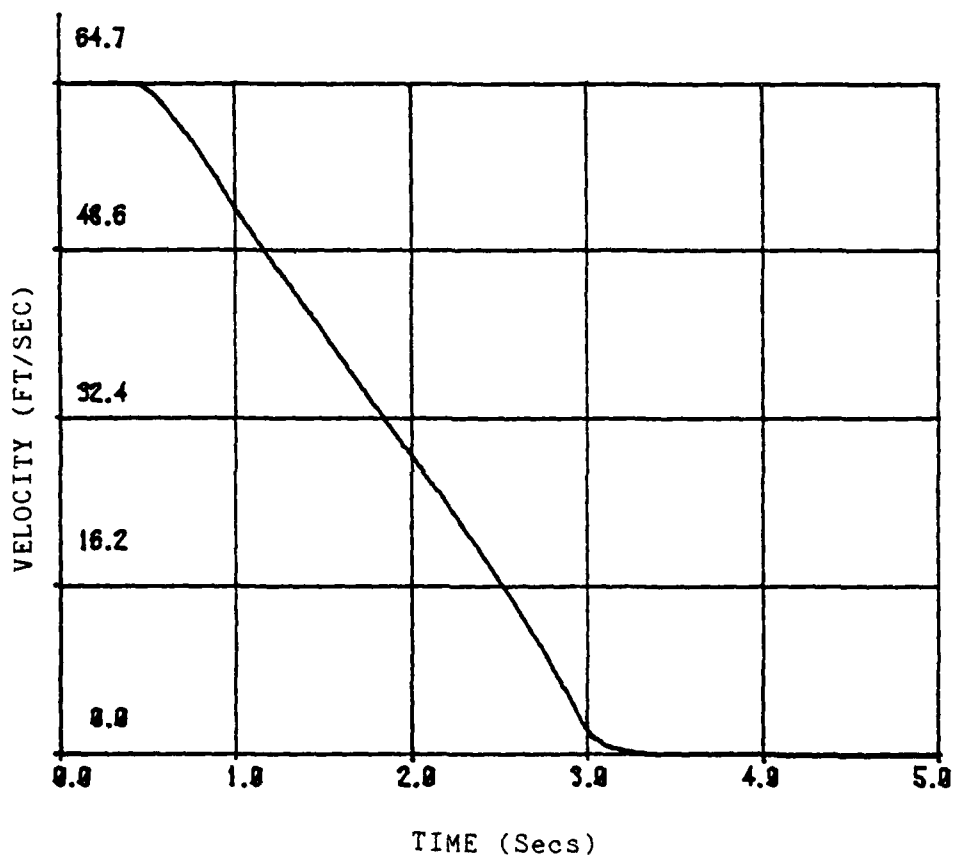


Figure 4.12 Velocity vs. Time June 18, 1982 Test Three

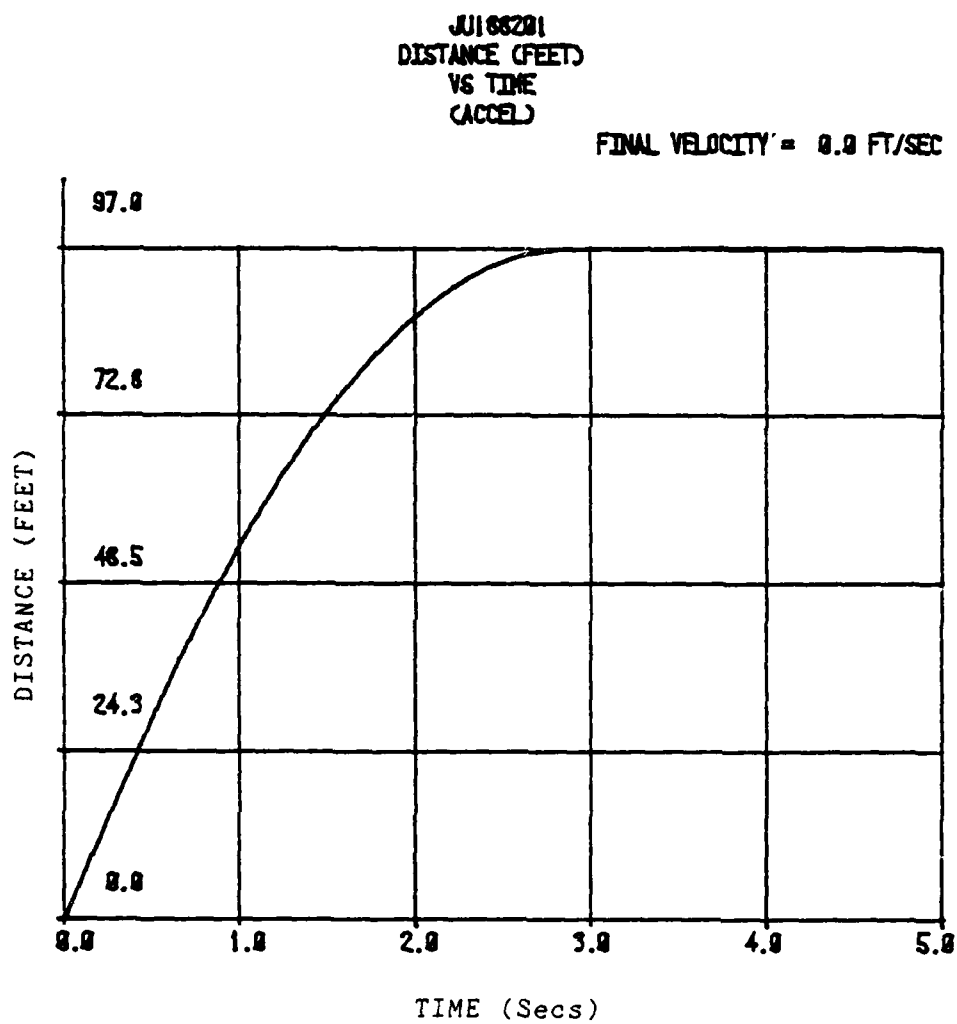


Figure 4.13 Distance vs. Time June 18, 1982 Test One

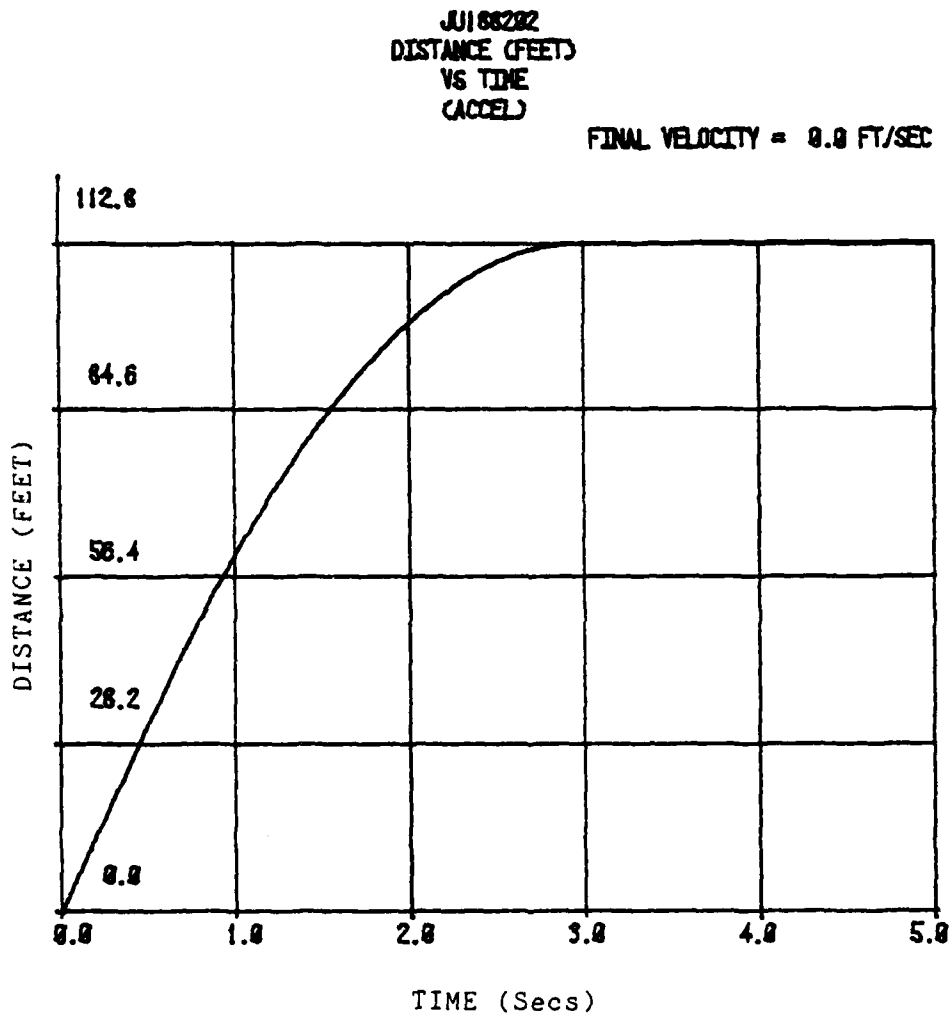


Figure 4.14 Distance vs. Time June 18, 1982 Test Two

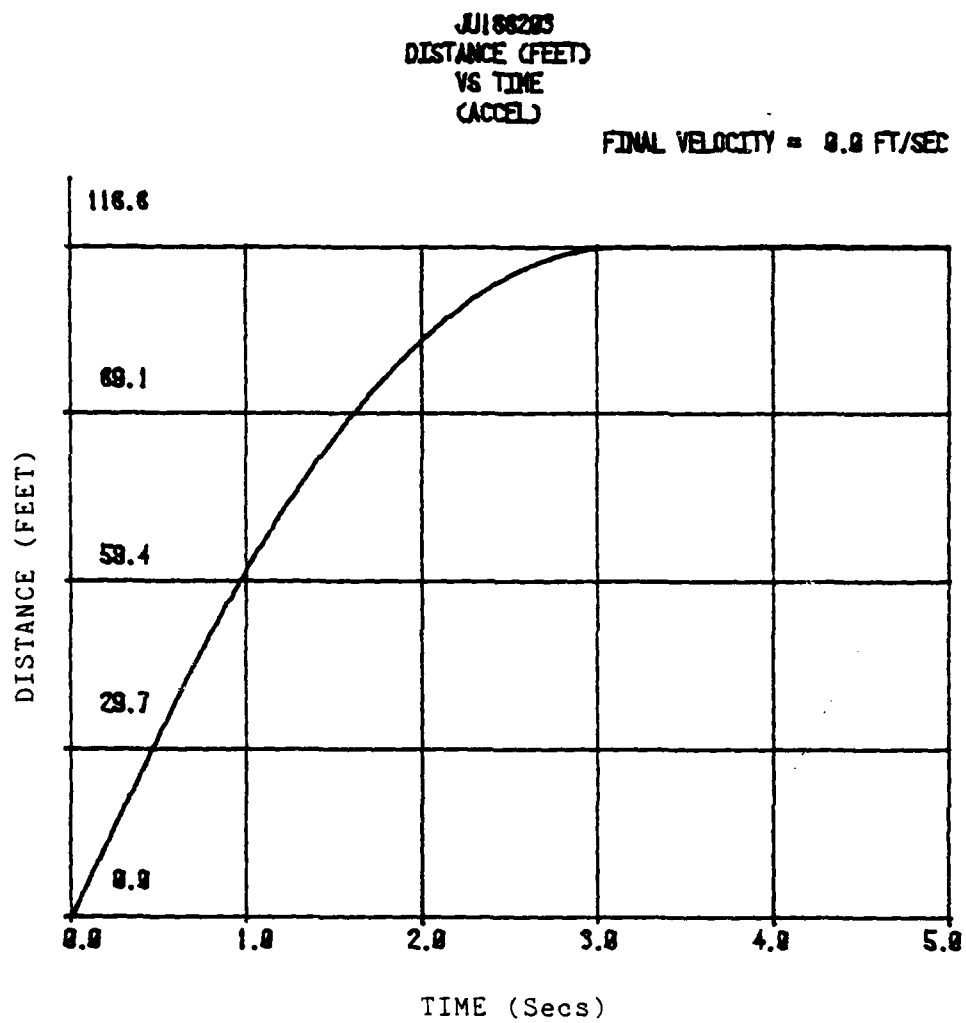


Figure 4.15 Distance vs. Time June 18, 1982 Test Three

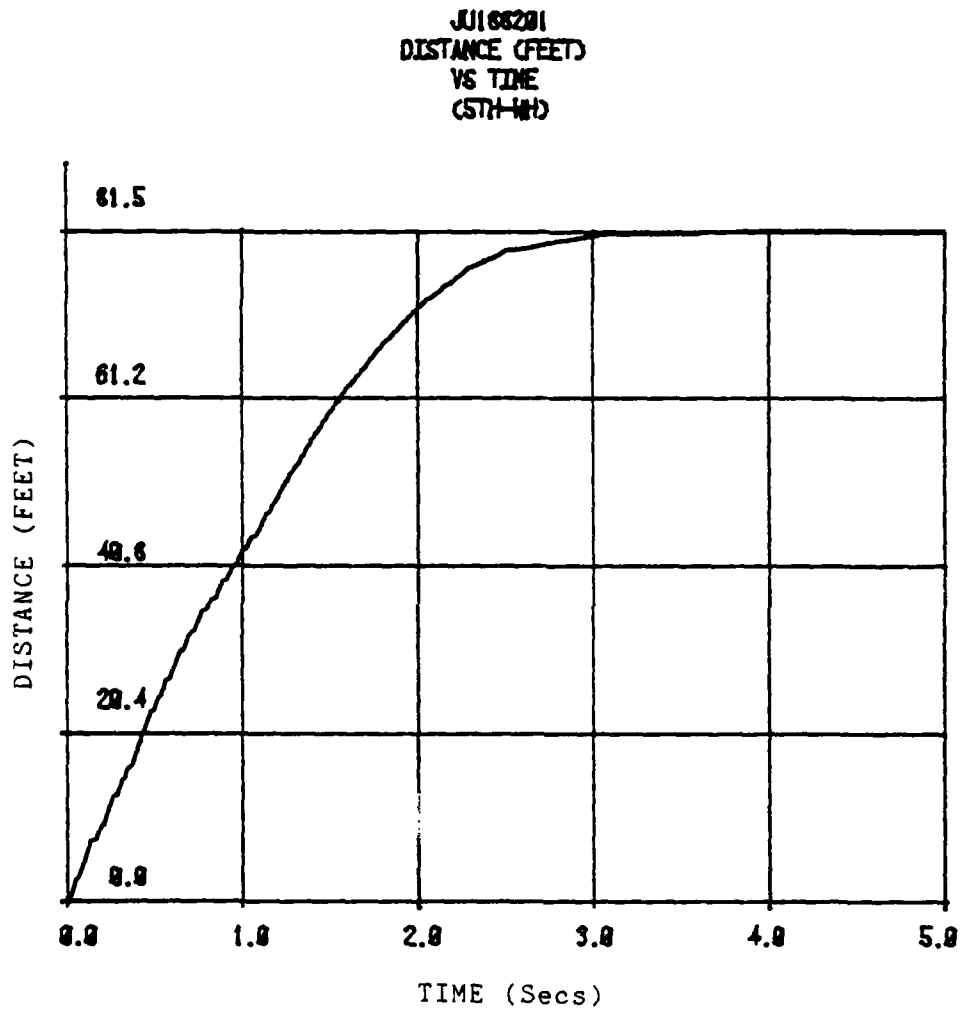


Figure 4.16 Distance vs. Time June 18, 1982 Test One  
Fifth-Wheel Data



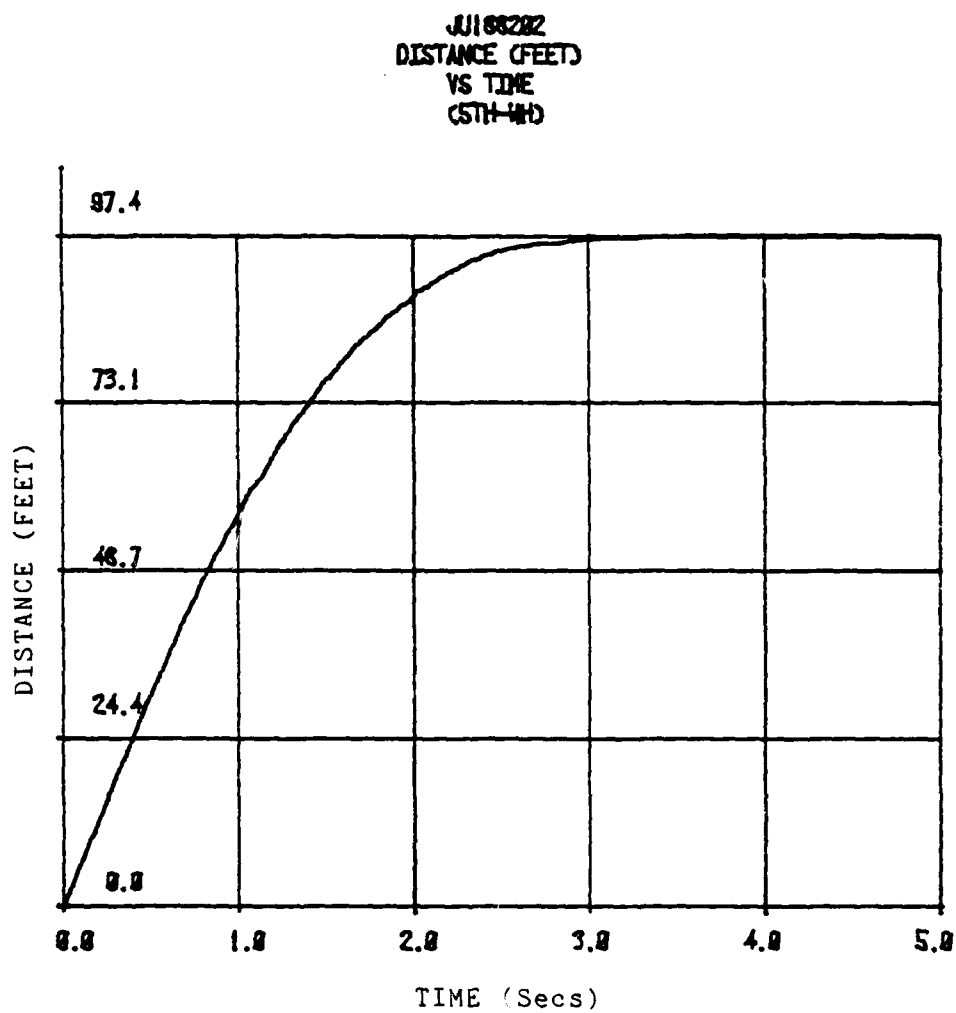


Figure 4.17 Distance vs. Time June 18, 1982 Test Two  
Fifth-Wheel Data

UNCLASSIFIED

AIR FORCE INST OF TECH WRIGHT-PATTERSON AFB OH F/G 13/6  
MEASUREMENT OF VEHICLE TIRE-TO-ROAD COEFFICIENT OF FRICTION WIT--ETC(U)  
AUG 62 R L COKE  
AFIT/CI/NR/82-35T NI

**N**

2 OF 2  
ADA  
1191-2

END  
DATE  
FILMED  
10-82  
DTIC

JU168203  
DISTANCE (FEET)  
VS TIME  
(5TH-WHEEL)

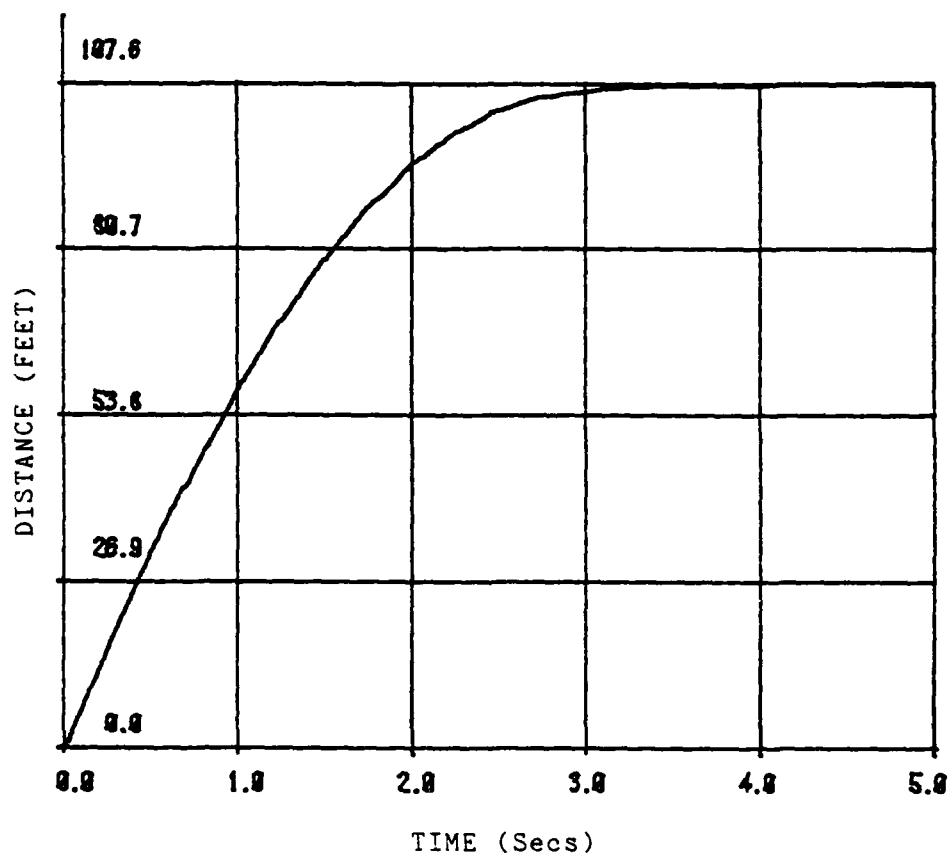


Figure 4.18 Distance vs. Time June 18, 1982 Test Three  
Fifth-Wheel Data

distance data obtained from the fifth-wheel to get the total energy and, therefore, the initial velocity. This integration yields results which are generally lower than the previous results. Close examination of the fifth-wheel distance versus time data reveals points in the curve where the distance did not increase for a short period of time. This indicates that the Hall Effect switch at times did not detect the presence of a magnet passing by it. Eyewitness observations of the fifth-wheel indicate that the fifth-wheel began to bounce severely during the skids which could account for lost pulses. Therefore, the loss of accurate distance versus time data results. During the approach to the skid, the fifth-wheel did not bounce making the initial velocity measurement still valid. Work is currently under way which should correct the fifth-wheel device.

Table 4.1 includes the initial velocity as calculated by Equation (13) using the fifth-wheel as the distance data and the length of the skid marks left by the tires on the pavement. It also lists the distance as measured by the fifth-wheel and the distance calculated by the double integration of the deceleration versus time data.

Figure 4.19 is a plot of the distance versus velocity data obtained from the double and single integration of the adjusted deceleration versus time data using the higher

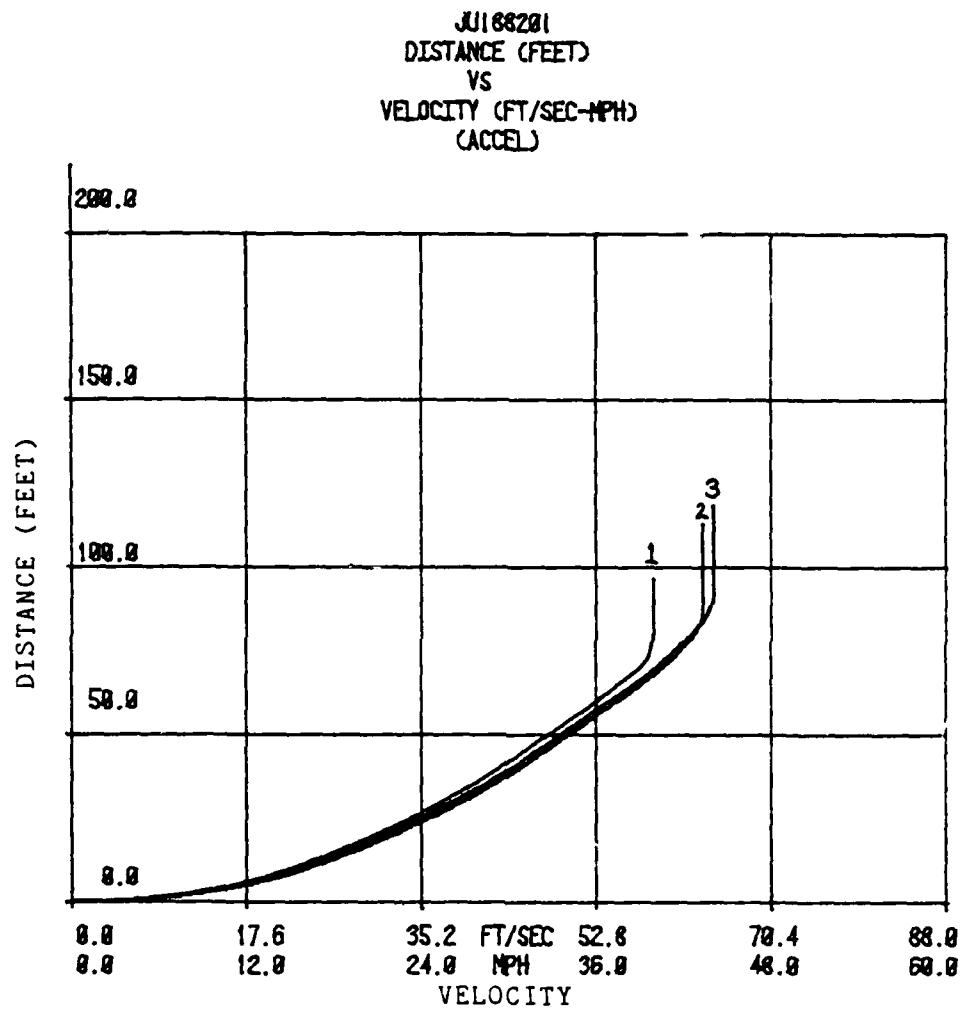
recalibrated one-g value. All three curves from the testing done at test site two are contained on the same set of coordinates. The origin of these coordinates is the point where the vehicle has stopped after the skid. From this plot it can be seen that the distance versus velocity curves tend to fall along the same path. The three tests at site two were done at three different initial velocities so the curves do not end at the same point or velocity. By knowing the skid length of a vehicle which was involved in an accident being reconstructed at the same site, the initial velocity can be estimated. The length of the skid marks would be marked off on the distance scale and the point where that measurement intersects the distance versus velocity curve would indicate the minimum velocity at which the vehicle was traveling. If the velocity is beyond the range of the curve, the curve can be extended in a straight line as an estimate of distance versus velocity characteristics.

Figure 4.20 represents an example of the above procedure using Figure 4.19 as a data base. In a hypothetical example: if a vehicle's skid marks were 65 feet long and it was estimated that it was going 15 miles per hour at impact, the initial velocity can be estimated by adding 65 feet to the skid length which would result from a skid at 15 miles per hour. Using Figure 4.20, it is

estimated that the vehicle was going a minimum of 42 miles per hour at the onset of the skid.

The results for the skid tests done at sites one and three are tabulated in Tables 4.3, and 4.4, and the distance versus velocity curves are contained in Figures 4.21, 4.22, and 4.23. The results from test site three had to be analyzed in two figures because three skid tests were performed on a three and one half degree grade going uphill and two were performed on the same grade going downhill. The deceleration of the vehicle is affected by the slope of the road surface because of the effect of gravity acting on the vehicle. This is indicated by the deceleration versus time curves which show a higher deceleration rate on the uphill skid than on the downhill skid. See Appendix A for the plots of the data for the tests done at sites one and Appendix B for plots of data from site three.

Careful examination of the deceleration versus time data curves for all the tests reveals that there are differences in the characteristics of the coefficient of friction from one road surface to another. The tests done on relatively unused surfaces (test site one and three) show that the deceleration and coefficient of friction tend to remain relatively constant, while on a smooth polished surface (test site two) the coefficient of friction tends to rise dramatically when the speed decreases. This could be



1 = Skid Test No. One  
2 = Skid Test No. Two  
3 = Skid Test No. Three

Figure 4.19 Distance vs. Velocity Test Site Two

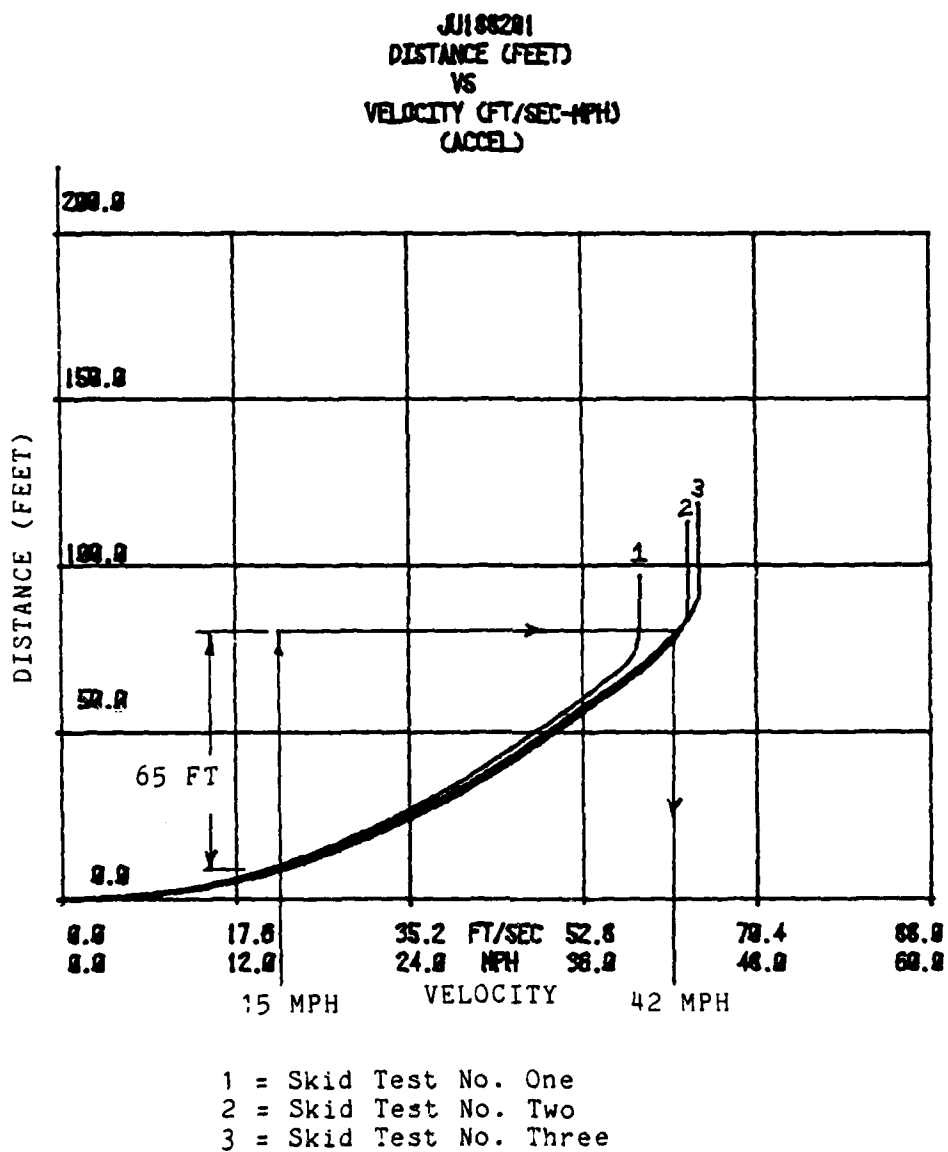
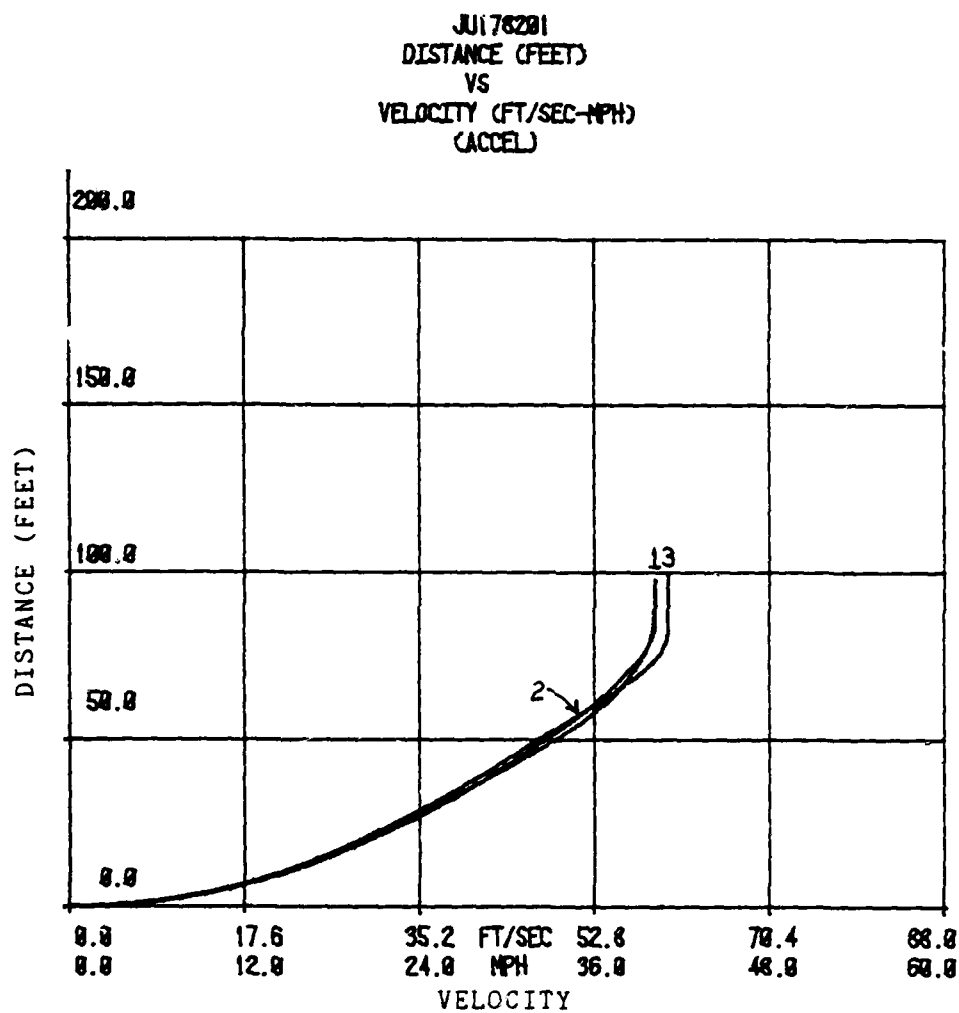


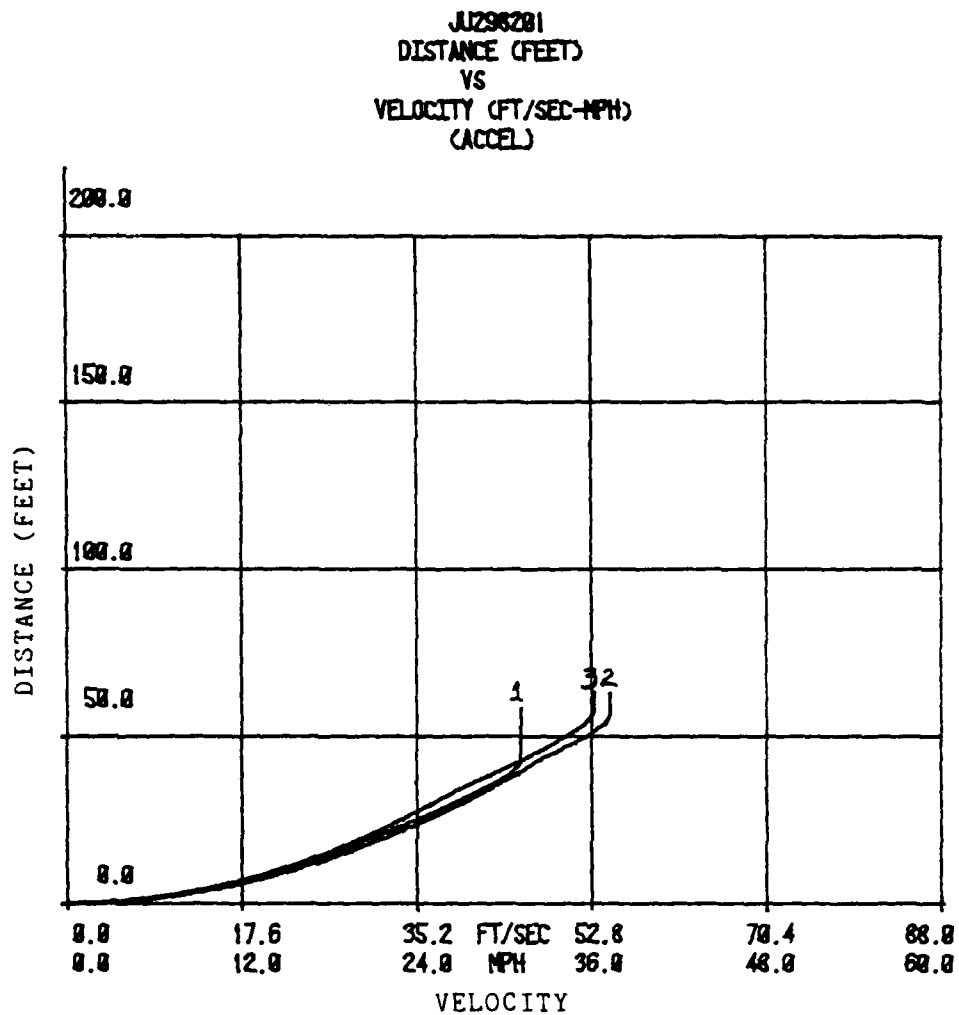
Figure 4.20 Distance vs. Velocity Test Site Two  
Example Velocity Estimation





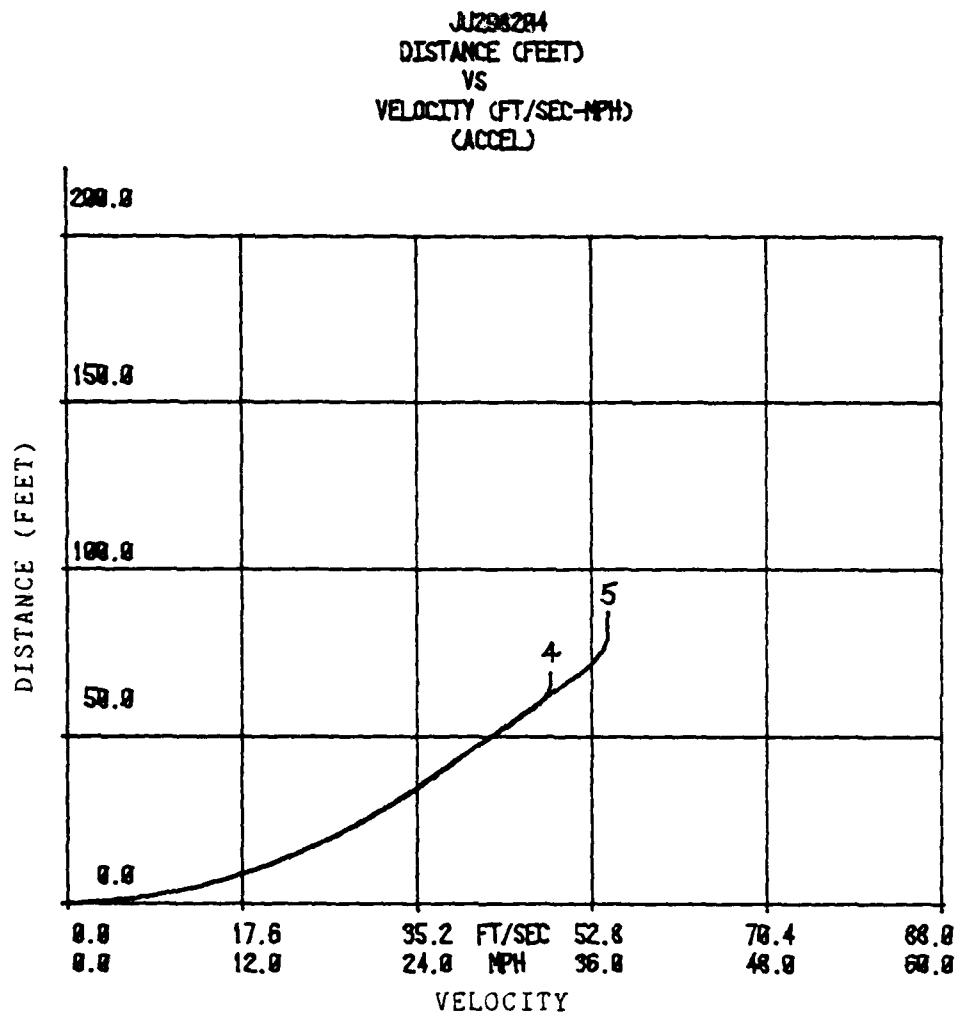
- 1 = Skid Test No. One  
2 = Skid Test No. Two  
3 = Skid Test No. Three

Figure 4.21 Distance vs. Velocity Test Site One



1 = Skid Test No. 1  
2 = Skid Test No. 2  
3 = Skid Test No. 3

Figure 4.22 Distance vs. Velocity Test Site Three  
Uphill Skid Tests



4 = Skid Test No. Four  
5 = Skid Test No. Five

Figure 4.23 Distance vs. Velocity Test Site Three  
Downhill Skid Tests

Description	Test Number		
	1	2	3
1. Initial Velocity (5th-Wh)	40 MPH	40 MPH	41 MPH
2. Initial Calibration Value (HEX)	CD	A4	96
3. Calibration Range Adjust	CD -C9	B3 - B0	C0 - BC
4. Velocity Range Using Calib. Range	40.13-40.86 MPH	40.21 - 40.9 MPH	41.06-41.09 MPH
5. Fifth-Wheel Distance	83.4 FT	86.2 FT	89.1 FT
6. Skid Length Measurement	70.5 FT	66.5 FT	76 FT
7. Initial Velocity Using 5th-Wheel Energy	36.09-36.45 MPH	36.85-37.16 MPH	38.08-38.49 MPH
8. Calculated Distance Using Double Integration of Decel. Data	98.00-99.95 FT	97.89-99.56 FT	99.27-101.4 FT

Table 4.2 Results of Skid Tests at Site One  
June 17, 1982

Description	Test Number				
	1	2	3	4	5
1. Initial Velocity (5th-Wh)	31	37	36	33	37
2. Initial Calibration Value (HEX)	90	89	8D	A8	96
3. Calibration Range Adjust	C6-C1	87-85	93-90	D9-D4	CA-C6
4. Velocity Range Using Calib. Range	31.09-31.95 MPH	37.22-37.78 MPH	36.12-36.91 MPH	33.07-33.85 MPH	37.09-37.84 MPH
5. Fifth-Wheel Distance	50.8 FT	52.8 FT	54.5 FT	62.0 FT	63.7 FT
6. Skid Length Measurement	31 FT	49.3 FT	42.8 FT	60.0 FT	66.8 FT
7. Initial Velocity Using 5th-Wheel Energy	28.08-28.44 MPH	33.72-34.11 MPH	33.28-33.62 MPH	31.14-31.50 MPH	30.90-31.21 MPH
8. Calculated Distance Using Double Integration of Decel. Data	59.19-60.72 FT	63.10-64.10 FT	63.57-64.89 FT	69.35-70.99 FT	87.59-89.36 FT

Table 4.3 Results of Skid Tests at Site Three  
June 29, 1982

explained by the fact that adhesion tends to play more of a role in the friction process at low speeds on smooth surfaces. Each surface must be evaluated separately for an accurate representation of the coefficient of friction.

## CHAPTER V

### CONCLUSIONS AND RECOMMENDATIONS

#### Conclusions

Using a portable accelerometer mounted in a vehicle is a very accurate way to measure the coefficient of friction between a vehicle's tires and the road surface. With the accuracy of the fifth-wheel being within one mile per hour rounded down, the recalibrated accelerometer data is within two percent of the actual  $u$  when an initial velocity of 40 miles per hour is used. The exact accuracy will depend on the accuracy of the fifth-wheel at a given speed. This method closely duplicates many of the unknown variables which were present at the time of the accident which is being reconstructed.

The use of a microcomputer to record the information and to transmit it to a storage medium such as a cassette tape is a method which insures that all the data is received and recorded. This method provides for the analysis of the data with very little human interpretation and interaction.

The fifth-wheel as a velocity measuring device is an accurate way to record the initial velocity prior to the engagement of the brakes. Problems were encountered with using the fifth-wheel as a distance measuring device but

these problems appear to have acceptable solutions.

This total system is a very useful tool for use in the motor vehicle accident reconstruction field. Since all road surfaces are of different textures and made of different materials, the exact coefficient of friction at each accident site must be measured as accurately as possible. Previous methods tended to overestimate the coefficient of friction and, therefore, overestimate the initial velocity.

#### Recommendations

Problems were encountered with vibrations in the cantilever beam accelerometer during the skid tests even though a damper was used. It is recommended that a new approach be taken to improve the accelerometer package by improving the damper or designing a new type of accelerometer other than the cantilever beam type. Perhaps a fluidic column with a pressure transducer at the end toward the direction of the deceleration would be possible.

Another approach may be taken to damp out the unwanted vibrations of the beam. Analytical modeling with damping may be used to help offset the effects of the resonances during the digital analysis.

The fifth-wheel was also a source of problems during the skid tests. Accurate distance measurements were not obtained because of lost pulses caused by the fifth-



wheel bouncing which caused it to deflect. A method to minimize the bouncing of the fifth-wheel may eliminate the problem, if not a method to restrain the lateral movement of the wheel with the magnets mounted on it may be necessary. It may be necessary to convert the fifth-wheel system to an optical, rather than magnetic, system.

The fifth-wheel provided a means of determining the velocity at the time the brakes were applied. This velocity was updated and recorded once every second and was accurate to the next lower speed in miles per hour. It is recommended that the programming be altered to update the velocity every one half second and to display and store the velocity in tenths of miles per hour. This change will increase the accuracy to within one tenth of a mile per hour, rounded down to the nearest tenth. The recalibrated accelerometer data will be even closer to the actual  $\mu$ , perhaps within one percent.

APPENDIX

A

FIGURES FOR TEST SITE ONE

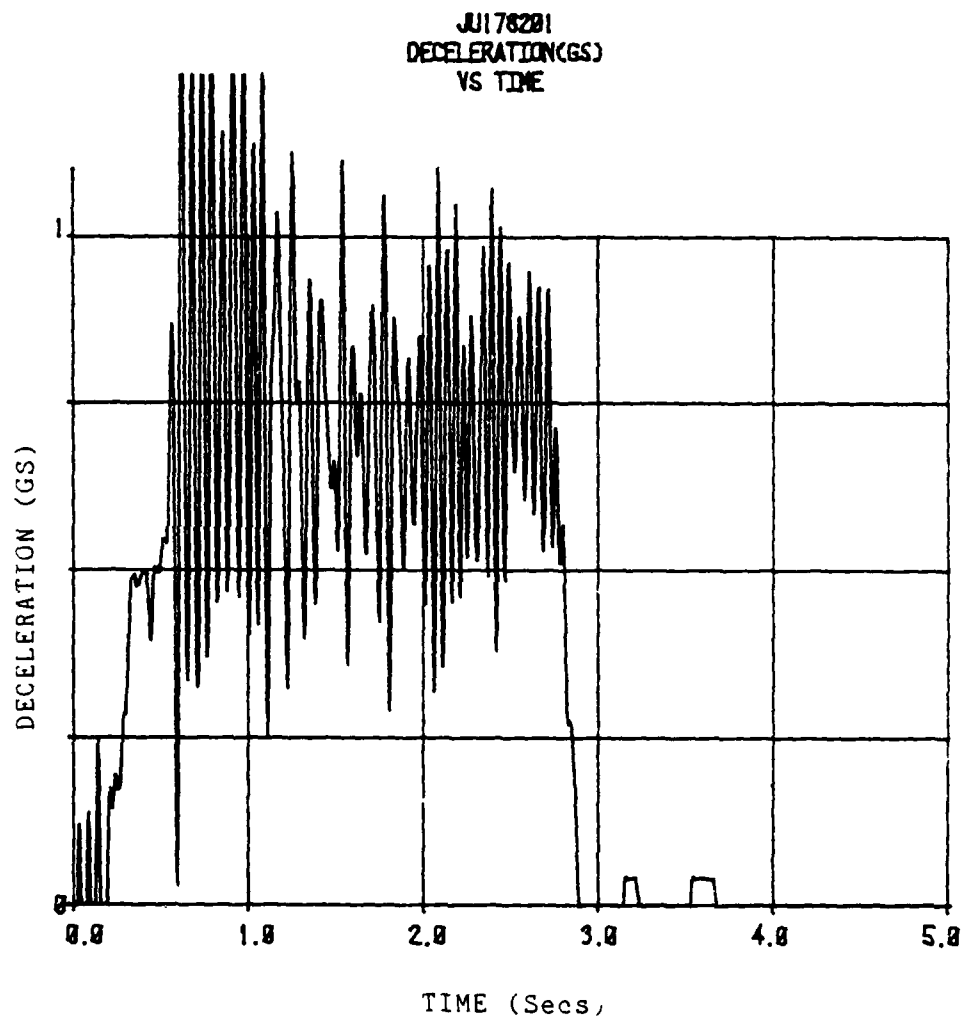


Figure A.1 Deceleration vs. Time June 17, 1982 Test One  
Unfiltered

JUL 7 82  
DECELERATION(GS)  
VS TIME

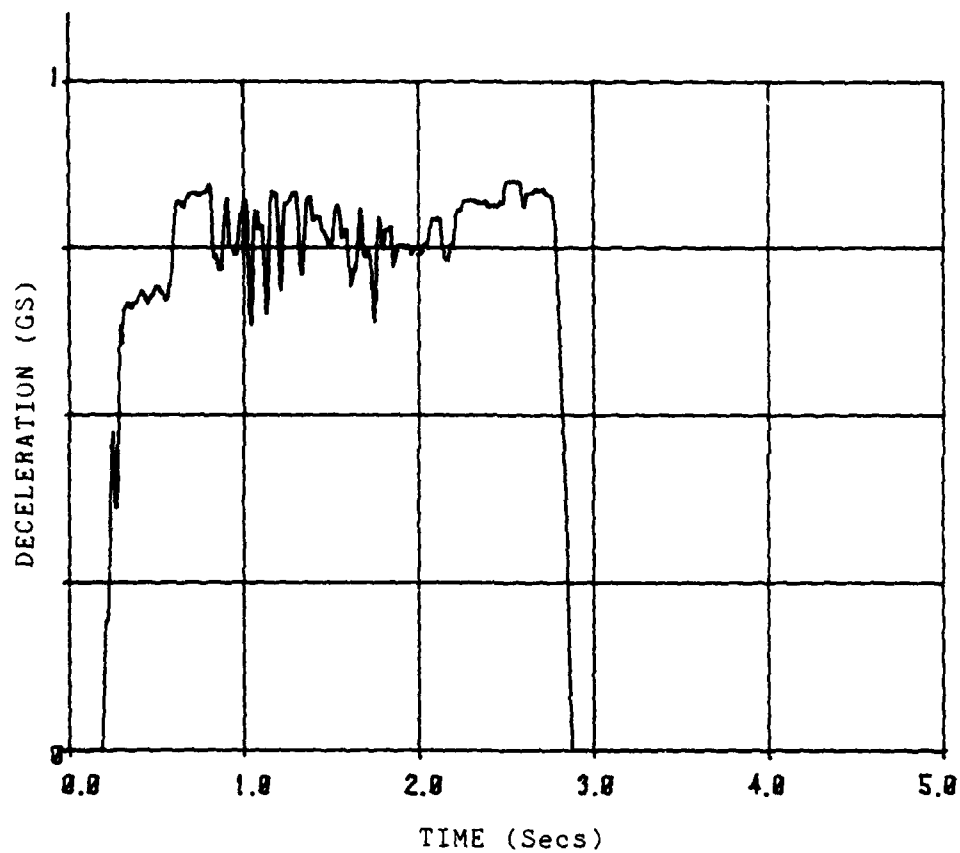


Figure A.2 Deceleration vs. Time June 17, 1982 Test Two  
Unfiltered

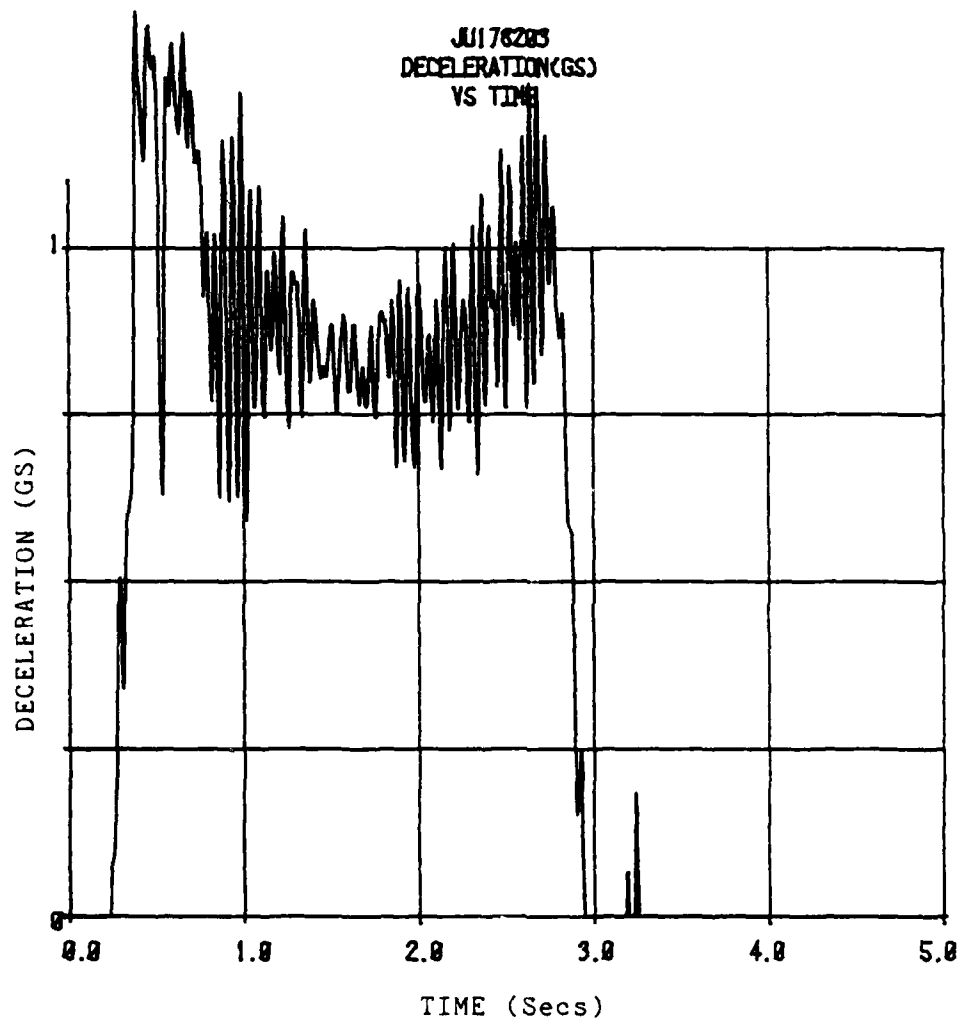


Figure A.3 Deceleration vs. Time June 17, 1982 Test  
Three Unfiltered

JU178281  
DECELERATION(GS)  
VS TIME

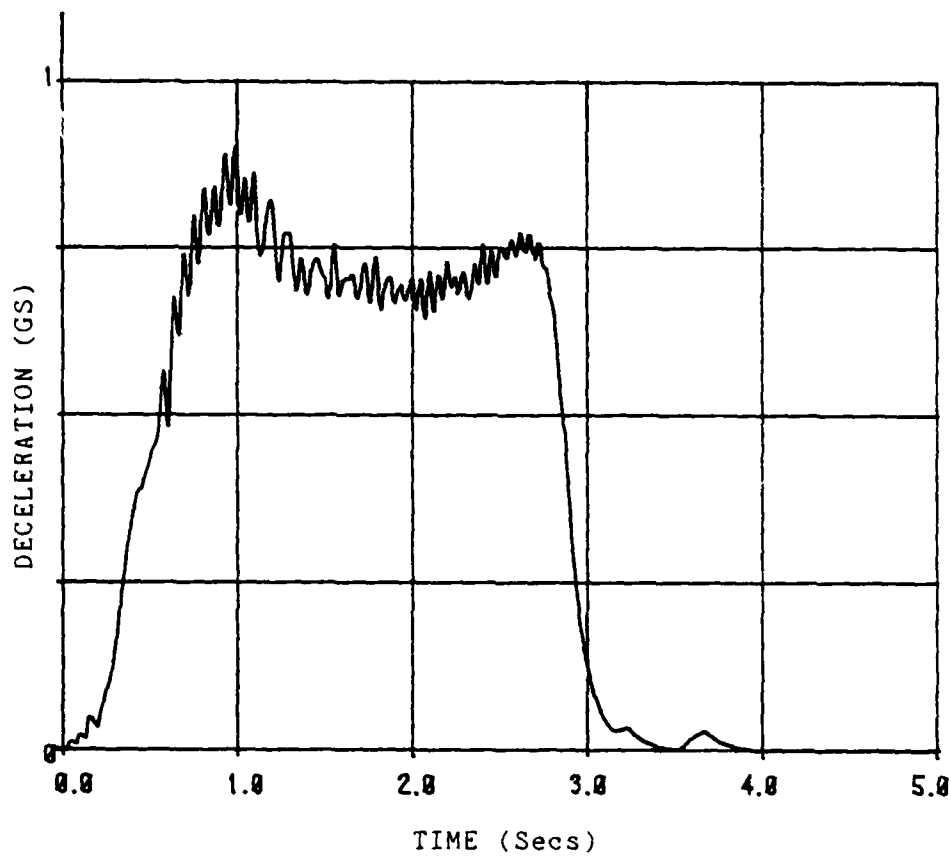


Figure A.4 Deceleration vs. Time June 17, 1982 Test One  
Filtered

JU178282  
DECELERATION(GS)  
VS TIME

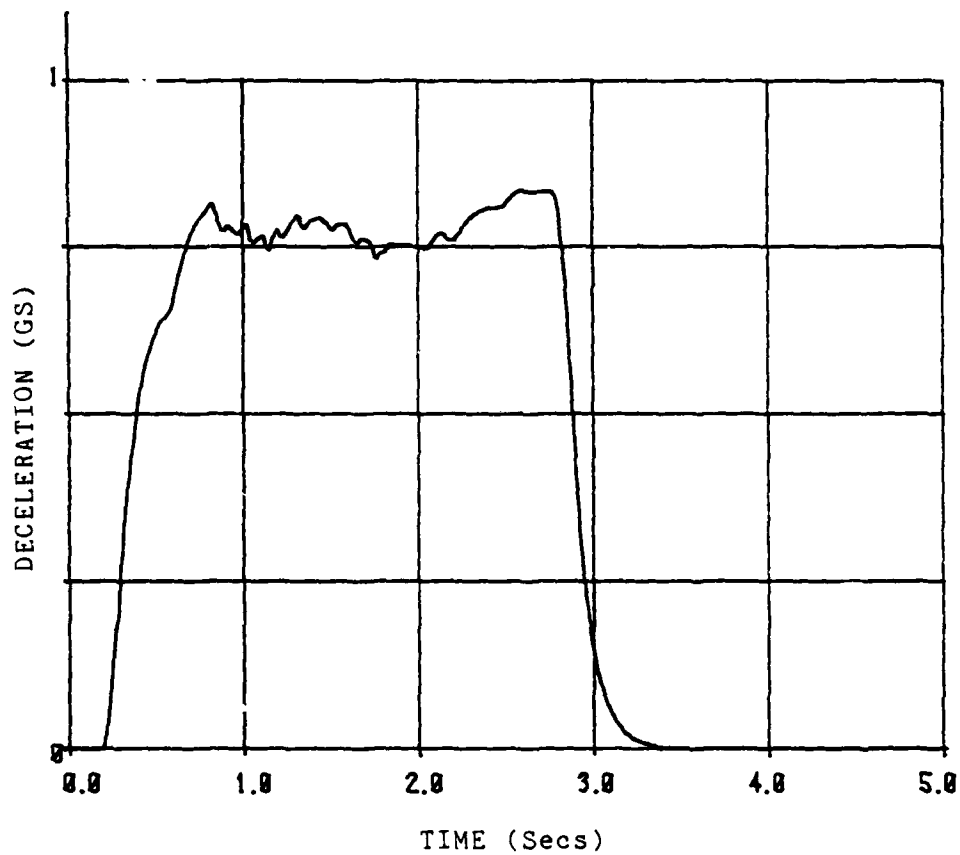


Figure A.5 Deceleration vs. Time June 17, 1982 Test Two  
Filtered

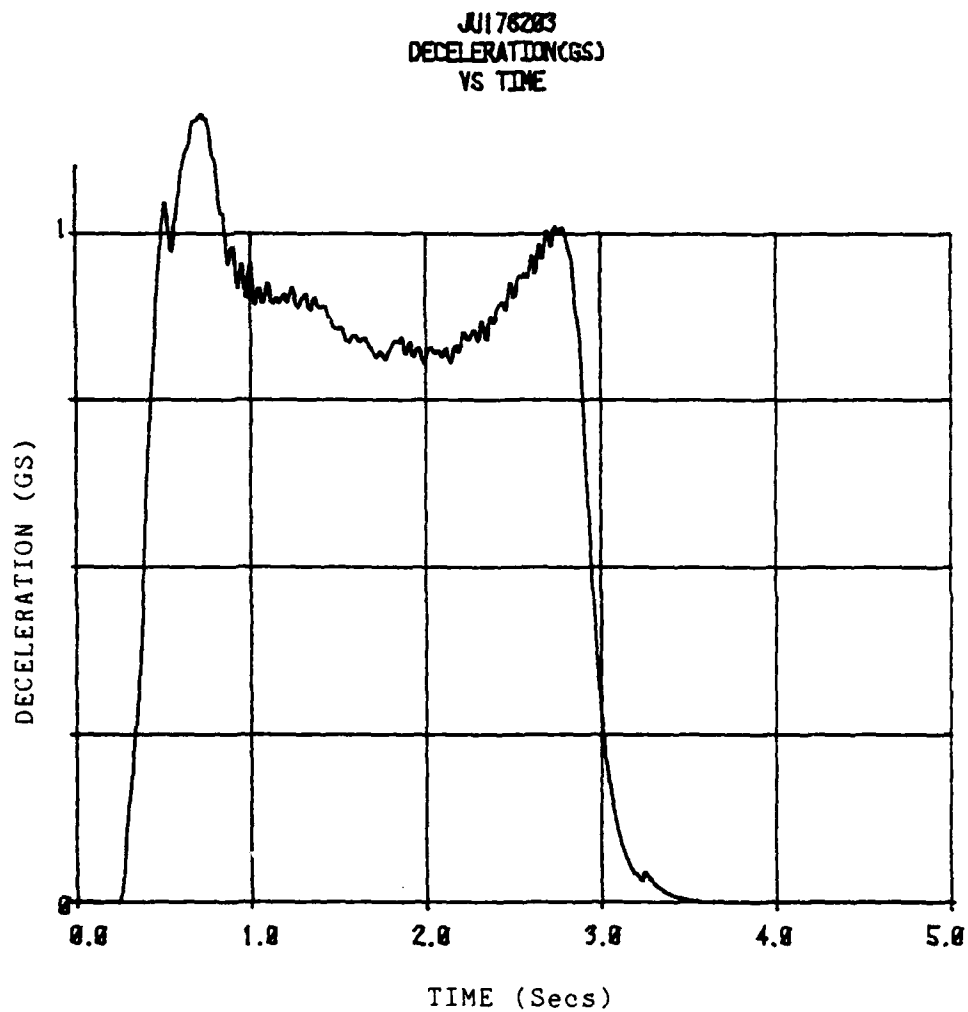


Figure A.6 Deceleration vs. Time June 17, 1982 Test  
Three Filtered



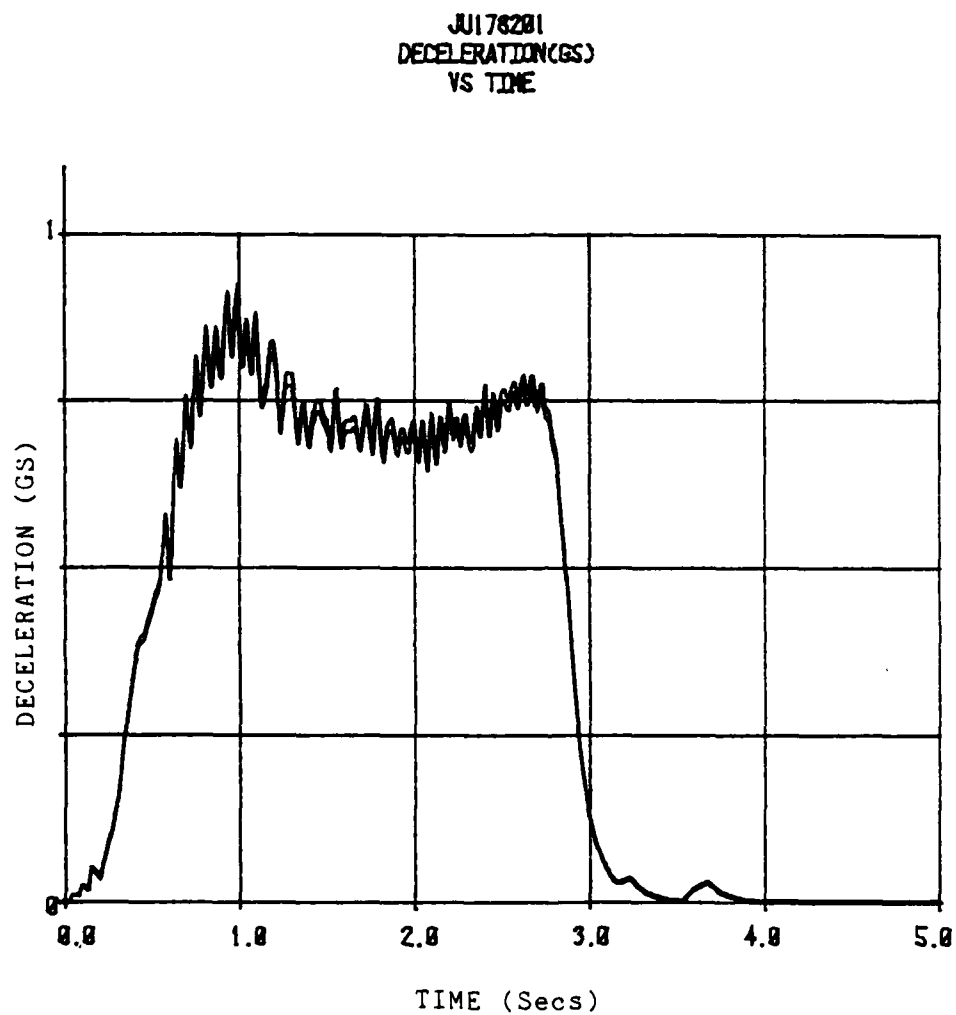


Figure A.7 Deceleration vs. Time June 17, 1982 Test One  
Filtered One-G Calibration Range

JU178282  
DECELERATION(GS)  
VS TIME

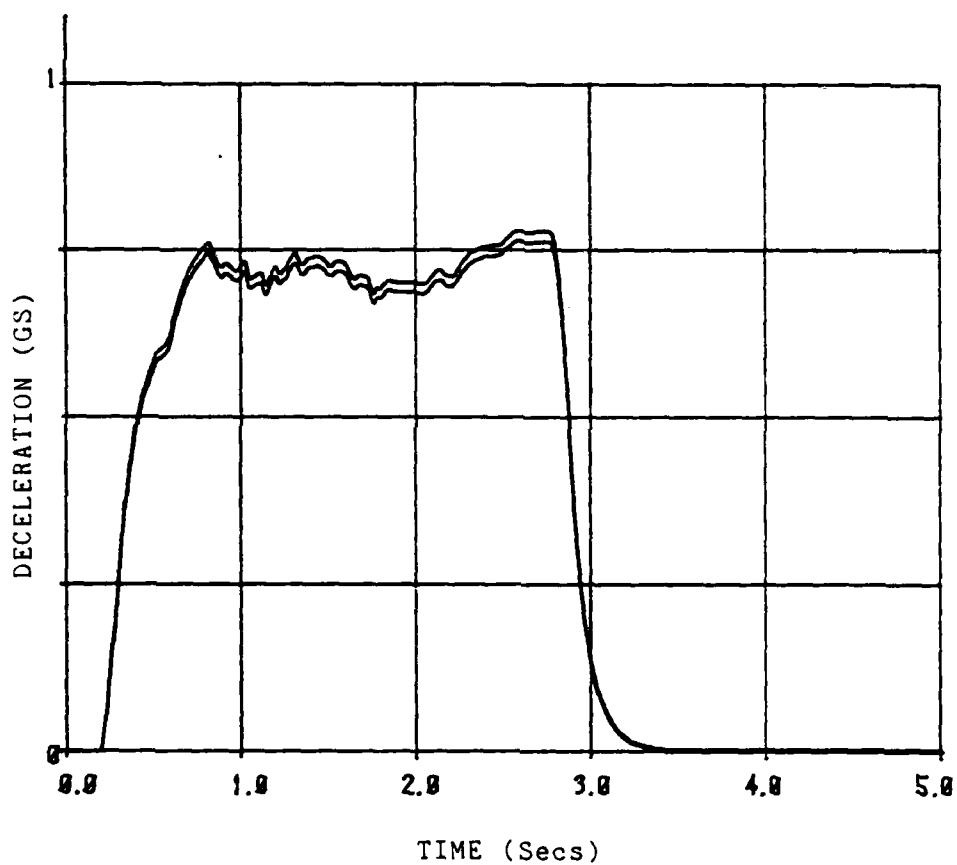


Figure A.8 Deceleration vs. Time June 17, 1982 Test Two  
Filtered One-G Calibration Range

JU176283  
DECELERATION(GS)  
VS TIME

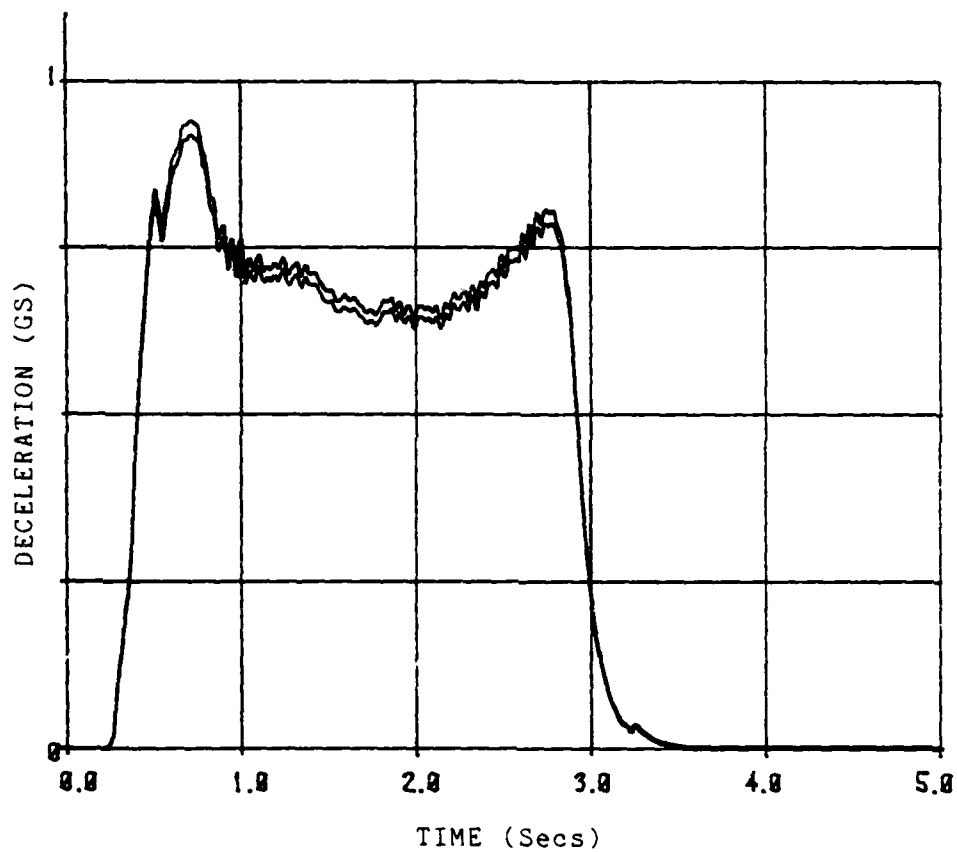


Figure A.9 Deceleration vs. Time June 17, 1982 Test  
Three Filtered One-G Calibration Range

JU178281  
VELOCITY (FT/SEC)  
VS TIME

FINAL VELOCITY = 0.0 FT/SEC

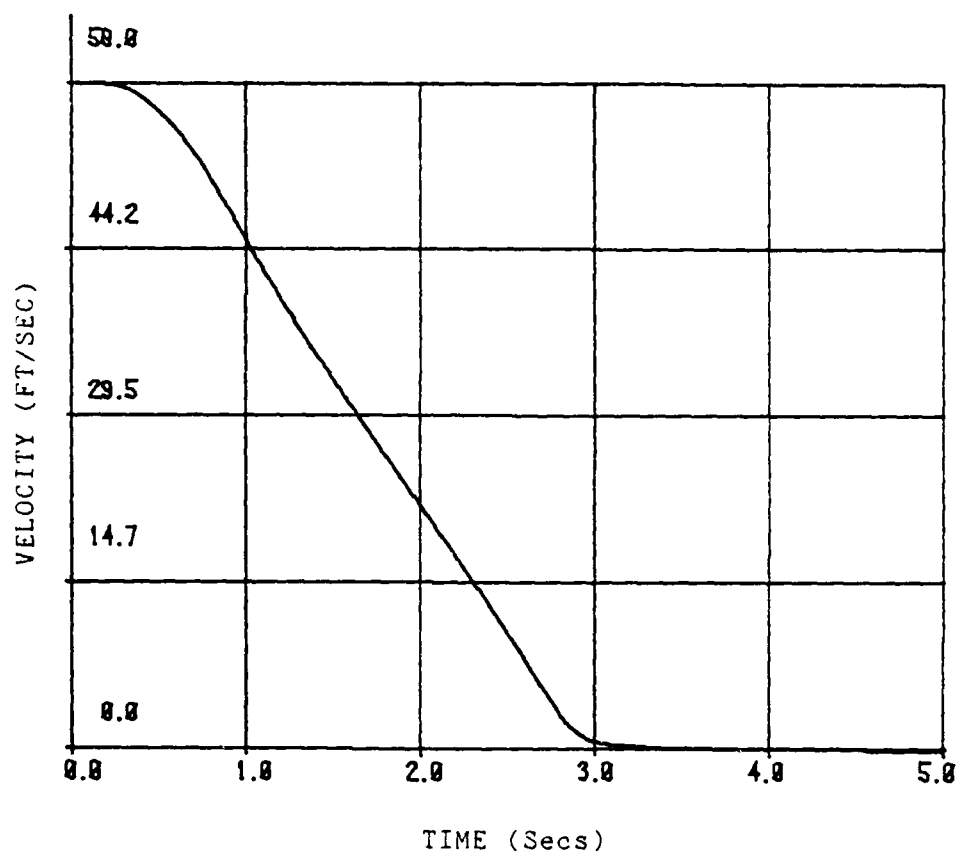


Figure A.10 Velocity vs. Time June 17, 1982 Test One

JU178202  
VELOCITY (FT/SEC)  
VS TIME

FINAL VELOCITY = 0.0 FT/SEC

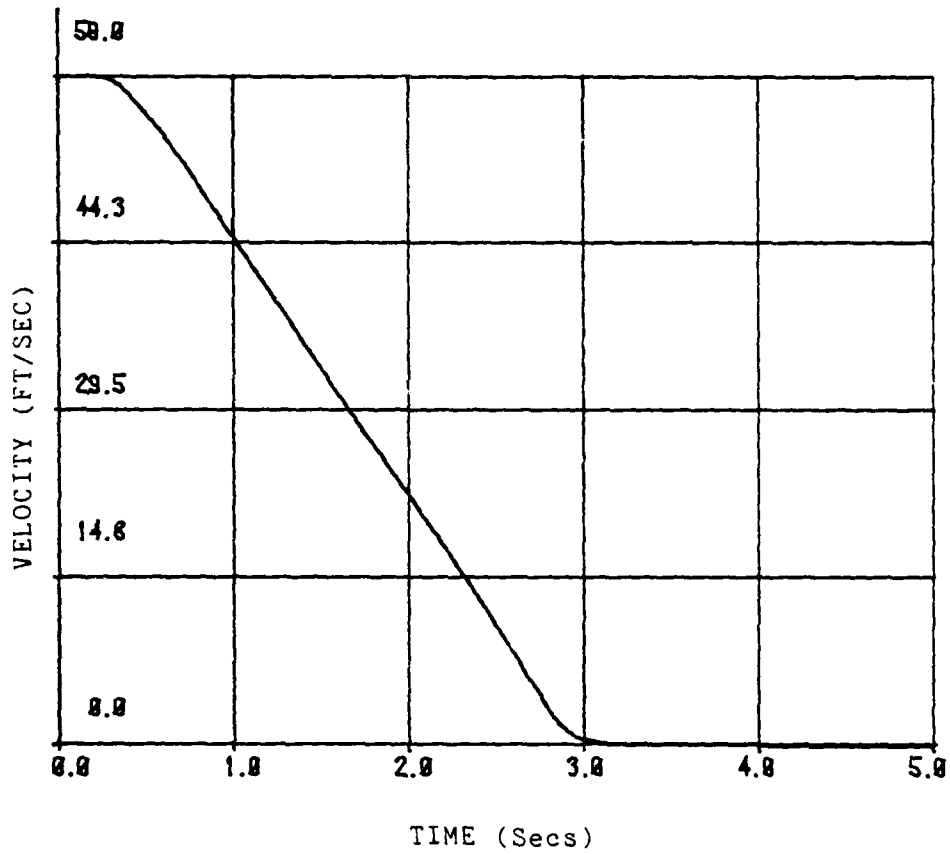


Figure A.11 Velocity vs. Time June 17, 1982 Test Two

JU176283  
VELOCITY (FT/SEC)  
VS TIME

FINAL VELOCITY = 8.8 FT/SEC

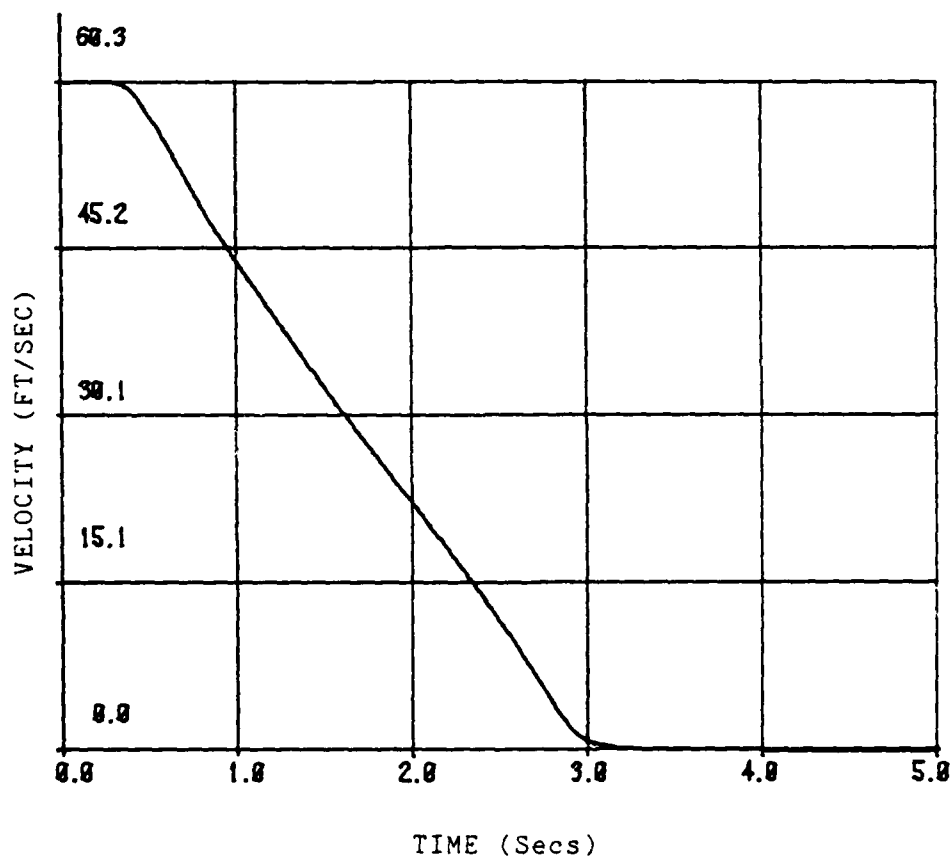


Figure A.12 Velocity vs. Time June 17, 1962 Test Three

JU178201  
DISTANCE (FEET)  
VS TIME  
(ACCEL)

FINAL VELOCITY = 0.0 FT/SEC

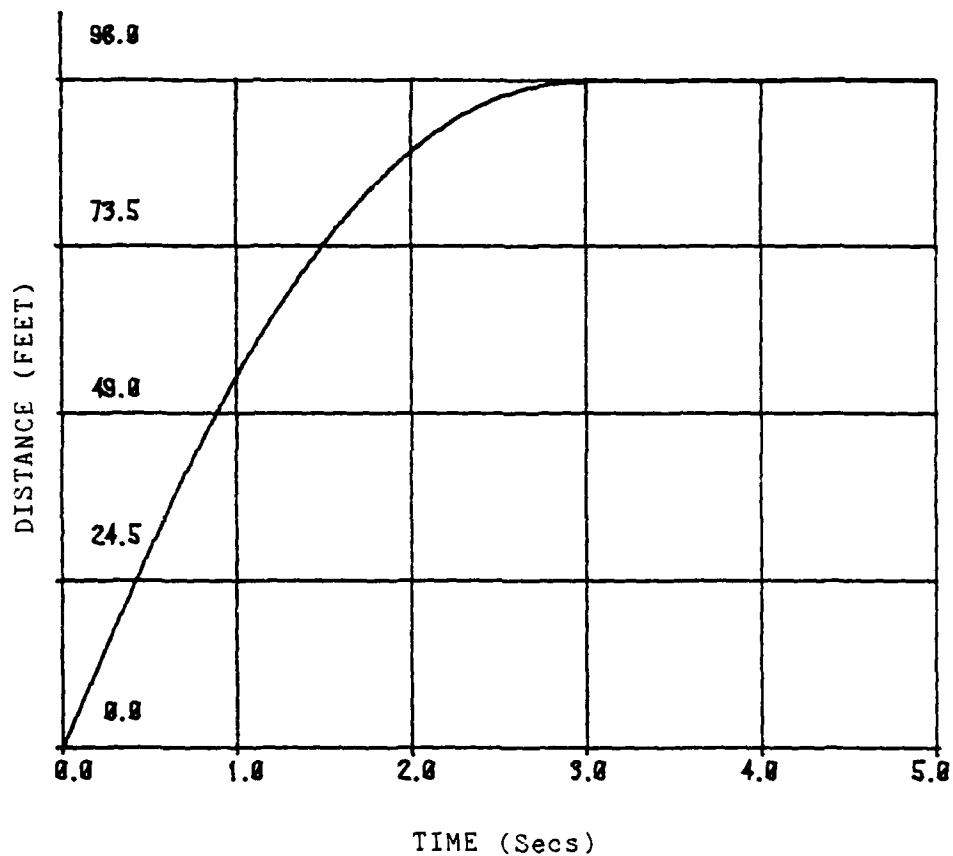


Figure A.13 Distance vs. Time June 17, 1982 Test One

JU178202  
DISTANCE (FEET)  
VS TIME  
(ACCEL)

FINAL VELOCITY = 0.0 FT/SEC

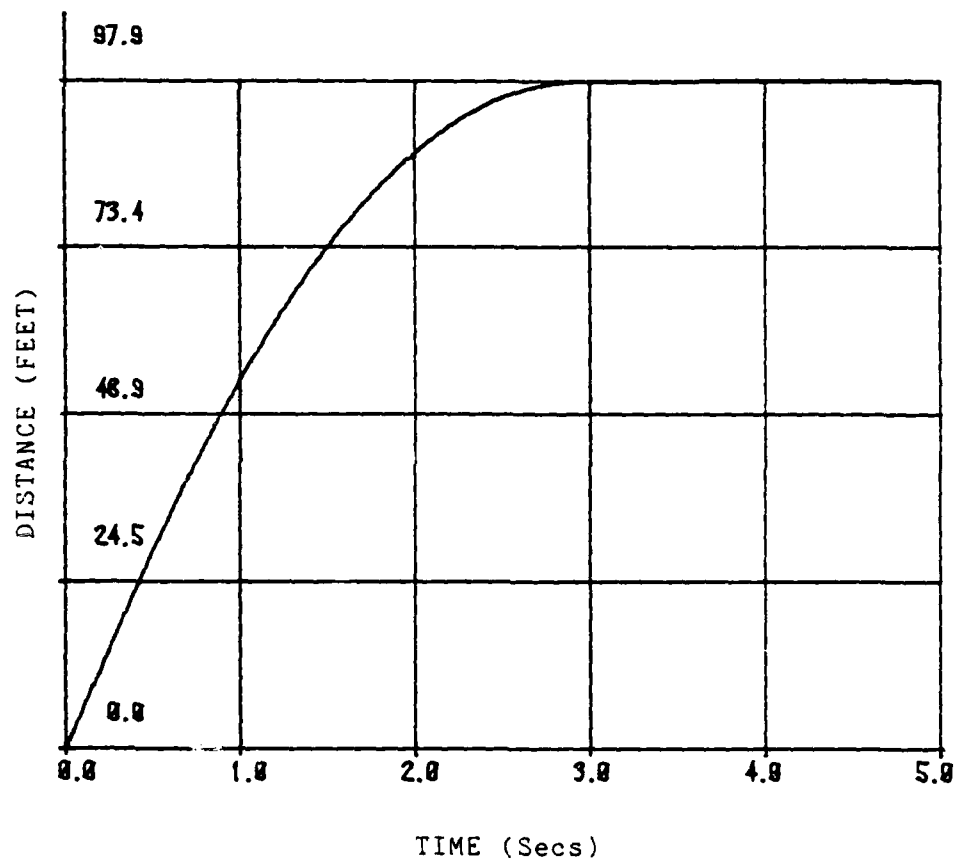


Figure A.14 Distance vs. Time June 17, 1982 Test Two



JU176283  
DISTANCE (FEET)  
VS TIME  
(ACCEL)

FINAL VELOCITY = 0.0 FT/SEC

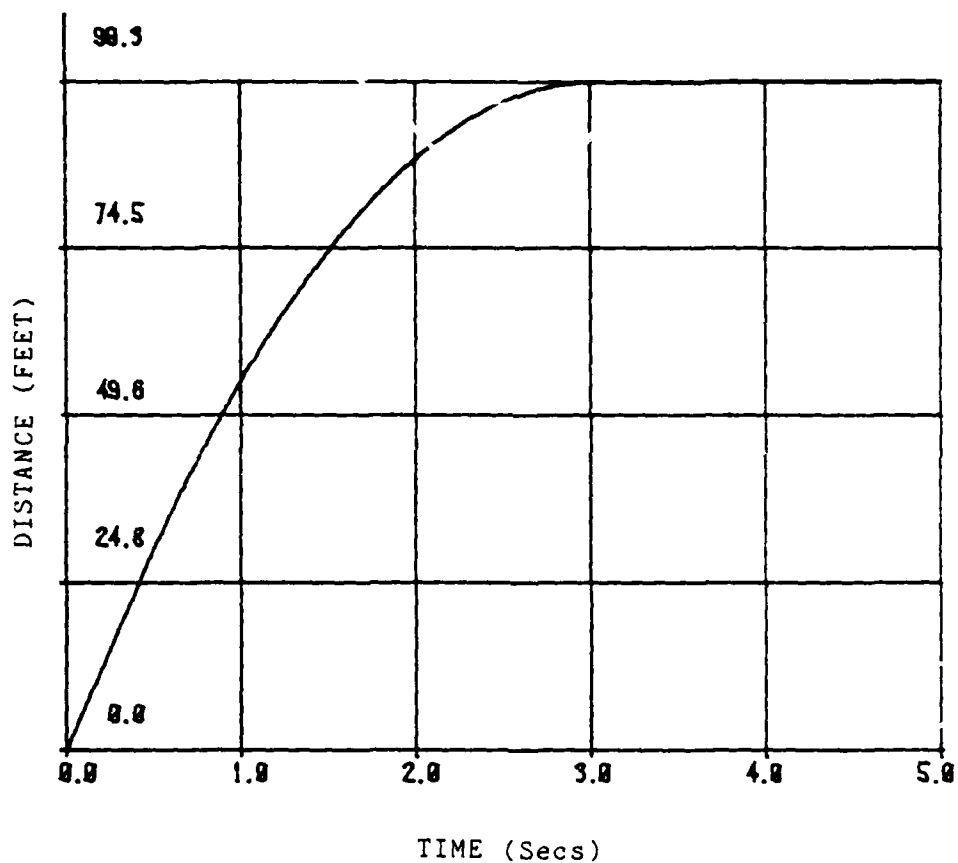


Figure A.15 Distance vs. Time June 17, 1982 Test Three

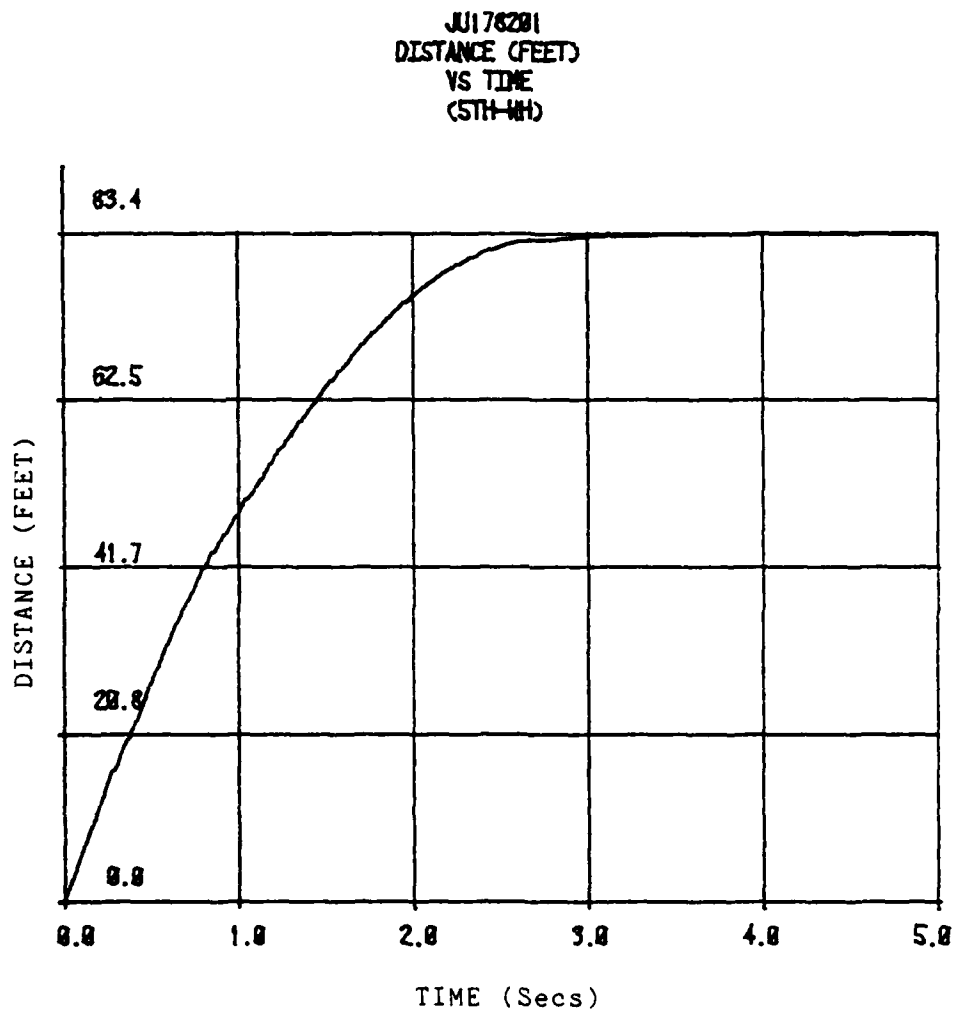


Figure A.16 Distance vs. Time June 17, 1982 Test One  
Fifth-Wheel Data

JU176282  
DISTANCE (FEET)  
VS TIME  
(STH-WH)

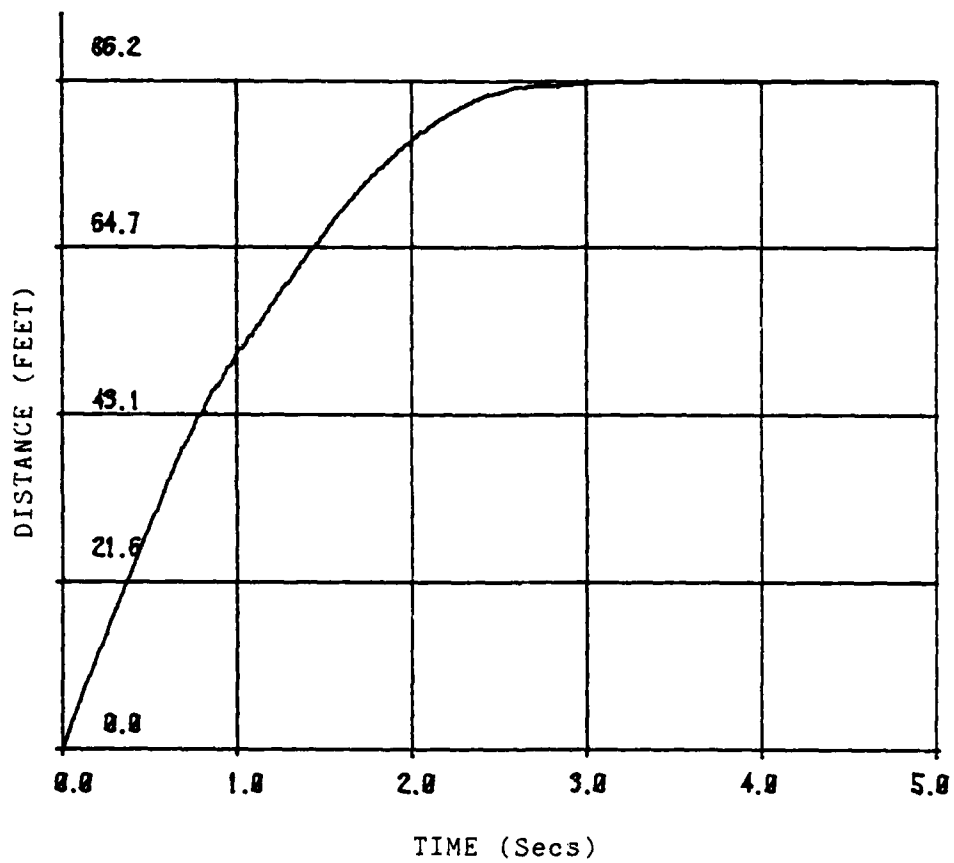


Figure A.17 Distance vs. Time June 17, 1982 Test Two  
Fifth-Wheel Data

JU178283  
DISTANCE (FEET)  
VS TIME  
(5TH-WHEEL)

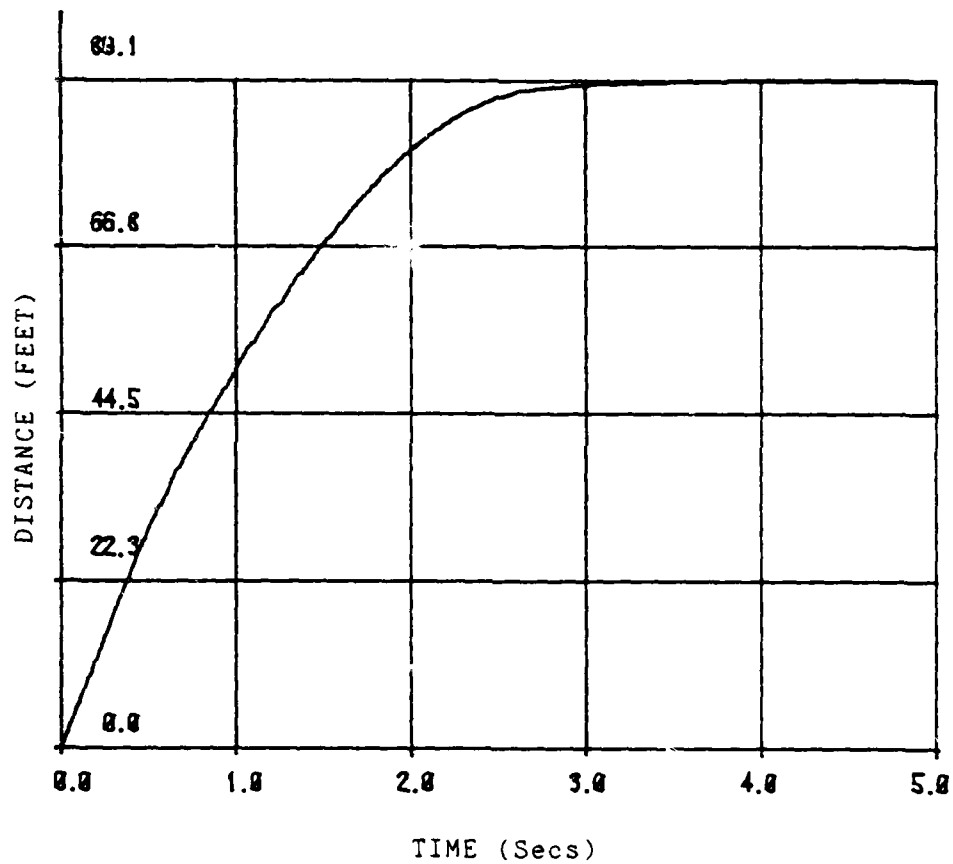


Figure A.18 Distance vs. Time June 17, 1982 Test Three  
Fifth-Wheel Data

APPENDIX

B

FIGURES FOR TEST SITE THREE

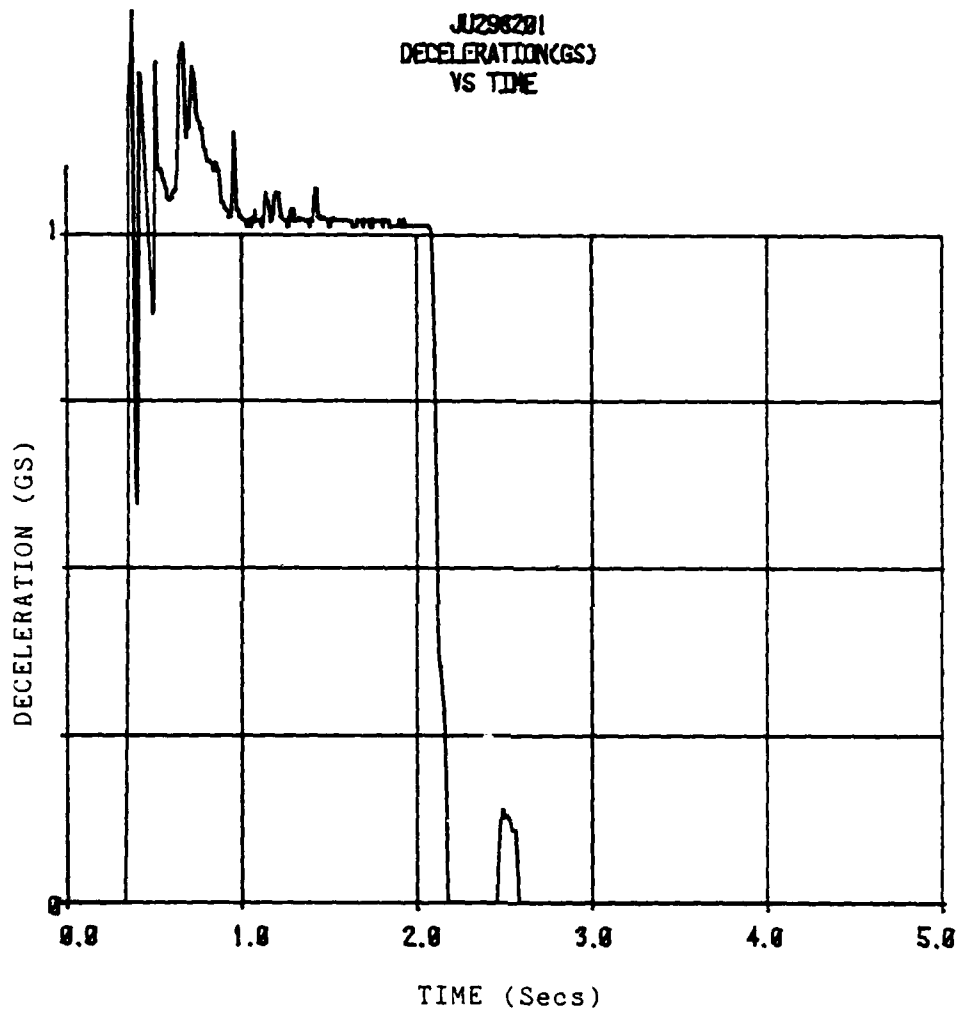


Figure B.1 Deceleration vs. Time June 29, 1982 Test One  
Unfiltered

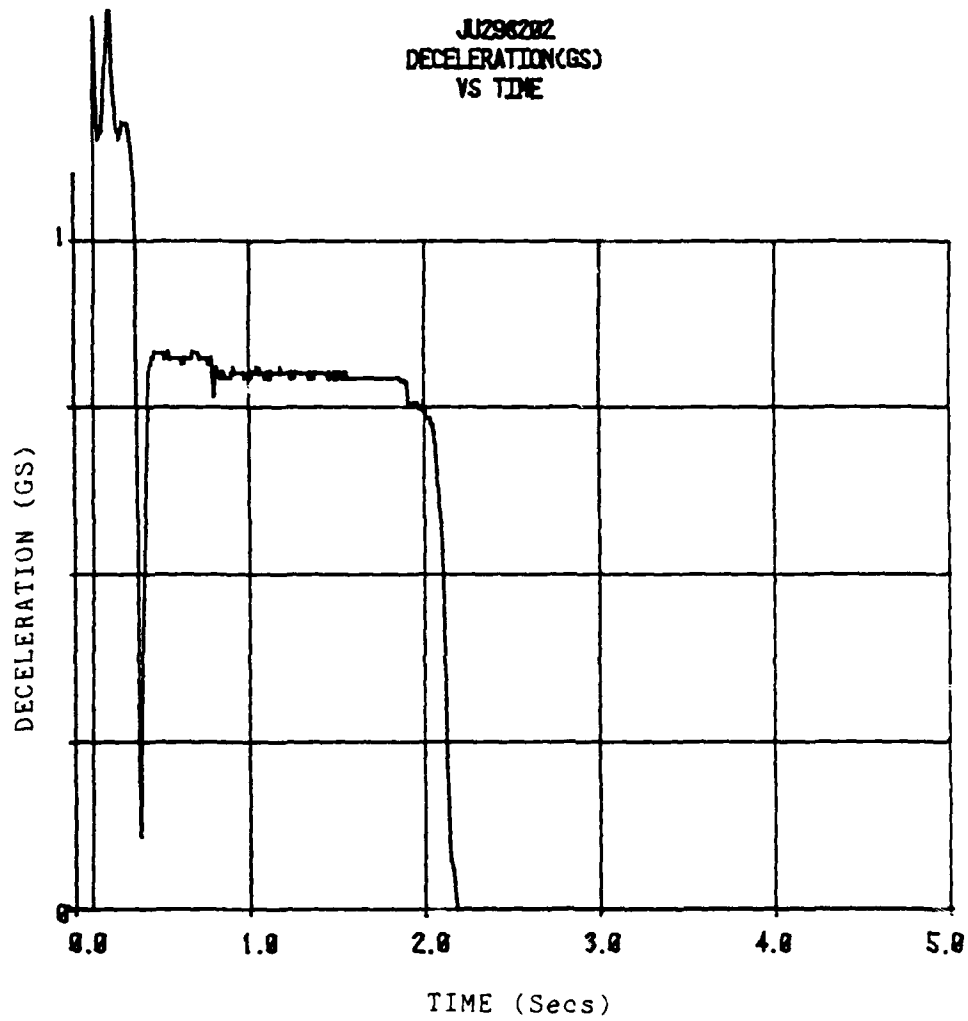


Figure B.2 Deceleration vs. Time June 29, 1982 Test Two  
Unfiltered

JJ296283  
DECELERATION(GS)  
VS TIME

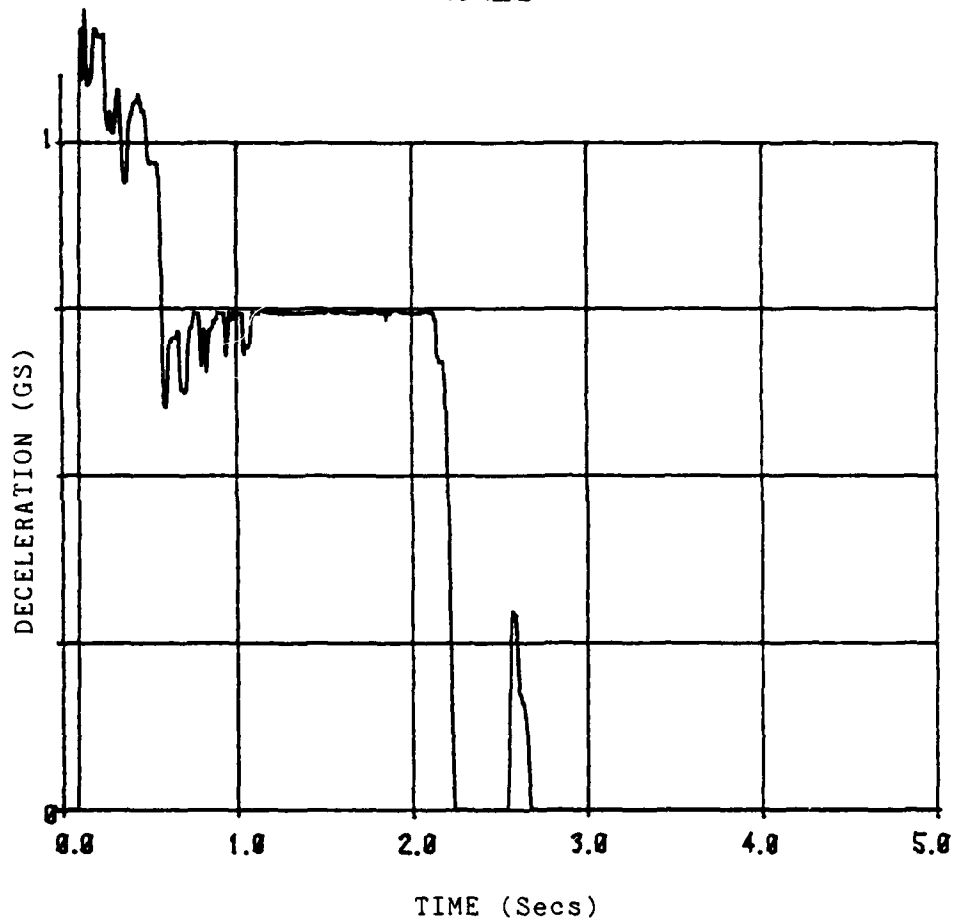


Figure B.3 Deceleration vs. Time June 29, 1982 Test  
Three Unfiltered



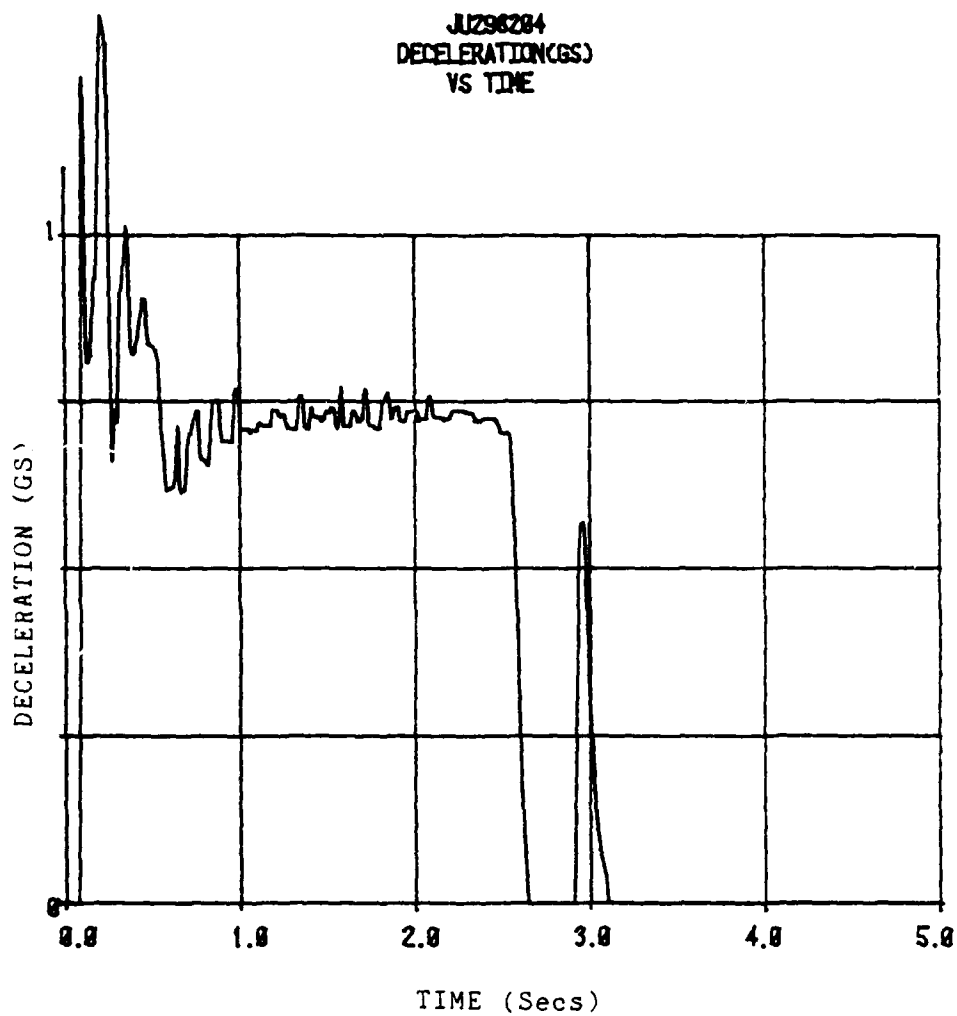


Figure B.4 Deceleration vs. Time June 29, 1982 Test Four  
Unfiltered

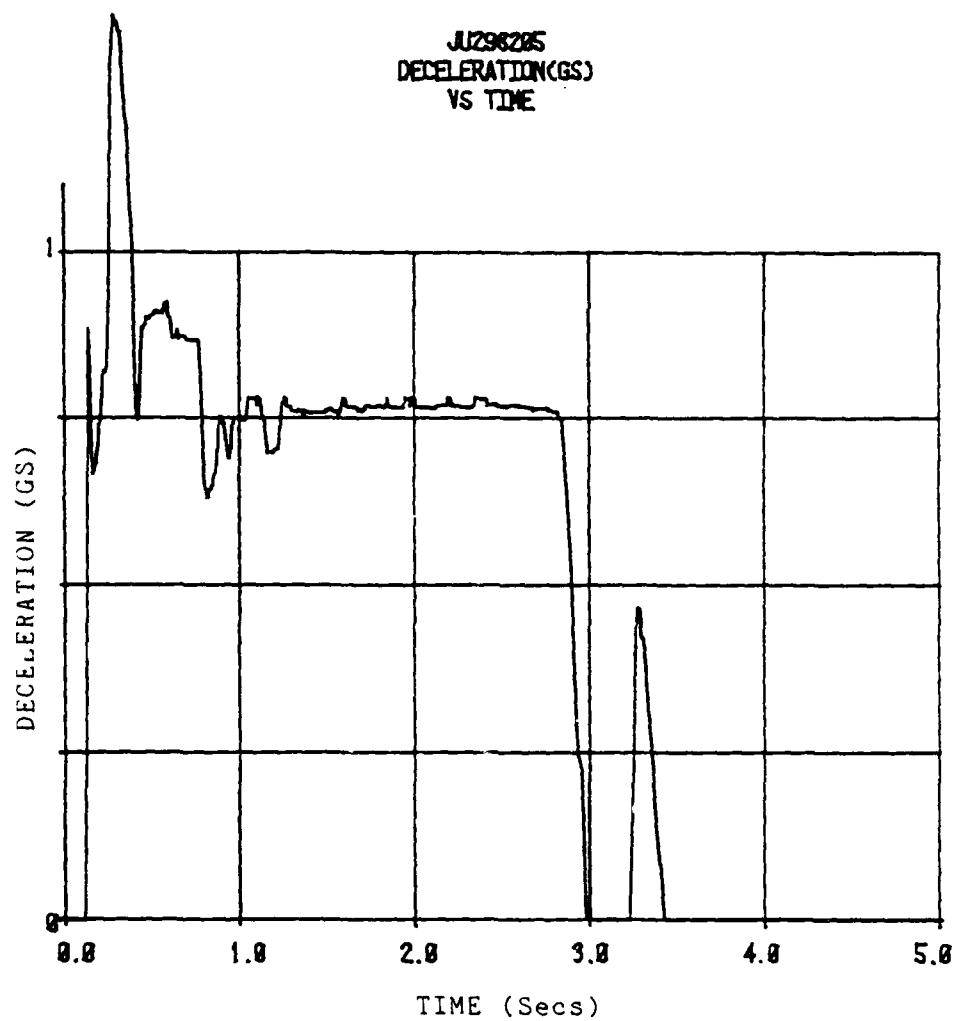


Figure B.5 Deceleration vs. Time June 29, 1982 Test Five  
Unfiltered

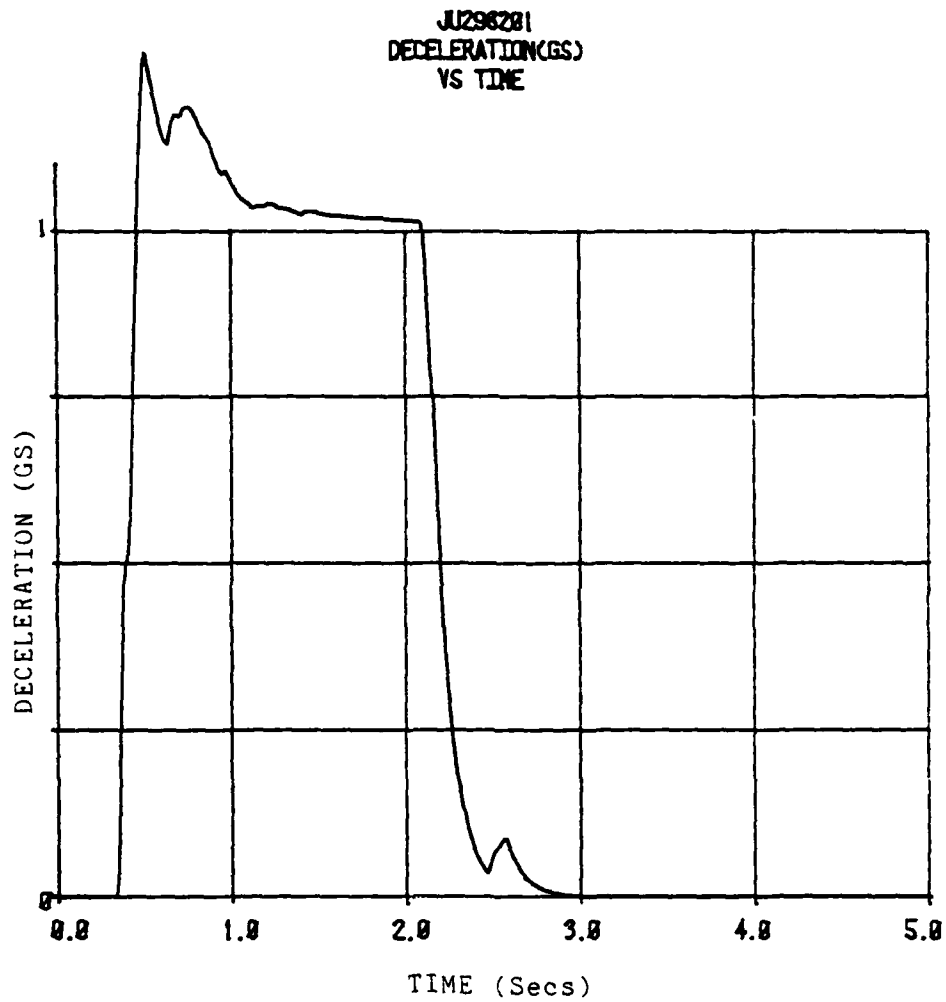


Figure B.6 Deceleration vs. Time June 29, 1982 Test One  
Filtered

JJ296282  
DECELERATION(GS)  
VS TIME

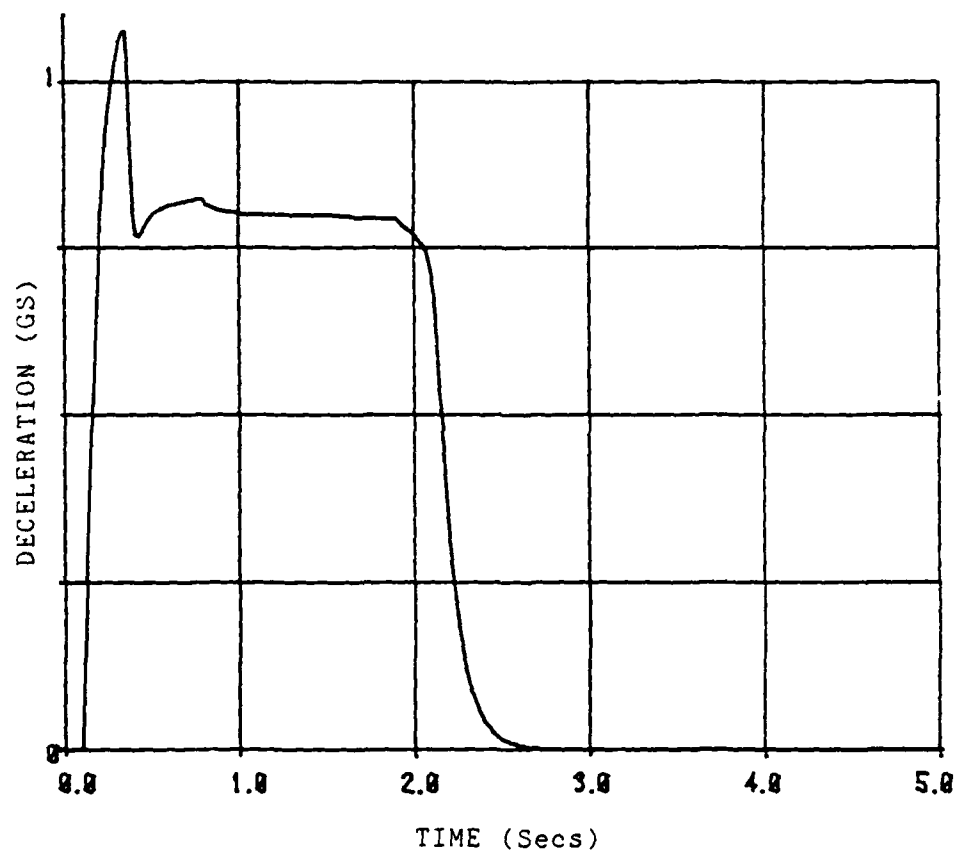


Figure B.7 Deceleration vs. Time June 29, 1982 Test Two  
Filtered

JJ298283  
DECELERATION(GS)  
VS TIME

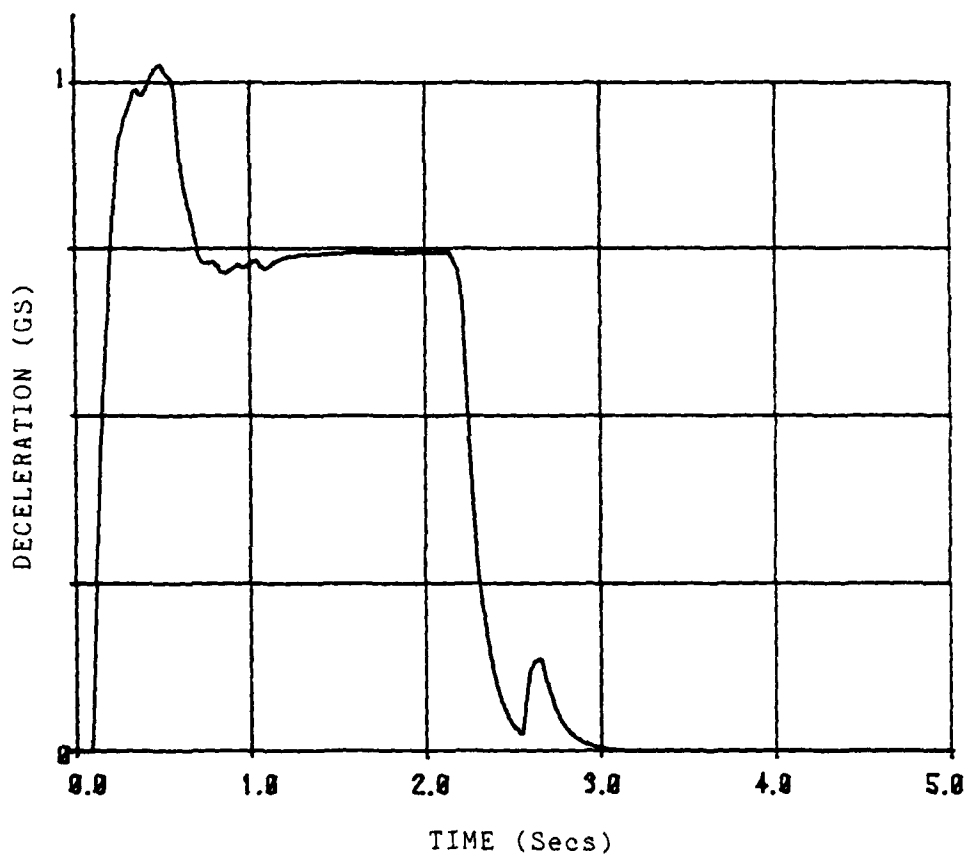


Figure B.8 Deceleration vs. Time June 29, 1982 Test  
Three Filtered

.J1298284  
DECELERATION(GS)  
VS TIME

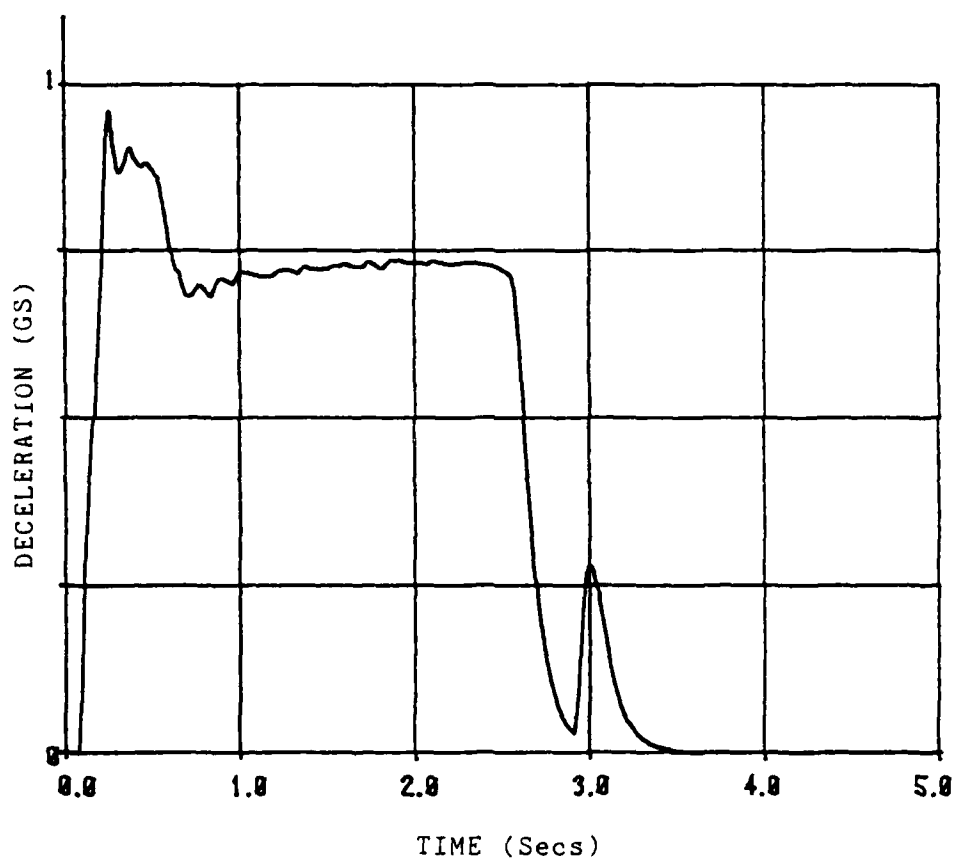


Figure B.9 Deceleration vs. Time June 29, 1982 Test Four  
Filtered

JUZ90205  
DECELERATION(GS)  
VS TIME

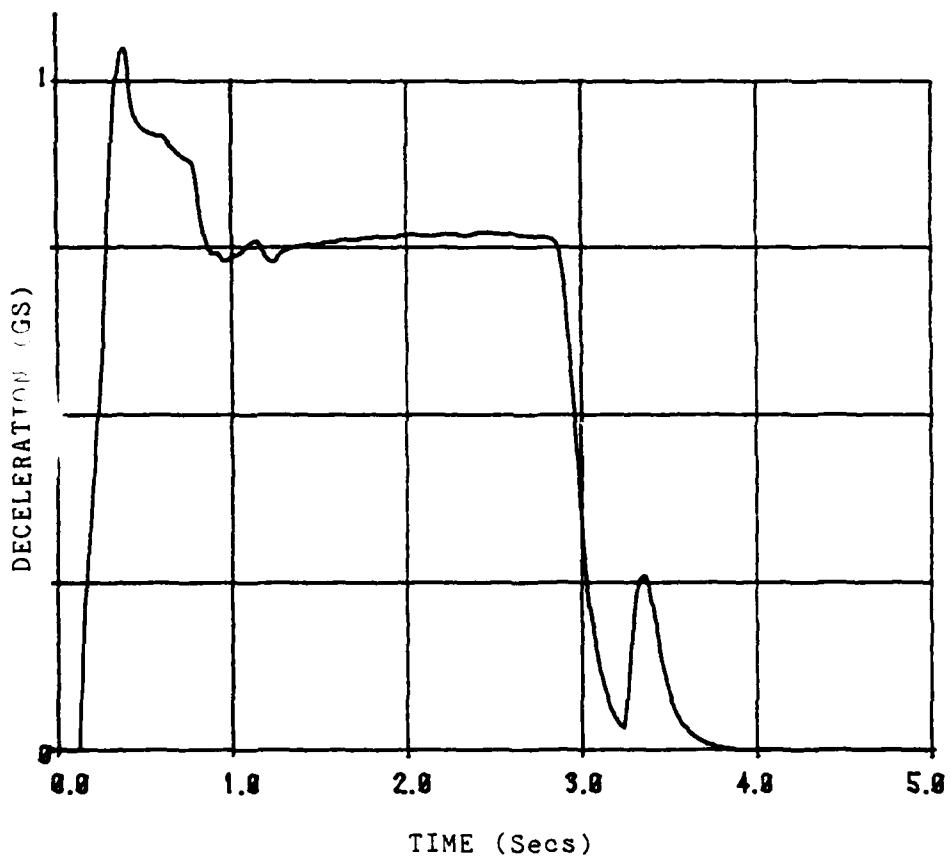


Figure B.10 Deceleration vs. Time June 29, 1982 Test  
Five Filtered

JJ298281  
DECELERATION(GS)  
VS TIME

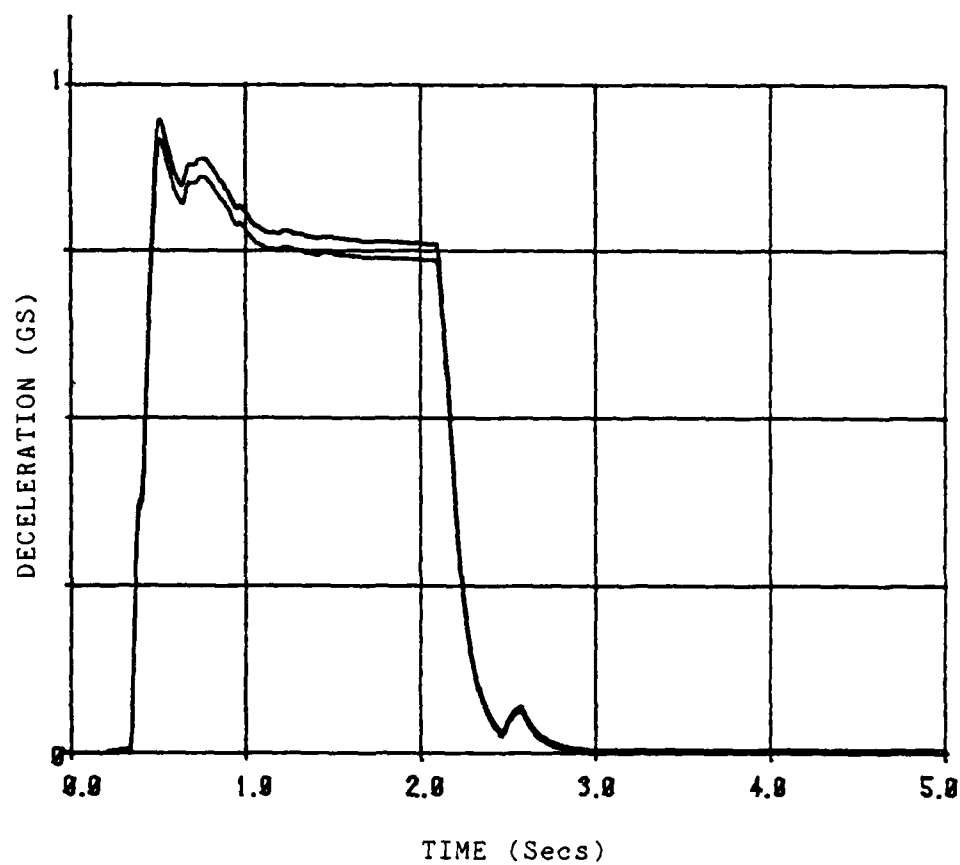


Figure B.11 Deceleration vs. Time June 29, 1982 Test One  
Filtered One-G Calibration Range



JUZ98282  
DECELERATION(GS)  
VS TIME

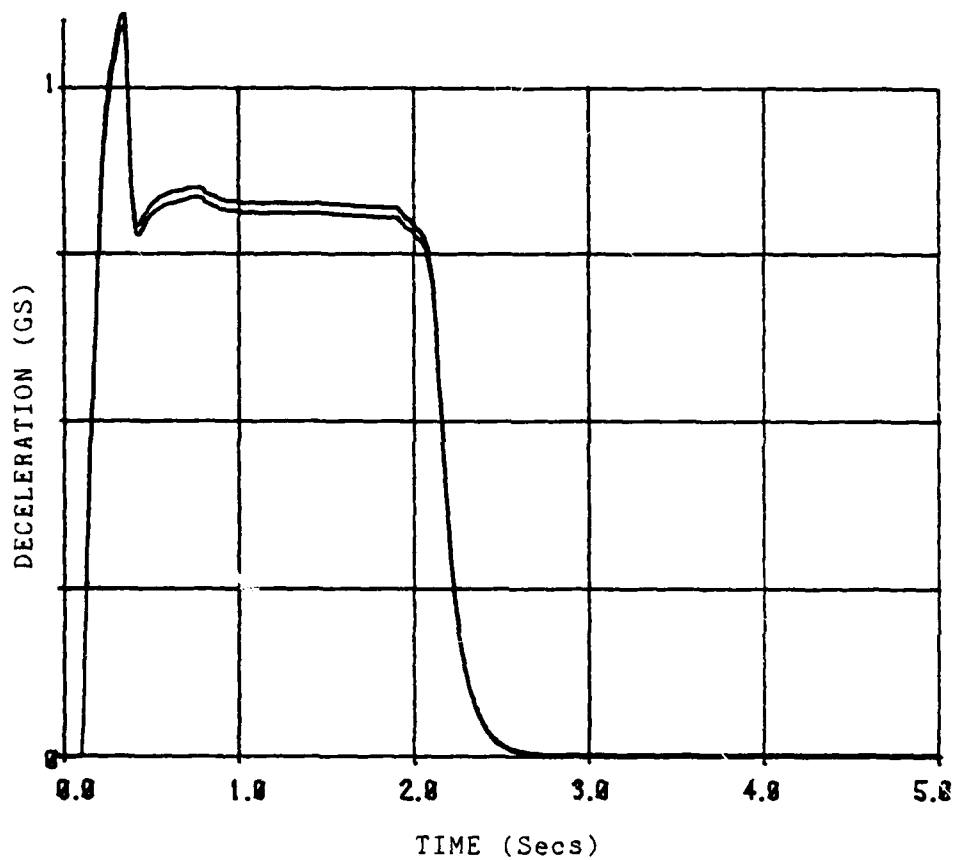


Figure B.12 Deceleration vs. Time June 29, 1982 Test Two  
Filtered One-G Calibration Range

JUZ98283  
DECELERATION(GS)  
VS TIME

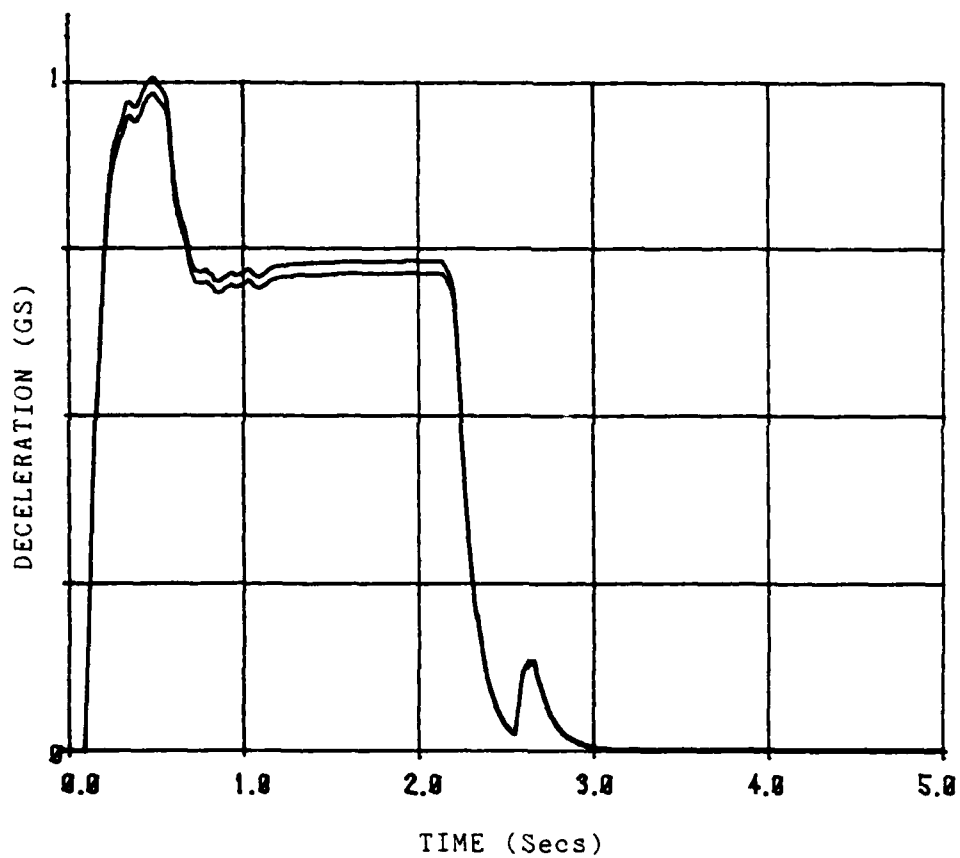


Figure B.13 Deceleration vs. Time June 29, 1982 Test  
Three Filtered One-G Calibration Range

JU298284  
DECELERATION(GS)  
VS TIME

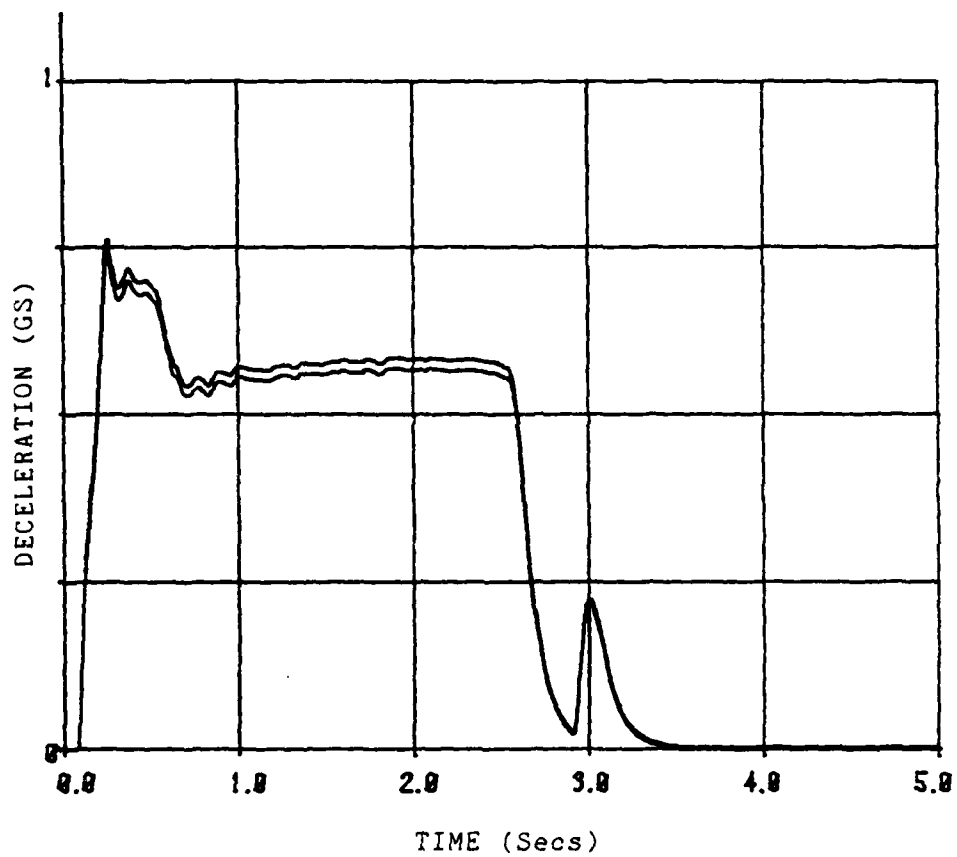


Figure B.14 Deceleration vs. Time June 29, 1982 Test  
Four Filtered One-G Calibration Range

JJ298205  
DECELERATION(GS)  
VS TIME

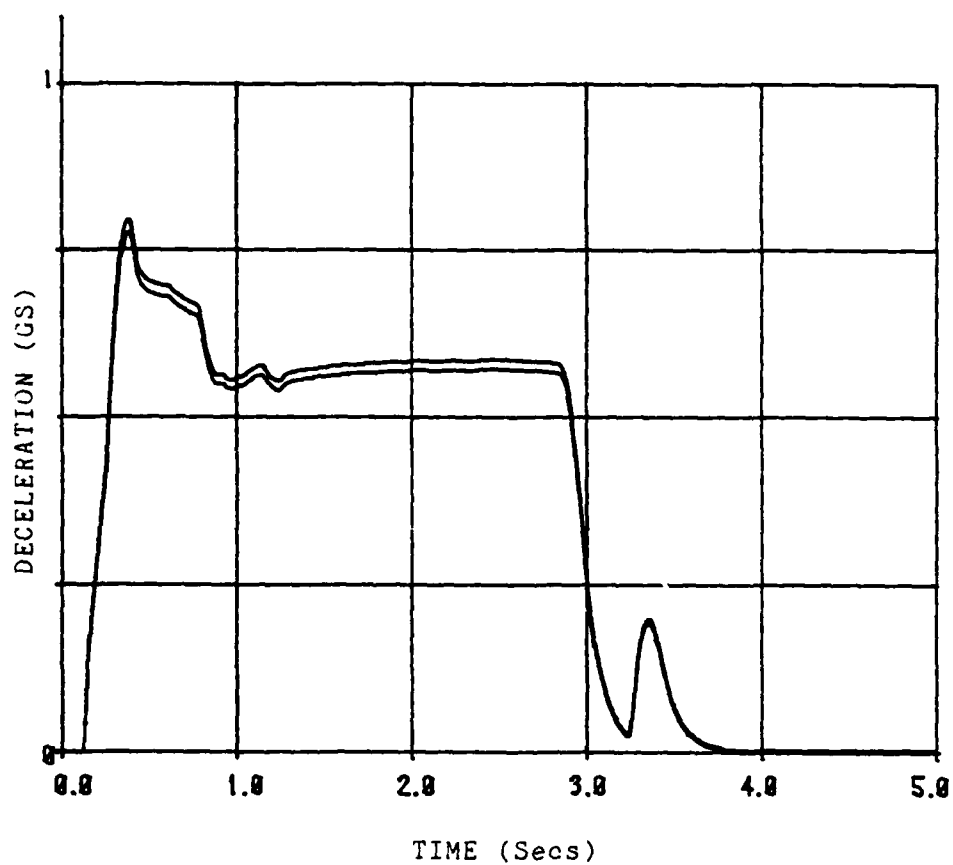


Figure B.15 Deceleration vs. Time June 29, 1982 Test  
Five Filtered One-G Calibration Range

JUZ98281  
VELOCITY (FT/SEC)  
VS TIME

FINAL VELOCITY = 0.0 FT/SEC

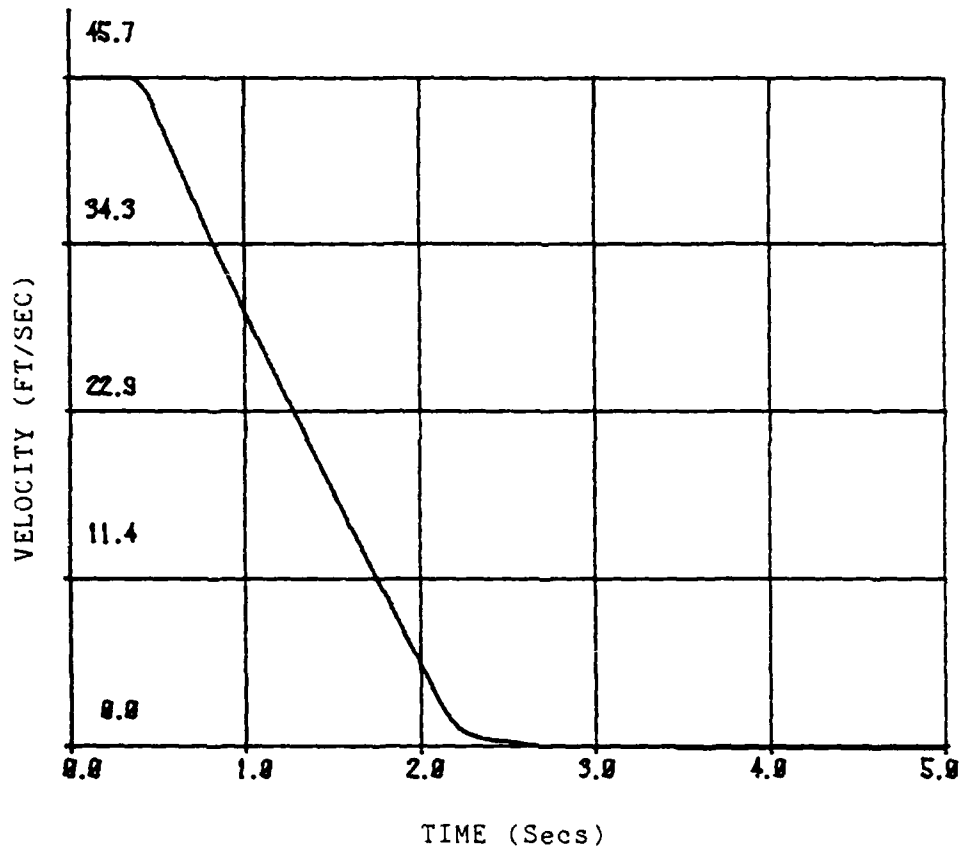


Figure B.16 Velocity vs. Time June 29, 1982 Test One

JJ296202  
VELOCITY (FT/SEC)  
VS TIME

FINAL VELOCITY = 8.8 FT/SEC

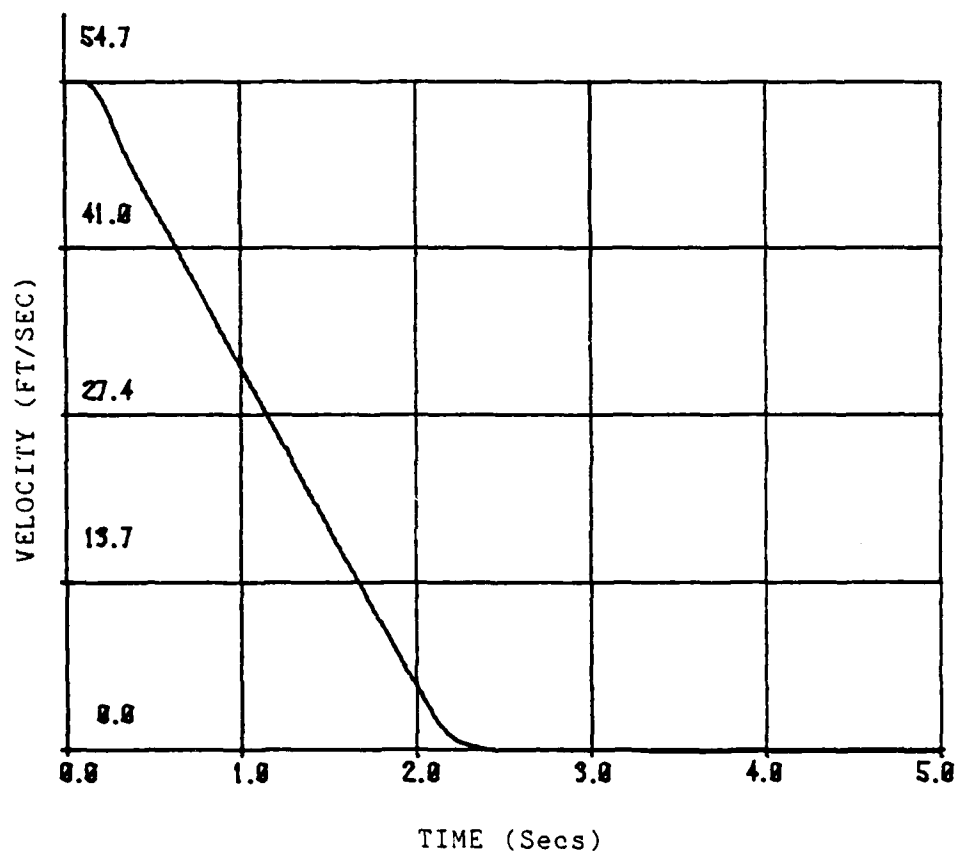


Figure B.17 Velocity vs. Time June 29, 1982 Test Two

JU296283  
VELOCITY (FT/SEC)  
VS TIME

FINAL VELOCITY = 0.8 FT/SEC

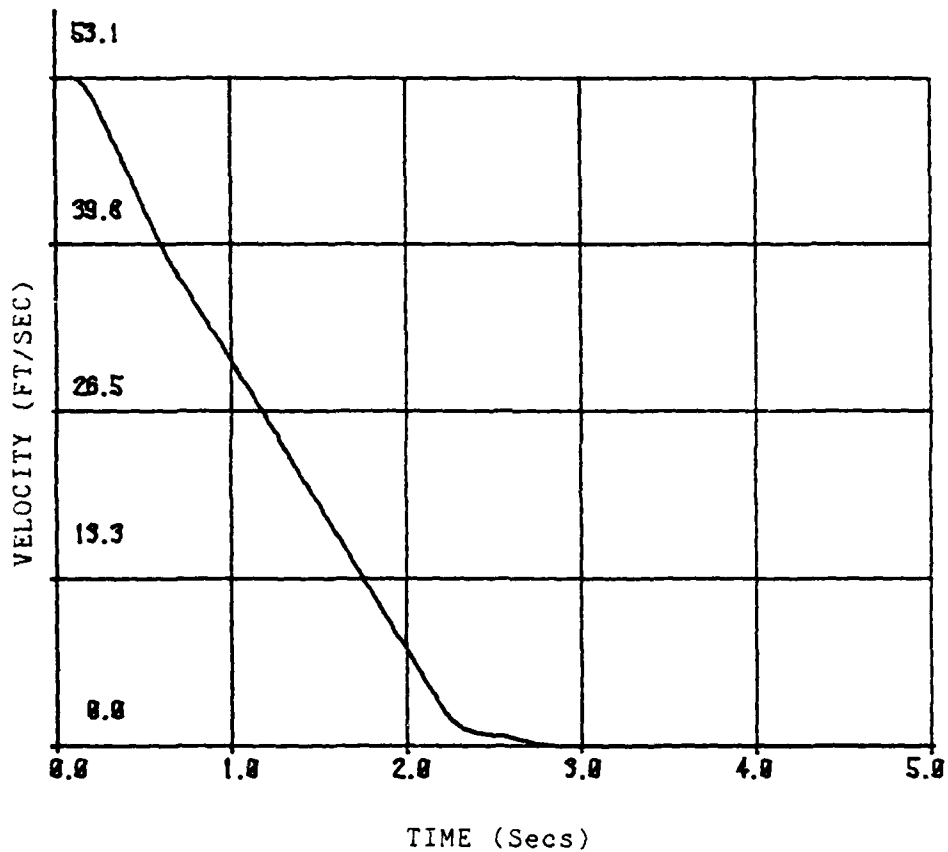


Figure B.18 Velocity vs. Time June 29, 1982 Test Three

JU298284  
VELOCITY (FT/SEC)  
VS TIME

FINAL VELOCITY = 0.0 FT/SEC

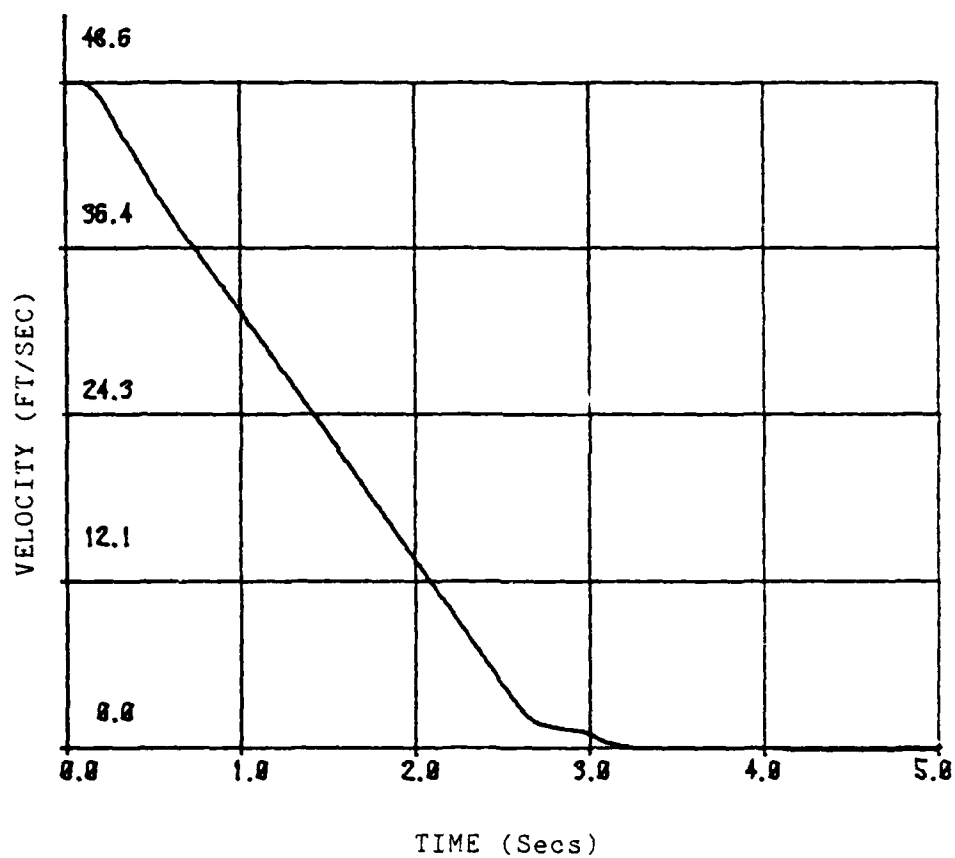


Figure B.19 Velocity vs. Time June 29, 1982 Test Four



JJ298285  
VELOCITY (FT/SEC)  
VS TIME

FINAL VELOCITY = 0.0 FT/SEC

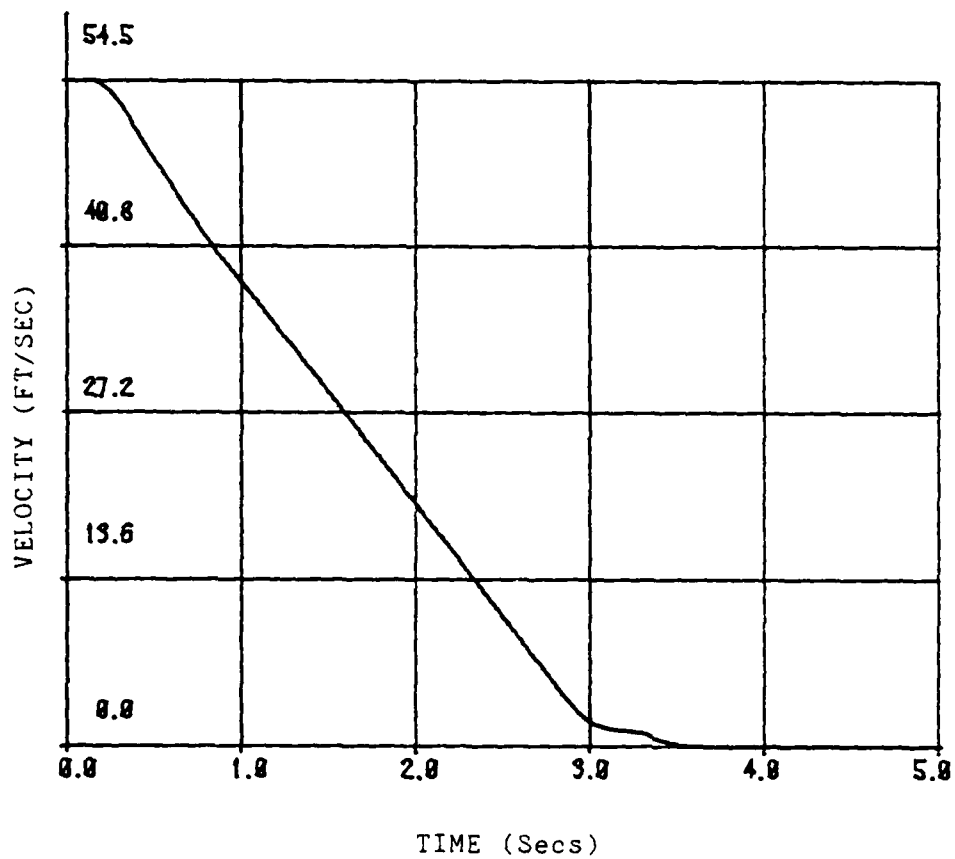


Figure B.20 Velocity vs. Time June 29, 1982 Test Five

JUZ98281  
DISTANCE (FEET)  
VS TIME  
(ACCEL)

FINAL VELOCITY = 8.8 FT/SEC

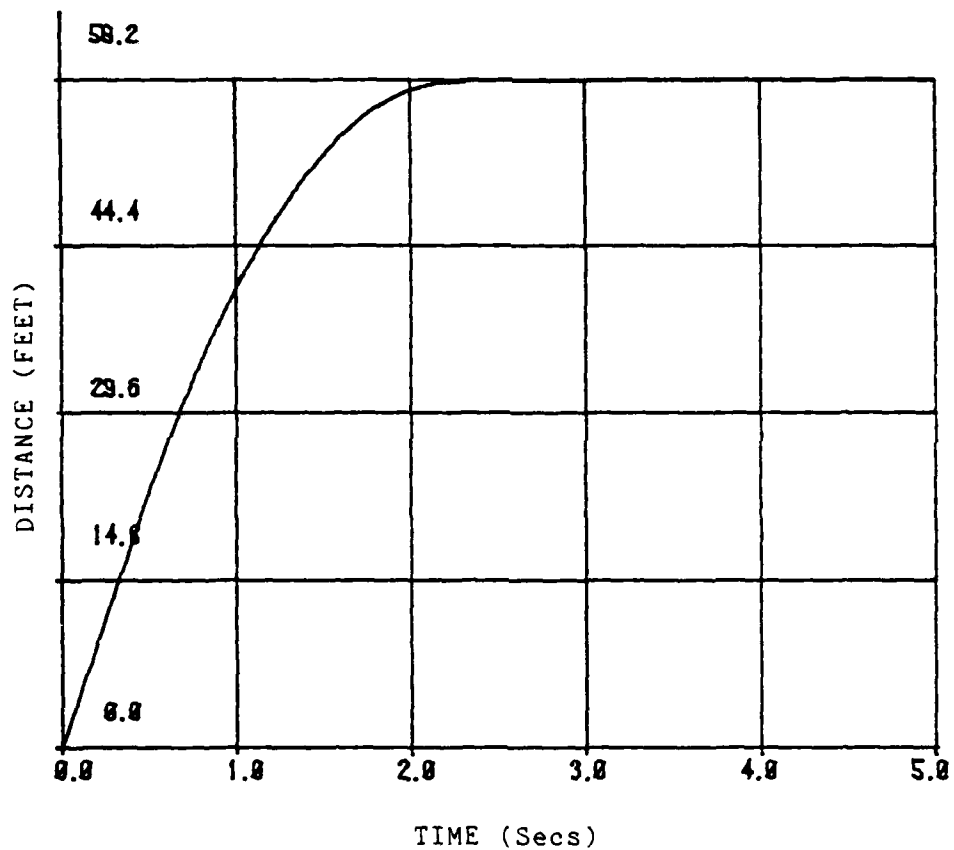


Figure B.21 Distance vs. Time June 29, 1982 Test One

JJ298282  
DISTANCE (FEET)  
VS TIME  
(ACCEL)

FINAL VELOCITY = 8.8 FT/SEC

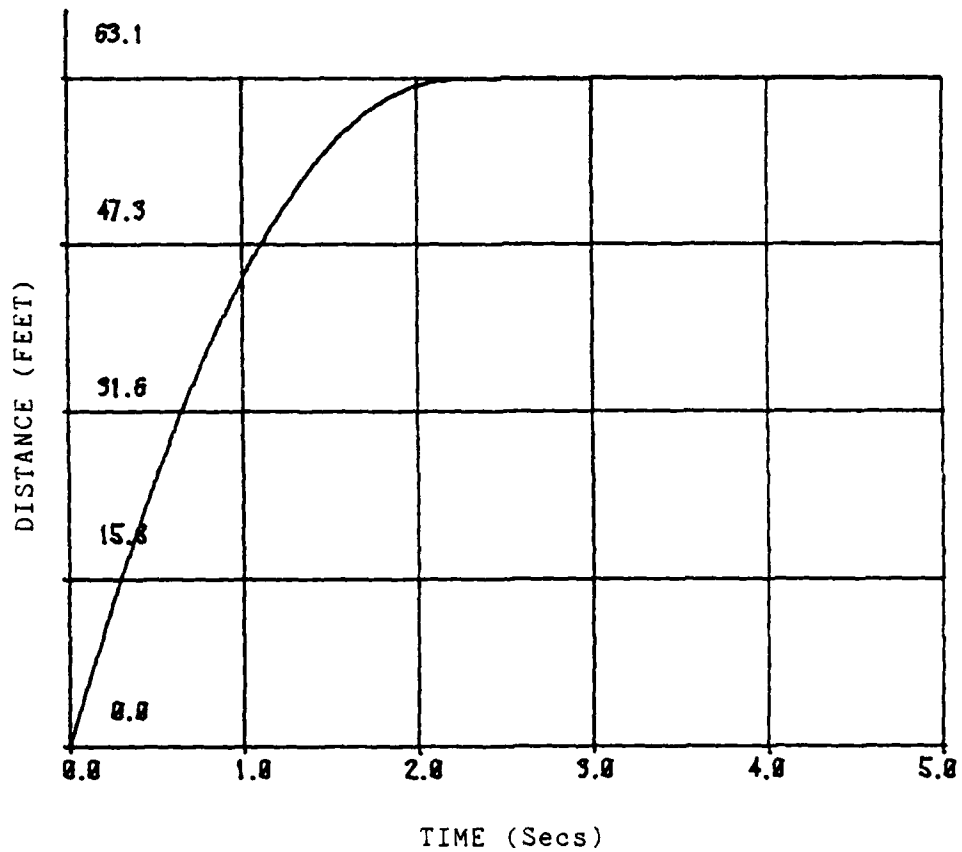


Figure B.22 Distance vs. Time June 29, 1982 Test Two

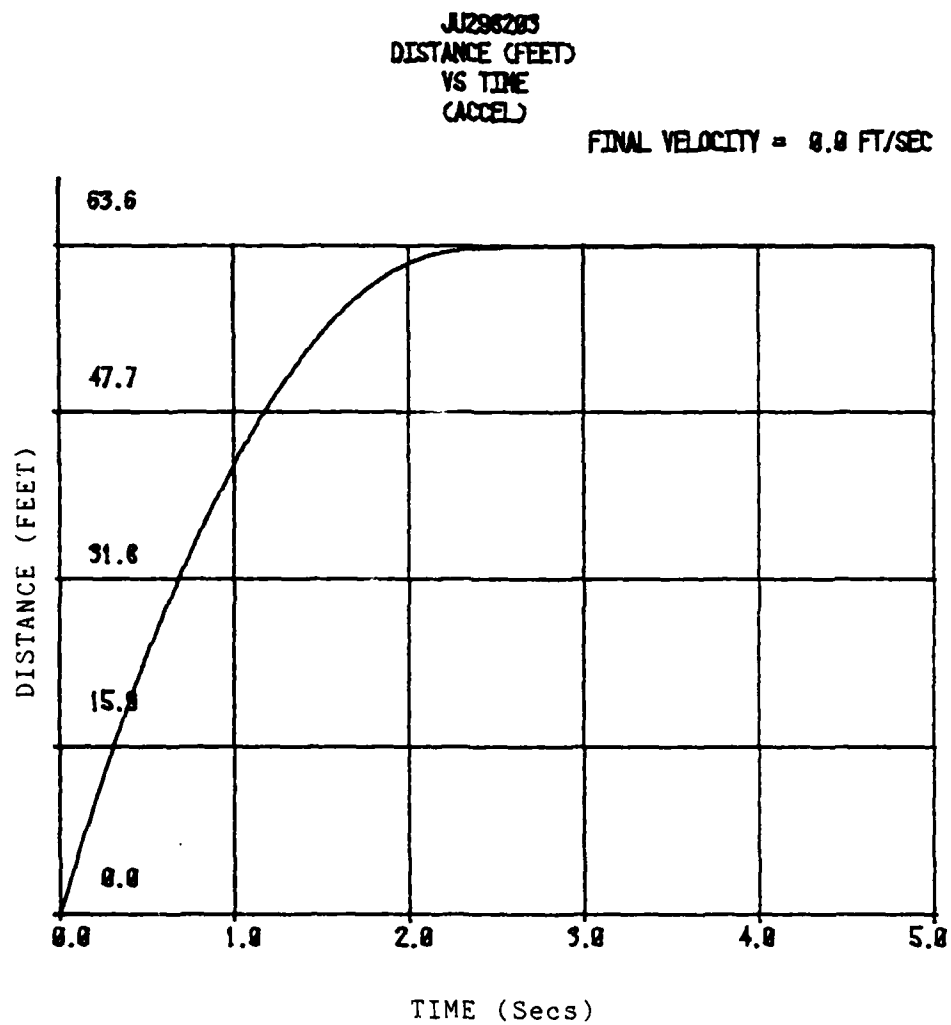


Figure B.23 Distance vs. Time June 29, 1982 Test Three

JJ296284  
DISTANCE (FEET)  
VS TIME  
(ACCEL)

FINAL VELOCITY = 8.8 FT/SEC

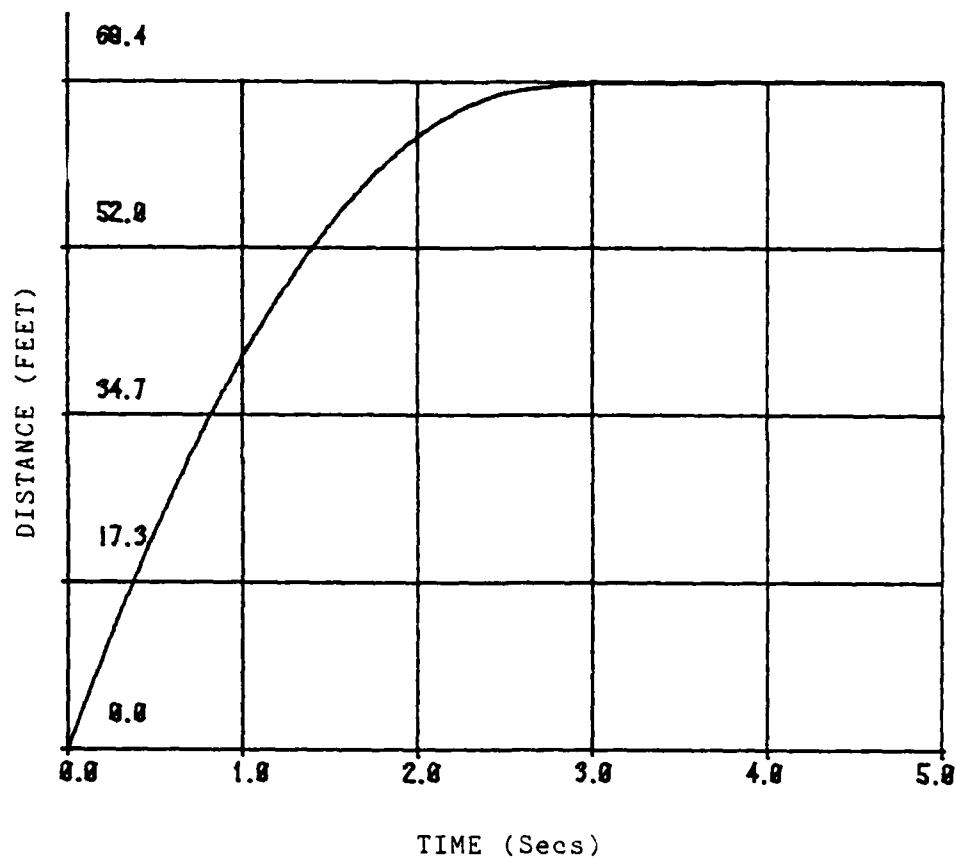


Figure B.24 Distance vs. Time June 29, 1982 Test Four

JJ296285  
DISTANCE (FEET)  
VS TIME  
(ACCEL)

FINAL VELOCITY = 0.0 FT/SEC

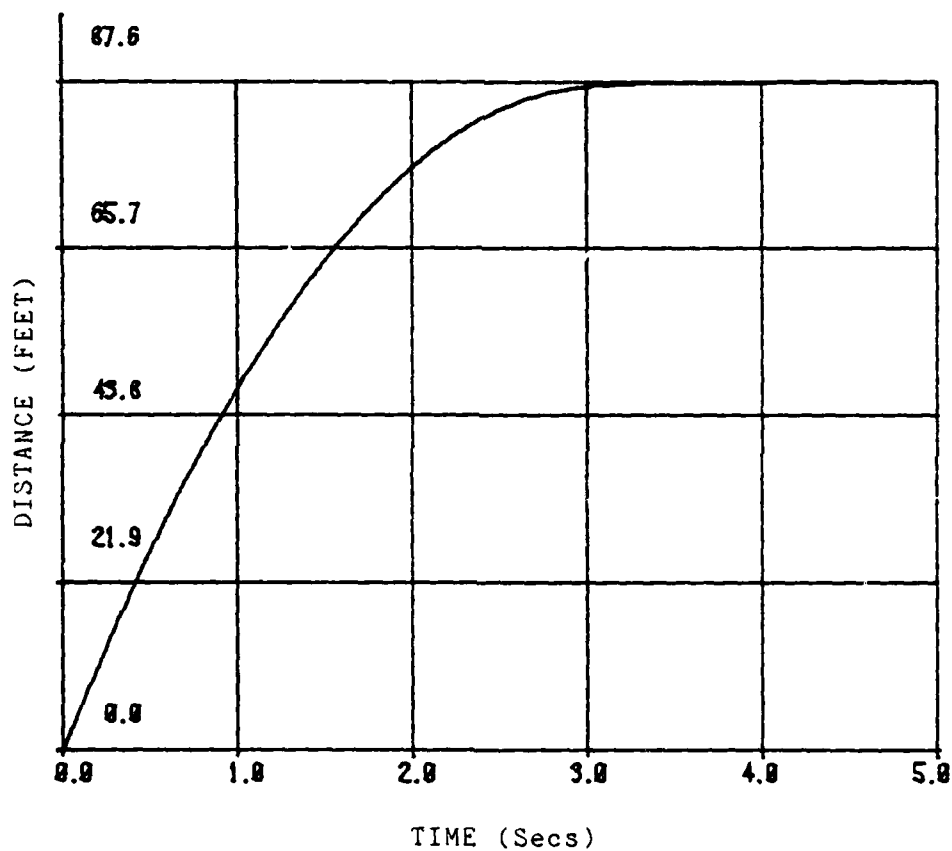


Figure B.25 Distance vs. Time June 29, 1982 Test Five

JJ298281  
DISTANCE (FEET)  
VS TIME  
(STH-MH)

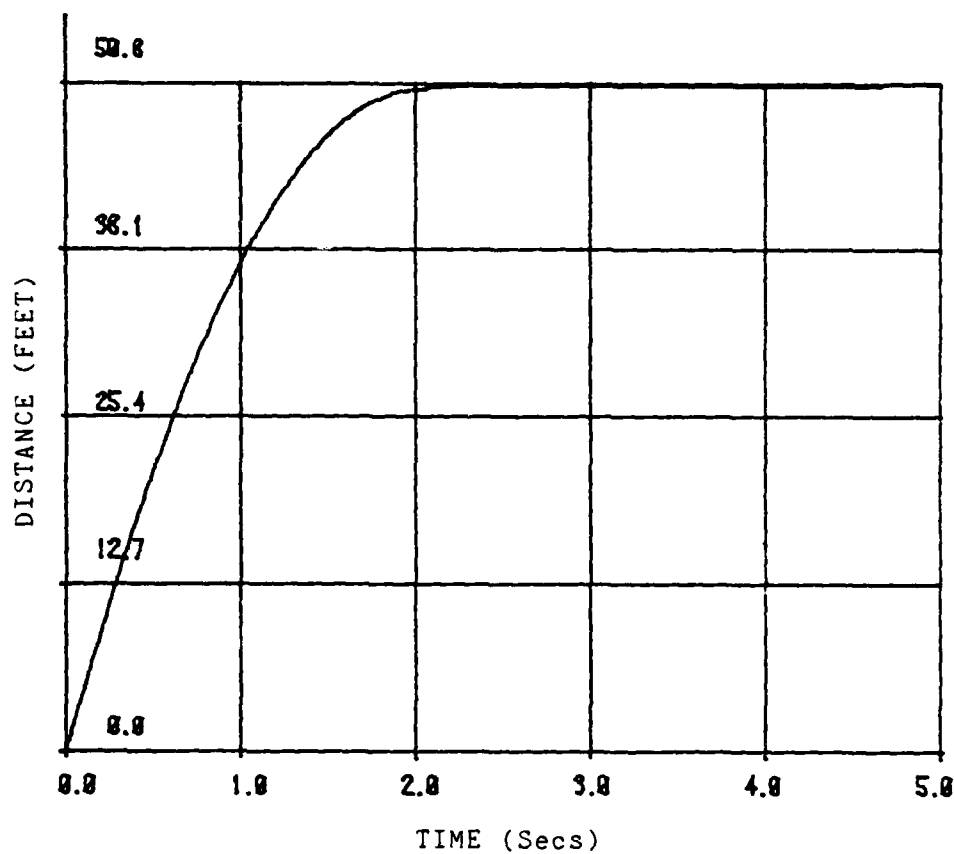


Figure B.26 Distance vs. Time June 29, 1982 Test One  
Fifth-Wheel Data

JJ298202  
DISTANCE (FEET)  
VS TIME  
(5TH-WHD)

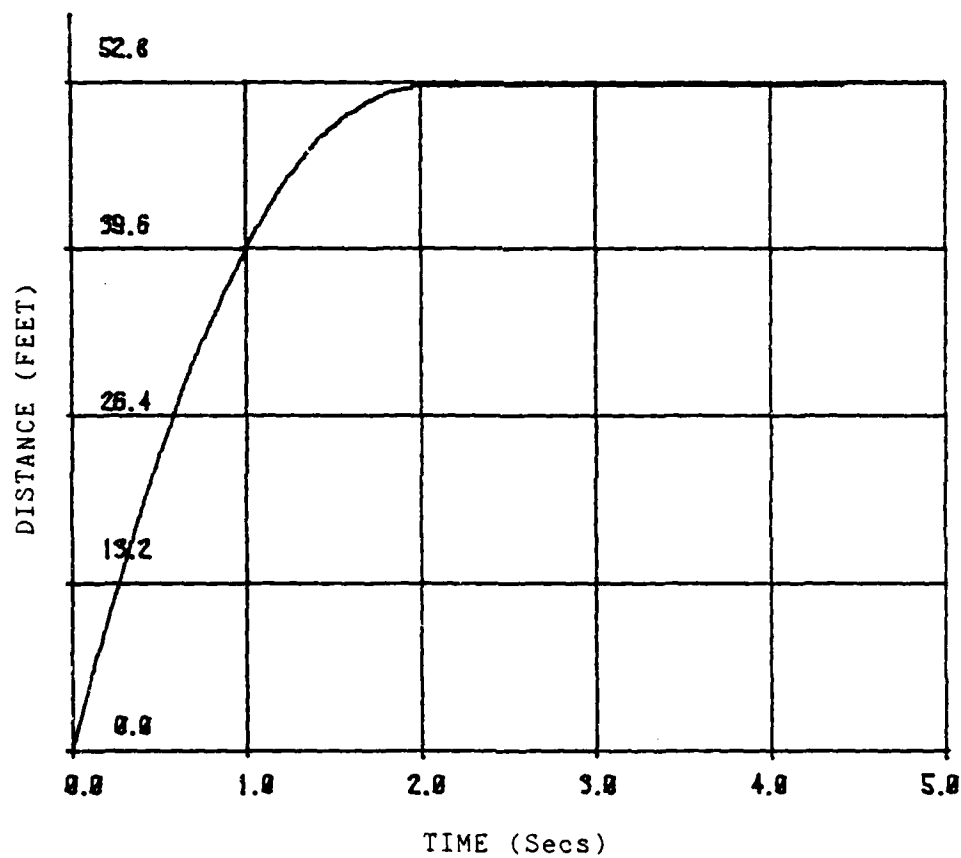


Figure B.27 Distance vs. Time June 29, 1982 Test Two  
Fifth-Wheel Data



J1298283  
DISTANCE (FEET)  
VS TIME  
(STH-44)

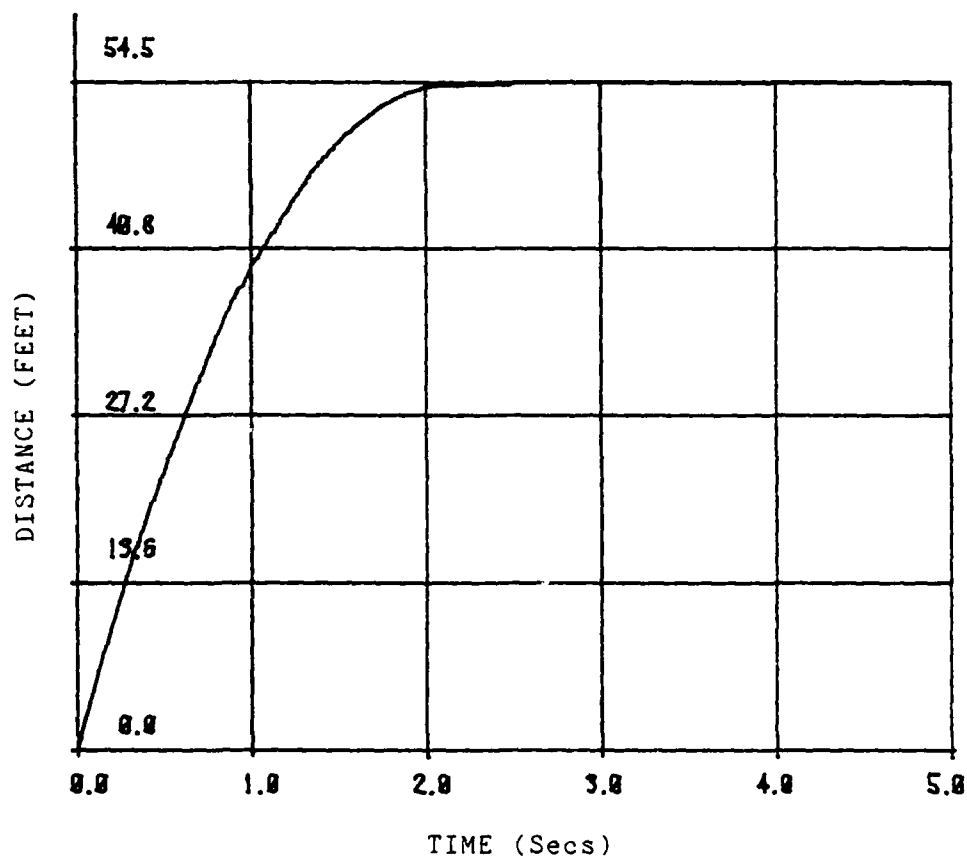


Figure B.28 Distance vs. Time June 29, 1982 Test Three  
Fifth-Wheel Data

JJ298284  
DISTANCE (FEET)  
VS TIME  
(STH-44)

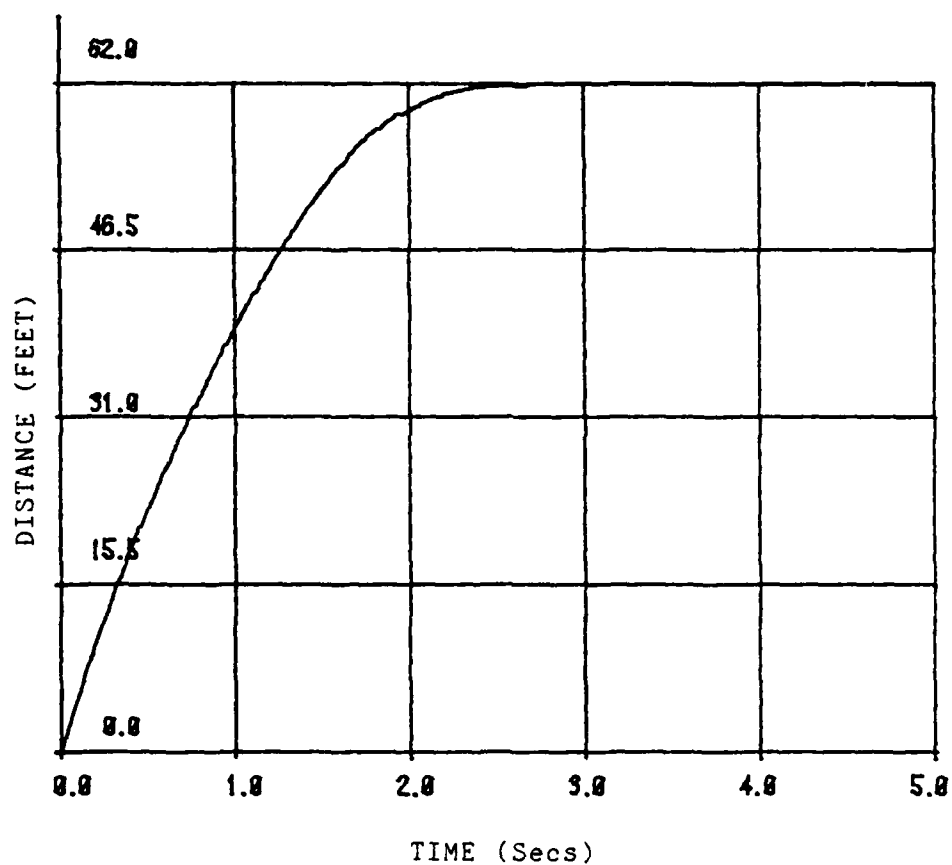


Figure B.29 Distance vs. Time June 29, 1982 Test Four  
Fifth-Wheel Data

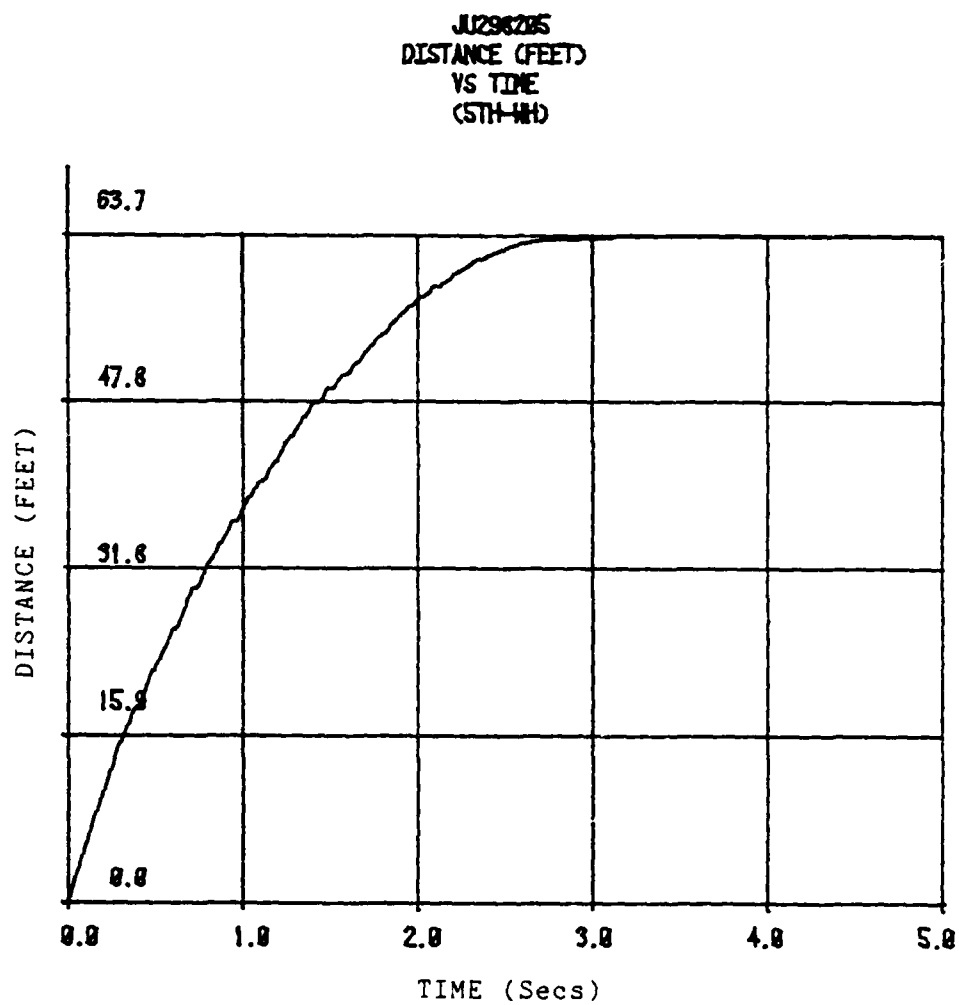


Figure B.30 Distance vs. Time June 29, 1982 Test Five  
Fifth-Wheel Data

REFERENCES

## REFERENCES

- [1] Limpert, Rudolf, Motor Vehicle Accident Reconstruction and Cause Analysis, Michie, Charlottesville, Va, 1978.
- [2] Nichols, F.P., Jr., Dillard, J.H., and Alwood, R.L., "Skid Resistance Pavements in Virginia," Highway Research Board, Bulletin 139, 1956, pp.35-59.
- [3] "Review of Laboratory and Field Methods of Measuring Road Surface Friction," Report of Subcommittee E to the First International Skid Prevention Conference, Charlottesville, Virginia, September 8-12, 1958, Highway Research Board, Bulletin 219, 1959, pp.52-55.
- [4] Dillard, J. H., "Measuring Pavement Slipperiness with a Pendulum Decelerometer," Highway Research Board, Bulletin 348, 1962, pp. 36-43.
- [5] Dillard, W. E., and Allen, T. M., "Comparison of Several Methods of Measuring Road Surface Friction," Highway Research Board, Bulletin 219, January 1959, pp. 25-51.
- [6] Marshall, A. F., and Gartner, W., Jr., "Skid Characteristics of Florida Pavements Determined by Tapley Decelerometer and Actual Stopping Distances," Highway Research Board, Bulletin 348, 1962, pp. 1-17.
- [7] Mercer, S., "Locked Wheel Skid Performance of Various Tires on Clean, Dry Road Surfaces," Highway Research Board, Bulletin 186, 1958, pp.8-25.
- [8] Grosch, K. A., "The Speed and Temperature Dependence of Rubber and its Bearing on the Skid Resistance of Tires," The Physics of Tire Traction, Theory, and Experiment (Hays, D. F., and Brown, A. L., ED) Plenum, New York, 1974; Symposium held at General Motors Research Laboratories, Warren, Michigan, Oct 8-9, 1973, pp.143-165.

## REFERENCES (Con't)

- [9] Ludeme, K. C., Moore, D. F., Schonfeld, R., Williams, and Yandell, W. O., "Tire Traction-The Role of the Pavement," The Physics of Tire Traction, Theory, and Experiment (Hays, D. F., and Brown, A. L., Ed) Plenum, New York, 1974; Symposium held at General Motors Research Laboratories, Warren, Michigan, Oct 8-9, 1973, pp. 361-376.
- [10] DeVinney, W. E., "Factors Affecting Tire Traction," SAE Paper No. 670461, SAE Transactions, May 1967, pp. 1649-1656.
- [11] Davisson, W.E., "Basic Test Methods for Evaluating Tire Traction," SAE Paper No. 680136, SAE Transactions, January 1968, pp. 561-570.
- [12] Yandell, W. O., "The Relationship Between the Stress Saturation of Sliding Rubber and the Load Dependence of Road Tyre Friction," The Physics of Tire Traction, Theory, and Experiment (Hays, D. F., and Brown, A. L., Ed) Plenum, New York, 1974; Symposium held at General Motors Research Laboratories, Warren, Michigan, Oct 8-9, 1973, pp. 311-323.
- [13] Clark, S. K., Kienle, R. N., Pacejka, H. B., and Peterson, R.F., "Tire Traction-The Role of the Tire," The Physics of Tire Traction, Theory and Experiment (Hays, D. F., and Brown, A. L., Ed) Plenum, New York, 1974; Symposium held at General Motors Research Laboratories, Warren, Michigan, Oct 8-9, 1973, pp. 361-376.
- [14] Peterson, R. F., Eckert, C. F., and Carr, C. I., "Tread Compound Effects in Tire Traction," The Physics of Tire Traction, Theory, and Experiment (Hays, D. F., and Brown, A. L., Ed), Plenum, New York, 1974; Symposium held at the General Motors Research Laboratories, Warren, Michigan, Oct 8-9, 1973, pp. 223-239.
- [15] White, A. M., and Thompson, H. O., "Tests for Coefficients of Friction by Skidding Car Method on Wet and Dry Surfaces," Highway Research Board, Bulletin 186, 1958, pp. 26-34.

## REFERENCES (Con't)

- [16] Segal, L., "Tire Traction on Dry Uncontaminated Surfaces," The Physics of Tire Traction, Theory, and Experiment (Hays, D. F., and Brown, A. L., Ed) Plenum, New York, 1974; Symposium held at the General Motors Research Laboratories, Warren, Michigan, Oct 8-9, 1973, pp. 65-98.
- [17] Grough, V. E., "A Tyre Engineer Looks Critically at Current Traction Physics," The Physics of Tire Traction, Theory, and Experiment (Hays, D. F., and Brown, A. L., Ed) Plenum, New York, 1974; Symposium held at the General Motors Research Laboratories, Warren, Michigan, Oct 8-9, 1973, pp.281-297.
- [18] Meyer, W. E., "Friction and Slipperiness," Highway Research Record, No. 214, 1968, pp. 13-17.
- [19] Meyer, W. E., and Kummer, H. W., "Pavement Friction and Temperature Effects," Highway Research Board, Special Report 101, 1969, pp. 47-55.
- [20] Schonfeld, R., "Pavement Surface Texture Classification and Skid Resistance Photo Interperetation," The Physics of Tire Traction, Theory, and Experiment (Hays, D. F., and Brown, A. L., Ed) Plenum, New York, 1974; Symposium held at the General Motors Research Laboratories, Warren, Michigan, Oct 8-9, 1973, pp. 325-338.
- [21] Close, W., "Locked Wheel Friction Tests on Wet Pavements," Highway Research Board, Bulletin 302, 1961, pp. 18-34.
- [22] Reid, S. W., "Measurement of Automobile Tire-To-Road Coefficient of Friction with a Portable Transducer," Thesis, The University of Texas, May 1981.
- [23] Rabinowicz, E., Friction and Wear of Materials, John Wiley & Sons, New York, 1965.
- [24] Calcote, L. R., "A Comparison of High-Speed Photography and Accelerometer Data Reducing Techniques," Experimental Mechanics, May 1977, pp. 167-171.

## REFERENCES Con't

- [25] Leventhal, L. A. 8080A/8085 Assembly Language Programming, Osborne/McGraw Hill, Inc. Berkley, California, 1978.
- [26] Bibbero, R. J., Microprocessors in Instruments and Control, John Wiley & Sons, New York, 1977.
- [27] Stark, P.A., Introduction to Numerical Methods, The MacMillan Co., New York, N.Y., 1970.



## VITA

Ronnie Lynn Coke was born in Madison, Wisconsin, on March 26, 1951. He is the second of two sons born to Evelyn K. Coke and Daniel H. Coke. After completing his work at LaFollette High School, Madison, Wisconsin, in 1969, he entered The University of Wisconsin at Madison. In 1972 he enlisted in The United States Air Force. On December 24, 1972, he married Ellen Mary Hase. Through an Air Force program, he entered The University of Utah in 1974. Graduating from The University of Utah in 1974, he received the degree of Bachelor of Science in Mechanical Engineering. During the following years, he remained in the Air Force serving tours of duty at Kelly AFB, San Antonio, Texas, and at Hofn NYI, Iceland. His son, John Thomas Coke, was born on July 26, 1977. In January 1981, he entered The Graduate School of The University of Texas at Austin.

Permanent Address: 4701 Steinhauer Trail  
Madison, Wisconsin 53716

This thesis was types by the author.

MEASUREMENT OF VEHICLE TIRE-TO-ROAD  
COEFFICIENT OF FRICTION WITH A  
PORTABLE MICROCOMPUTERIZED  
TRANSDUCER

BY

RONNIE LYNN COKE, B.S.  
CAPT, USAF  
26 JULY 1982  
164 PAGES

THESIS

Presented to the Faculty of the Graduate School of  
The University of Texas at Austin  
in Partial Fulfillment  
of the Requirements  
for the Degree of  
MASTER OF SCIENCE IN ENGINEERING

THE UNIVERSITY OF TEXAS AT AUSTIN  
August 1982

## ABSTRACT

Accurate measurement of the tire-to-road coefficient of friction is a necessary factor in the analysis of vehicle dynamics when sliding composes part of the motion. In the past, numerous methods have been used to measure the coefficient of friction but the results of these methods seldom agree or yield the requisite accuracy necessary for a detailed analysis of vehicle dynamics.

Tire traction is a complex process which has many variables. The method of using a portable accelerometer and a microcomputerized data acquisition and storage device was chosen as the best way to measure the coefficient of friction because it permits a test procedure which closely approximates the event being analyzed. Therefore, leaving the least number of variables unaccounted for.

A portable accelerometer/microcomputer device was implemented and used at three different skid test sites. Skid test results from the accelerometer, verified by an independent fifth-wheel device, confirm the accuracy of using this type of device and procedure to determine the coefficient of friction.

## REFERENCES

- [1] Limpert, Rudolf, Motor Vehicle Accident Reconstruction and Cause Analysis, Michie, Charlottesville, Va, 1978.
- [2] Nichols, F.P., Jr., Dillard, J.H., and Alwood, R.L., "Skid Resistance Pavements in Virginia," Highway Research Board, Bulletin 139, 1956, pp.35-59.
- [3] "Review of Laboratory and Field Methods of Measuring Road Surface Friction," Report of Subcommittee E to the First International Skid Prevention Conference, Charlottesville, Virginia, September 8-12, 1958, Highway Research Board, Bulletin 219, 1959, pp.52-55.
- [4] Dillard, J. H., "Measuring Pavement Slipperiness with a Pendulum Decelerometer," Highway Research Board, Bulletin 348, 1962, pp. 36-43.
- [5] Dillard, W. E., and Allen, T. M., "Comparison of Several Methods of Measuring Road Surface Friction," Highway Research Board, Bulletin 219, January 1959, pp. 25-51.
- [6] Marshall, A. F., and Gartner, W., Jr., "Skid Characteristics of Florida Pavements Determined by Tapley Decelerometer and Actual Stopping Distances," Highway Research Board, Bulletin 348, 1962, pp. 1-17.
- [7] Mercer, S., "Locked Wheel Skid Performance of Various Tires on Clean, Dry Road Surfaces," Highway Research Board, Bulletin 186, 1958, pp.8-25.
- [8] Grosch, K. A., "The Speed and Temperature Dependence of Rubber and its Bearing on the Skid Resistance of Tires," The Physics of Tire Traction, Theory, and Experiment (Hays, D. F., and Brown, A. L., ED) Plenum, New York, 1974; Symposium held at General Motors Research Laboratories, Warren, Michigan, Oct 8-9, 1973, pp.143-165.

## REFERENCES (Con't)

- [9] Ludeme, K. C., Moore, D. F., Schonfeld, R., Williams, and Yandell, W. O., "Tire Traction-The Role of the Pavement," The Physics of Tire Traction, Theory, and Experiment (Hays, D. F., and Brown, A. L., Ed) Plenum, New York, 1974; Symposium held at General Motors Research Laboratories, Warren, Michigan, Oct 8-9, 1973, pp. 361-376.
- [10] DeVinney, W. E., "Factors Affecting Tire Traction," SAE Paper No. 670461, SAE Transactions, May 1967, pp. 1649-1656.
- [11] Davisson, W.E., "Basic Test Methods for Evaluating Tire Traction," SAE Paper No. 680136, SAE Transactions, January 1968, pp. 561-570.
- [12] Yandell, W. O., "The Relationship Between the Stress Saturation of Sliding Rubber and the Load Dependence of Road Tyre Friction," The Physics of Tire Traction, Theory, and Experiment (Hays, D. F., and Brown, A. L., Ed) Plenum, New York, 1974; Symposium held at General Motors Research Laboratories, Warren, Michigan, Oct 8-9, 1973, pp. 311-323.
- [13] Clark, S. K., Kienle, R. N., Pacejka, H. B., and Peterson, R.F., "Tire Traction-The Role of the Tire," The Physics of Tire Traction, Theory and Experiment (Hays, D. F., and Brown, A. L., Ed) Plenum, New York, 1974; Symposium held at General Motors Research Laboratories, Warren, Michigan, Oct 8-9, 1973, pp. 361-376.
- [14] Peterson, R. F., Eckert, C. F., and Carr, C. I., "Tread Compound Effects in Tire Traction," The Physics of Tire Traction, Theory, and Experiment (Hays, D. F., and Brown, A. L., Ed), Plenum, New York, 1974; Symposium held at the General Motors Research Laboratories, Warren, Michigan, Oct 8-9, 1973, pp. 223-239.
- [15] White, A. M., and Thompson, H. O., "Tests for Coefficients of Friction by Skidding Car Method on Wet and Dry Surfaces," Highway Research Board, Bulletin 186, 1958, pp. 26-34.

## REFERENCES (Con't)

- [16] Segal, L., "Tire Traction on Dry Uncontaminated Surfaces," The Physics of Tire Traction, Theory, and Experiment (Hays, D. F., and Brown, A. L., Ed) Plenum, New York, 1974; Symposium held at the General Motors Research Laboratories, Warren, Michigan, Oct 8-9, 1973, pp. 65-98.
- [17] Grough, V. E., "A Tyre Engineer Looks Critically at Current Traction Physics," The Physics of Tire Traction, Theory, and Experiment (Hays, D. F., and Brown, A. L., Ed) Plenum, New York, 1974; Symposium held at the General Motors Research Laboratories, Warren, Michigan, Oct 8-9, 1973, pp.281-297.
- [18] Meyer, W. E., "Friction and Slipperiness," Highway Research Record, No. 214, 1968, pp. 13-17.
- [19] Meyer, W. E., and Kummer, H. W., "Pavement Friction and Temperature Effects," Highway Research Board, Special Report 101, 1969, pp. 47-55.
- [20] Schonfeld, R., "Pavement Surface Texture Classification and Skid Resistance Photo Interpretation," The Physics of Tire Traction, Theory, and Experiment (Hays, D. F., and Brown, A. L., Ed) Plenum, New York, 1974; Symposium held at the General Motors Research Laboratories, Warren, Michigan, Oct 8-9, 1973, pp. 325-338.
- [21] Close, W., "Locked Wheel Friction Tests on Wet Pavements," Highway Research Board, Bulletin 302, 1961, pp. 18-34.
- [22] Reid, S. W., "Measurement of Automobile Tire-To-Road Coefficient of Friction with a Portable Transducer," Thesis, The University of Texas, May 1981.
- [23] Rabinowicz, E., Friction and Wear of Materials, John Wiley & Sons, New York, 1965.
- [24] Calcote, L. R., "A Comparison of High-Speed Photography and Accelerometer Data Reducing Techniques," Experimental Mechanics, May 1977, pp. 167-171.

## REFERENCES Con't

- [25] Leventhal, L. A. 8080A/8085 Assembly Language Programming, Osborne/McGraw Hill, Inc. Berkley, California, 1978.
- [26] Bibbero, R. J., Microprocessors in Instruments and Control, John Wiley & Sons, New York, 1977.
- [27] Stark, P.A., Introduction to Numerical Methods, The MacMillan Co., New York, N.Y., 1970.

MEASUREMENT OF VEHICLE TIRE-TO-ROAD  
COEFFICIENT OF FRICTION WITH A  
PORTABLE MICROCOMPUTERIZED  
TRANSDUCER

BY

RONNIE LYNN COKE, B.S.  
CAPT, USAF  
26 JULY 1982  
164 PAGES

THESIS

Presented to the Faculty of the Graduate School of  
The University of Texas at Austin  
in Partial Fulfillment  
of the Requirements  
for the Degree of  
MASTER OF SCIENCE IN ENGINEERING

THE UNIVERSITY OF TEXAS AT AUSTIN  
August 1982



ATE  
MED  
-8